

Multinuclear fingerprinting

Gonzalo G. Rodriguez^{1,2}, Zidan Yu^{1,3,4}, Lauren O'Donnell^{1,5}, Martijn A. Cloos^{1,6} & Guillaume Madelin^{1,3*}

¹Center for Biomedical Imaging, Department of Radiology, New York University Grossman School of Medicine, New York, NY, USA; ²NMR Signal Enhancement, Max Planck Institute for Multidisciplinary Sciences, Göttingen, Germany; ³Vilcek Institute of Graduate Biomedical Sciences, New York University Grossman School of Medicine, New York, NY, USA; ⁴Philips, Best, The Netherlands; ⁵JEOL USA, Peabody, MA, USA; ⁶Donders Center for Cognitive Neuroimaging, Radboud University, Nijmegen, The Netherlands; *Corresponding author: guillaume.madelin@nyulangone.org

Manuscript compiled on May 25, 2026

We developed a new magnetic resonance imaging method called multinuclear fingerprinting (MNF) which leverages simultaneously-acquired proton (^1H) and sodium (^{23}Na) data to generate seven quantitative maps of the whole brain: proton density (PD), T_1 and T_2 relaxation times from water, and tissue sodium concentration (TSC), T_1 , $T_{2,\text{short}}$ and $T_{2,\text{long}}$ from Na^+ ions. MNF consists of two parts: (1) simultaneous $^1\text{H}/^{23}\text{Na}$ magnetic resonance fingerprinting (MRF), and (2) a super-resolution (SR) algorithm to increase the ^{23}Na resolution to match the ^1H resolution. It was tested on the brain of seven healthy subjects at 7 T, with a final resolution of $1.5 \times 1.5 \times 5 \text{ mm}^3$ for all maps acquired in 13 min. MNF could provide new fundamental insights into the inter-relationship between morphology (*i.e.* tissue structure from the ^1H maps) and physiology (*i.e.* ion homeostasis from the ^{23}Na maps) *in vivo* to help improve our understanding of the human brain in general, and to study neuropathologies and their treatments. Since all $^1\text{H}/^{23}\text{Na}$ MRF data is acquired simultaneously, all images are exactly co-registered with identical spatial and temporal resolutions. MNF could be useful in future longitudinal studies for assessing local time-dependent and conjoint $^1\text{H}/^{23}\text{Na}$ MR changes during tasks or interventions. MNF was initially developed for neuroimaging, but it can be adapted to any other parts of the body.

Sodium ions (Na^+) play an essential role in brain physiological processes such as cellular homeostasis (the maintenance of stable internal cell conditions of pH, temperature, ion concentration, and volume) and propagation of action potentials in neurons. The steady-state maintenance of the electrochemical gradient between intracellular and extracellular spaces is particularly important for ionic homeostasis. Well-defined transmembrane ionic gradients are necessary to absorb vital substrates (*e.g.* glucose), to release products (*e.g.* neurotransmitters), regulate intracellular metabolite concentrations (*e.g.* ions), allow energy production (*e.g.* oxidative phosphorylation), eliminate toxic byproducts (*e.g.* amyloid oligomers), and control cell volume by regulation of the water osmotic pressure (1, 2). Sodium homeostasis itself is regulated by the Na^+/K^+ -ATPase (sodium-potassium pump) which requires about 50% of the energy produced within the cells for normal brain function (3), and therefore relies on an efficient and well maintained cellular energetic metabolism.

High-resolution imaging of sodium in the living human brain could therefore provide a wealth of new information leading to a better understanding of brain physiology in both health and disease (4). It is possible to detect sodium ions *in vivo* non-invasively with

sodium magnetic resonance imaging (^{23}Na MRI), but so far low signal-to-noise ratio (SNR), long acquisition times and low resolution have been major hurdles for its application in clinical work or in basic brain research. Unlike conventional hydrogen (^1H , proton) MRI, a cornerstone of modern-day healthcare and neuroscience, it is much more difficult to capture clear sodium images since the ^{23}Na signal is about 20,000 times lower than the ^1H signal in brain (5, 6). Moreover, while ^1H nuclei have a spin $\frac{1}{2}$, leading to relatively simple dynamics producing an MR signal that persists tens or hundreds of milliseconds, ^{23}Na nuclei have a spin $\frac{3}{2}$ and undergo complicated quadrupolar dynamics resulting in an MR signal that disappears quickly within a few milliseconds, making it difficult to detect with standard MR techniques (7, 8).

In order to improve the temporal and spatial efficiency of ^{23}Na MRI *in vivo*, as well as its clinical significance in conjunction with ^1H MRI, we developed a new imaging method called multinuclear fingerprinting (MNF) that can provide quantitative images with both morphological (^1H from water) and physiological (^{23}Na from Na^+) information in a single MR data acquisition. MNF consists of a new magnetic resonance fingerprinting (MRF) (10, 11) pulse sequence that can ac-

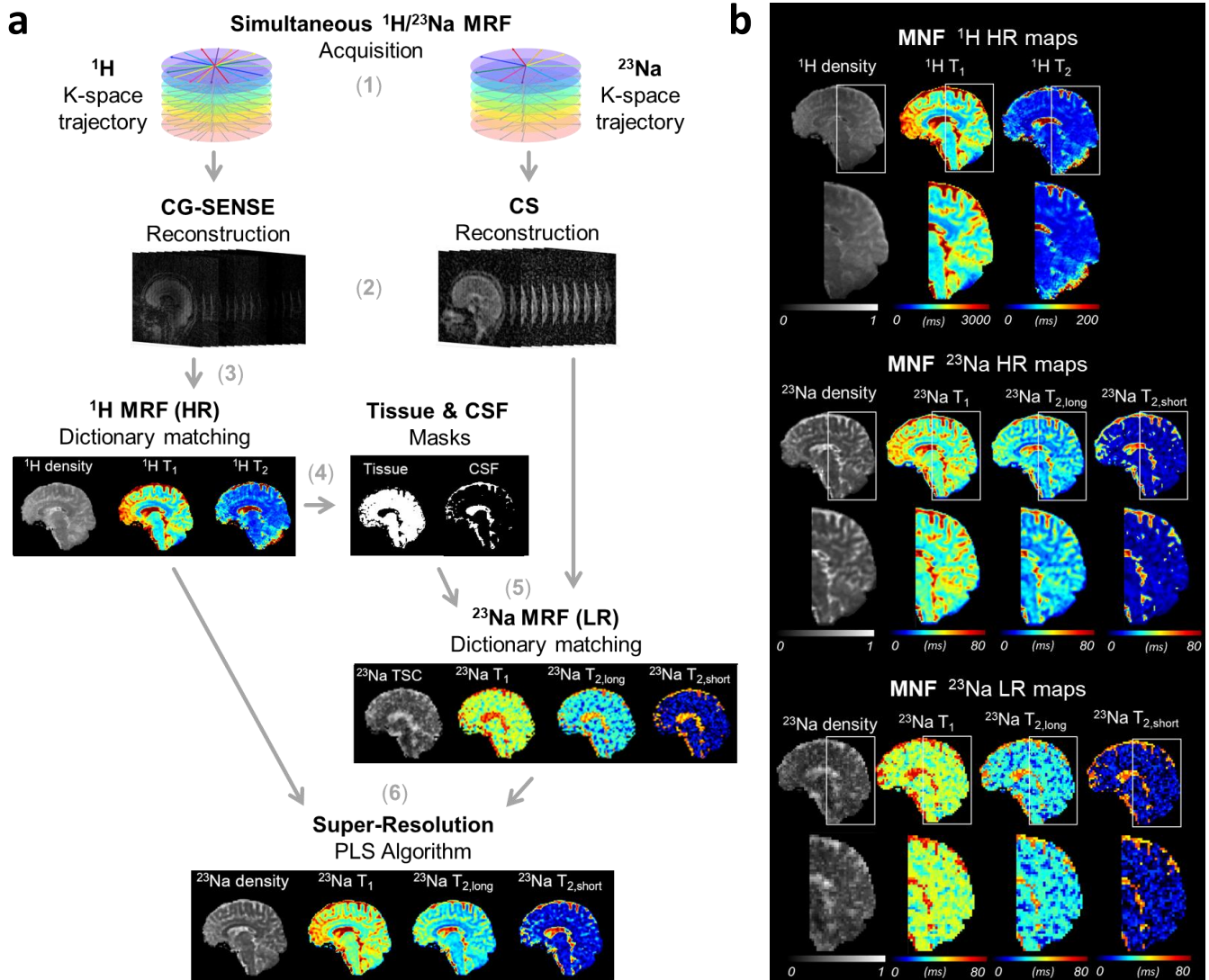


Figure 1. The multinuclear fingerprinting (MNF) method. (a) MNF consists of: (1) simultaneous $^1\text{H}/^{23}\text{Na}$ MRF data acquisition; (2) separate reconstructions of HR ^1H images (using CG-SENSE) and LR ^{23}Na images (using CS) from data acquired after each pulse of their respective MRF acquisitions; (3) MR fingerprints dictionary matching of the ^1H MRF images to generate quantitative HR maps of ^1H density, and relaxation times T_1 and T_2 ; (4) Brain tissue (gray + white matters) and CSF masking from the HR ^1H MRF maps; (5) MR fingerprints dictionary matching of the ^{23}Na MRF images to generate quantitative LR maps of ^{23}Na density, and relaxation times T_1 , $T_{2,\text{short}}$ and $T_{2,\text{long}}$, using the downsampled (LR) masks, and with different MR fingerprints dictionaries for fluids (CSF) and brain tissue; (6) Application of a PLS super-resolution algorithm optimized for these data to generate HR ^{23}Na maps (9). (b) Examples of sagittal slices from MNF from the quantitative 3D maps of ^1H density, T_1 and T_2 , and ^{23}Na density, T_1 , $T_{2,\text{short}}$ and $T_{2,\text{long}}$ in a healthy brain. The part of each map within the white rectangle is zoomed in below its respective map. For the ^{23}Na data, we show the maps before (LR) and after (HR) application of the super-resolution algorithm. Resolution = $1.5 \times 1.5 \text{ mm}^2$ for the HR slices, and $2.85 \times 2.85 \text{ mm}^2$ for the LR slices. *Abbreviations:* CG-SENSE = Conjugate Gradient Sensitivity Encoding; CS = Compressed Sensing; CSF = Cerebrospinal Fluid; PLS = Partial Least Square; LR = Low Resolution ($2.85 \times 2.85 \times 5 \text{ mm}^3$); HR = High Resolution ($1.5 \times 1.5 \times 5 \text{ mm}^3$)

quire and characterize both ^1H and ^{23}Na spin dynamics simultaneously to infer their respective local MR properties (density and relaxation times), combined with a specially-designed super-resolution (SR) algorithm. This MRF+SR process results in a set of ^1H and ^{23}Na maps of the whole brain with exact co-registration, as well as identical spatial and temporal resolutions.

In summary, to develop MNE, we first modified an

ultra-high field (7 T) MRI system such that it can record MR signals from multiple nuclei simultaneously (12, 13). We then developed a new simultaneous 3D $^1\text{H}/^{23}\text{Na}$ MRF pulse sequence, based on our previous work on simultaneous ^1H MRF/ ^{23}Na MRI (13–15), to generate four "low-resolution" (LR, $2.85 \times 2.85 \times 5 \text{ mm}^3$) ^{23}Na maps (tissue sodium concentration [TSC], T_1 , $T_{2,\text{short}}$ and $T_{2,\text{long}}$), and three "high-resolution" (HR, $1.5 \times 1.5 \times 5 \text{ mm}^3$) ^1H

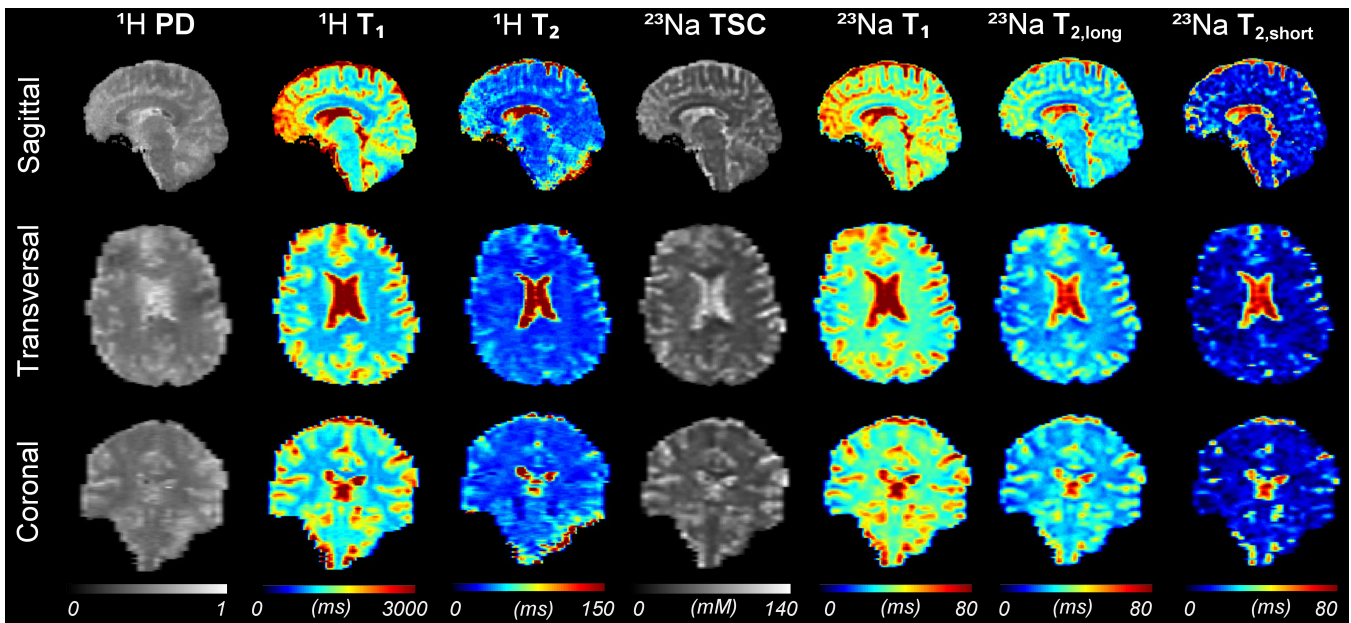


Figure 2. Examples of the seven MNF HR ^1H and ^{23}Na maps of a whole brain. Representative sagittal, transversal and coronal slices include proton density (PD), T_1 and T_2 from ^1H , and tissue sodium concentration (TSC), T_1 , $T_{2,\text{short}}$ and $T_{2,\text{long}}$ from ^{23}Na . Resolution = $1.5 \times 1.5 \times 5 \text{ mm}^3$, TA = 13 min.

maps (proton density [PD], T_1 and T_2) of the whole brain in a single 13-min acquisition. Finally, we implemented an iterative SR algorithm based on partial least square regression to model the voxelwise relationship between all the HR ^1H and LR ^{23}Na maps to derive the final HR ^{23}Na maps on a subject-by-subject basis (9, 16). The MNF pipeline is schematically summarized in Figure 1.

Since all MNF maps are acquired co-registered and simultaneously, they undergo the same local B_0 inhomogeneities, head motion, or pulsations from blood and cerebrospinal fluid (CSF), that can influence local MR signals. This could prove useful for: (1) for trying to reduce scan time by acquiring all multinuclear data in one single sequence instead of two consecutive sequences; (2) for studying the inter-relationship of brain morphology and physiology conjointly; and (3) for future dynamic or longitudinal studies to assess the simultaneous changes in local water and Na^+ concentrations, and their respective relaxation times, during tasks or interventions.

We expect that the possibility to provide new ^{23}Na -based physiological maps alongside morphological ^1H -based maps with MNF will enable scientists and clinicians to directly assess ion homeostasis linked to cellular energy processes and related morphological tissue changes, bridge the gap in resolution that has held back our ability to study metabolism in the human brain *in vivo*, and help better understand brain pathologies or monitor therapies. Although it was initially developed for neuroimaging, MNF can be adapted and optimized for any other parts of the body.

Results

MNF maps

Figure 2 shows representative examples of the seven 3D MNF HR ^1H and ^{23}Na maps in a healthy brain. These maps were all acquired simultaneously in 13 min and all have a spatial resolution of $1.5 \times 1.5 \times 5 \text{ mm}^3$ after application of the SR algorithm. Notice that the slight radial undersampling artifacts noticeable in the frontal lobe area on the PD and ^1H T_2 sagittal maps did not affect the ^{23}Na HR maps generated by the SR algorithm. Pre-processed full datasets from ^1H MRF (PD, T_1 , T_2 and B_1^+) are shown in Figure S1, and full datasets from ^{23}Na MRF (sodium density [SD], T_1 , $T_{2,\text{short}}$, $T_{2,\text{long}}$, ΔB_1^+ and Δf_0) are shown in Figure S2 in Supplementary Information. Only the seven maps of PD, T_1 , T_2 (from ^1H MRF) and TSC (derived from SD), T_1 , $T_{2,\text{short}}$ and $T_{2,\text{long}}$ (from ^{23}Na MRF) are shown as meaningful results with this method. The B_1^+ (from ^1H MRF), ΔB_1^+ and Δf_0 (from ^{23}Na MRF) parameters were only included in the simulation models used to calculate the respective fingerprint dictionaries as complementary information used to improve the estimation of the seven final MNF maps.

Measurements

In the following sections, the *final* mean and standard deviation (std) correspond to the mean \pm one std value of the measurements calculated for each subject using three different statistical methods (standard, jackknife, bootstrap) as described in details in "Meth-

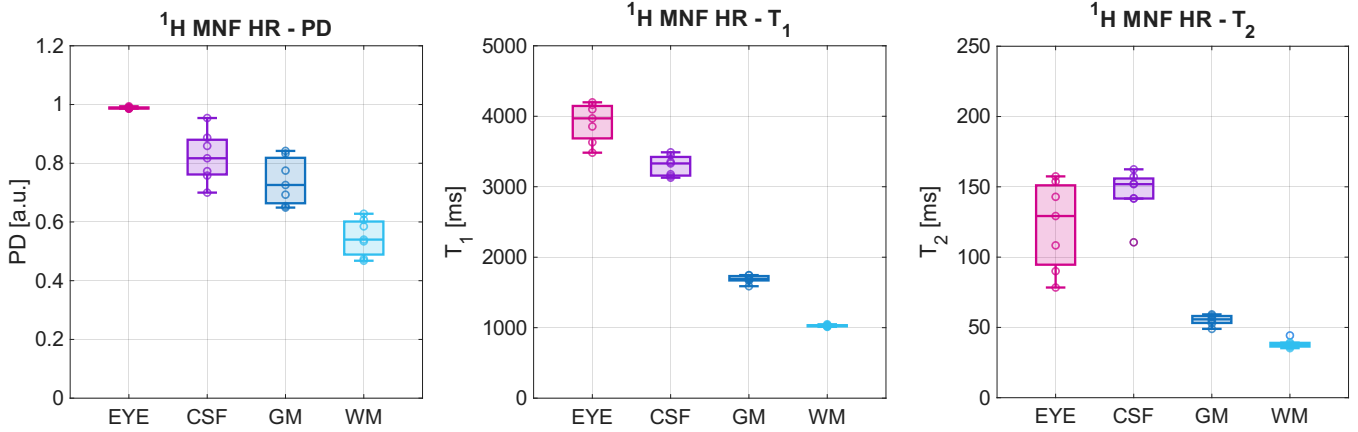


Figure 3. ^1H MNF HR measurements. The boxplots show distributions and median values of final mean values (from the standard method) of the mean measurements from the N_{ROI} and N_{REF} values (histograms) from $N = 7$ subjects, from the ^1H MNF HR data (PD, T_1 , T_2), in the EYE, CSF, GM and WM ROIs. Highest values used were $N_{\text{ROI}} = 5\%$ to 100% by steps of 5% (20 values), $N_{\text{REF}} = 5\%$ to 100% by steps of 5% (20 values).

ods/Statistical analysis", while the *overall* mean corresponds to the mean \pm one std of the final mean and of the final std values calculated over all subjects for each statistical method.

Figure 3 shows boxplots of the final mean values of the ^1H MNF HR data from $N = 7$ subjects, calculated using the standard statistical method. This data includes PD, T_1 , and T_2 measured in four regions-of-interest (ROI): the vitreous humor of the eyes (EYE), cerebrospinal fluid (CSF), gray matter (GM) and white matter (WM). We can see that PD measurements present quite a large variability between subjects, except for PD in the EYE which was used as a reference. Relaxation times values in EYE and CSF are also quite variable, while T_1 and T_2 in GM and WM were pretty consistent with each other for all subjects.

Figure 4 shows boxplots of the final mean values of the ^{23}Na MNF HR and LR data from $N = 7$ subjects, and of the FLORET (FLO) data acquired as a reference method on two subjects, all calculated using the standard statistical method. This data includes TSC, T_1 , $T_{2,\text{short}}$, and $T_{2,\text{long}}$ measured in the EYE, CSF, GM and WM. Overall, ^{23}Na MNF HR seems to overestimate TSC and relaxation time values compared to ^{23}Na MNF LR and FLORET data, except for WM relaxation times.

Table 1 (placed after References) presents a summary of the overall means and standard deviations from ^1H MNF HR, ^{23}Na MNF HR and LR in the EYE, CSF, GM and WM. See Tables S1-S3 in Supplementary Information for a detailed summary of all the mean value measurements in each subject. We can see that the overall mean values are identical for all three statistical methods, but that the overall standard deviations (*i.e.* the mean uncertainty of the measurements over all subjects) are different: of the order of $12.49 \pm 7.85\%$ (range [3.22%, 32.92%])

for the standard method, of the order of $0.03 \pm 0.03\%$ (range [0.00%, 0.12%]) for jackknife, and of the order of $0.63 \pm 0.40\%$ (range [0.16%, 1.66%]) for bootstrap.

Individual measurements for each subject are presented in Supplementary Information. Figures S3-S25 show measurement histograms for single values of N_{REF} (80%) and N_{ROI} (90%). Figures S26-S31 show boxplots of the mean values measured in all seven subjects with single values of N_{ROI} (80%) and N_{REF} (90%). Figures S32-S54 show histograms of mean values from multiple measurements with both N_{REF} and N_{ROI} ranging from 5% to 100% by steps of 5%. Figures S55-S59 show boxplots of the mean values of the mean measurements using N_{ROI} and N_{REF} from 5% to 100% by steps of 5%.

Validation

Table 2 (placed after References) presents a comparison of the overall mean values (standard statistical method) from ^1H MNF HR measured *in vivo* in brain at 7 T with values from the literature, in EYE, CSF, GM and WM. We can see that mean PD and ^1H relaxation times measured with ^1H MNF HR are within or close to (within one std) the ranges of values from the literature, which is particularly sparse for the EYE and CSF regions. The two main discrepancies are: (1) PD in CSF, which is quite low (0.81 ± 0.09) compared to an expected value of 0.99; and (2) T_2 in CSF, which is higher than the value from a unique reference.

Table 3 (placed after References) presents a comparison of the overall mean values (standard statistical method) from ^{23}Na MNF LR and HR measured *in vivo* in brain at 7 T with values from the literature, in EYE, CSF, GM and WM. Mean values measured from ^{23}Na MNF LR are within the range of values from the literature, except T_1 and $T_{2,\text{short}}$ in GM, and $T_{2,\text{short}}$ in WM,

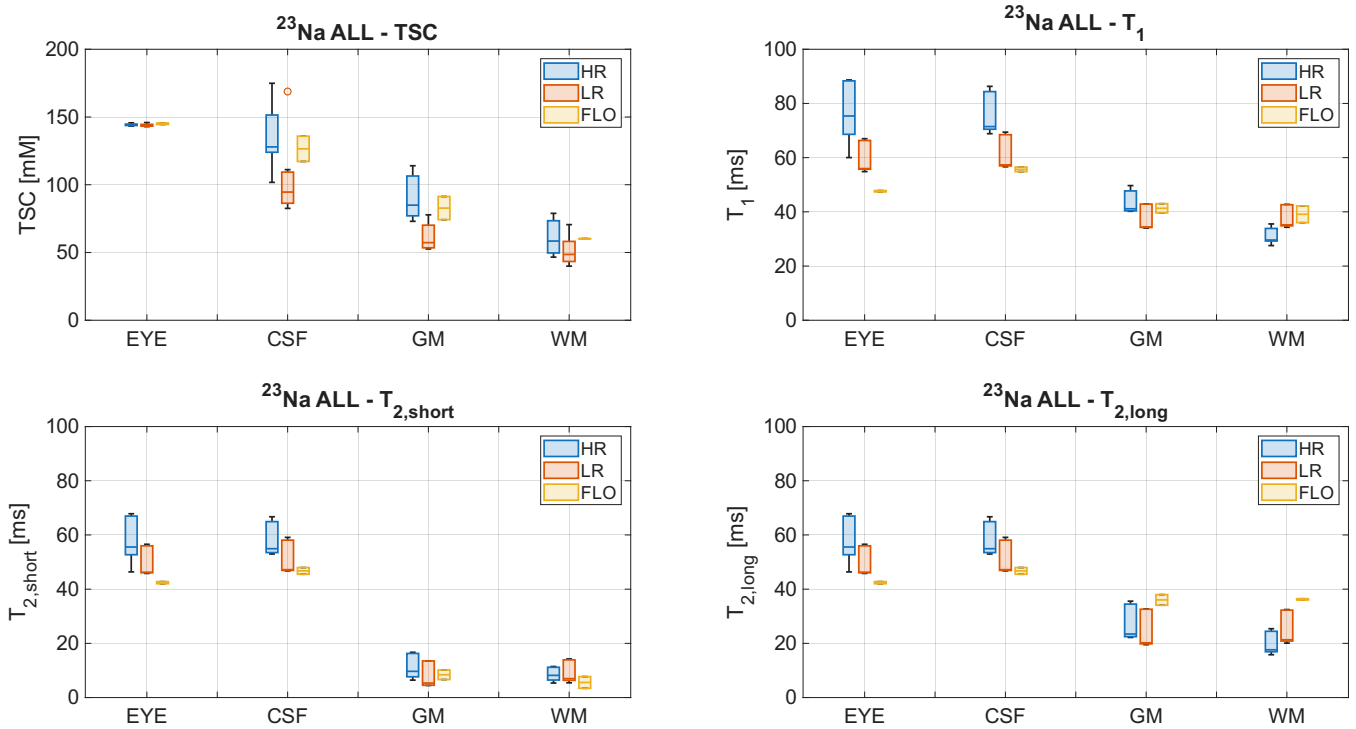


Figure 4. ^{23}Na MNF HR, LR, and FLORET measurements. The boxplots show distributions and median values of the final mean values (from the standard method) of the mean measurements from the N_{ROI} and N_{REF} values (histograms), from the ^{23}Na MNF HR (7 subjects), LR (7 subjects) and FLORET (FLO, 2 subjects: 5 and 6) data (TSC, T_1 , $T_{2,short}$, $T_{2,long}$), in the EYE, CSF, GM and WM ROIs. Highest values used were $N_{\text{ROI}} = 5\%$ to 100% by steps of 5% (20 values), $N_{\text{REF}} = 5\%$ to 100% by steps of 5% (20 values).

which are slightly above the range but still within one standard deviation. Most mean values measured from ^{23}Na MNF HR are in the higher part of, or above, the range of values from the literature, except WM T_1 which is slightly below this range.

The Wilcoxon rank-sum test did not detect any statistically significant difference (after Bonferroni correction) between the ^{23}Na MNF LR, ^{23}Na MNF HR and ^{23}Na FLORET measurements in GM, WM CSF and EYE, except in four cases, all of them only between HR and LR data: T_1 in EYE, CSF and WM, and TSC in GM (see Table S5 in Supplementary Information).

Discussion

Overall, both the ^1H MNF HR and the ^{23}Na MNF LR data reconstructed directly from the simultaneous $^1\text{H}/^{23}\text{Na}$ MRF acquisition provided mean values of PD, TSC and relaxation times from both nuclei that were similar to the values found in the sparse literature in healthy brain at 7 T. However, the application of the SR algorithm to the ^{23}Na MNF LR data to generate the HR maps had a tendency to slightly increase the values compared to literature. This could be explained by the reduction of partial volume effects (PVE) in the HR data combined with the fact that all the HR ^{23}Na values are compared

with values from the standard ^{23}Na MRI literature, which relies on data acquired with a low resolution similar to our ^{23}Na LR data (or even lower).

While absolute values measured in each healthy volunteer can be of interest for the diagnosis of brain pathologies, the main goal of MNF would be its application into longitudinal studies where the subjects will be scanned multiple times either during tasks, therapies, or simply to assess the potential evolution of pathologies over time without intervention. Quantitative changes in all these MNF metrics should provide more relevant information about brain morphological and physiological alterations in different conditions than the initial absolute value itself.

The systematic use of multiple values of N_{REF} highest voxel values for quantifying PD and TSC and of N_{ROI} for measuring mean values of all metrics in different ROIs can reduce the sensitivity of these measurements to subjective operator-dependent manual drawing of ROIs and to PVE at the borders of these ROIs. It should thus provide a more robust and automated quantification of MNF metrics in different regions of the brain. In addition, the application of resampling methods such as jackknife or bootstrapping can also significantly reduce uncertainties on these ROI-based quantitative estimates for each subject, where the mean std of the mean value measurements can go from more than 12% using

standard statistics to less than 1% with resampling.

The simultaneous acquisition of ^1H and ^{23}Na MRF data was made possible on our scanner at 7 T thanks to the insertion of an external frequency generator (local oscillator) in the radiofrequency (RF) cabinet of the system. However, such hardware modification can be difficult to carry out on clinical scanners at 3 T or 7 T. In that case, an alternative version of MNF needs to be developed with interleaved $^1\text{H}/^{23}\text{Na}$ MRF data acquisition instead of truly simultaneous (17, 18), where the signal of ^1H and ^{23}Na can be recorded through two different analog-to-digital converters (ADC) set up in close succession. In that case, ^1H and ^{23}Na MR raw data acquisitions will be delayed only by a few milliseconds and can be considered quasi-simultaneous.

Further improvements of MNF to increase spatial resolution in all directions and reduce total scan time will include stack-of-spirals or 3D spiral (FLORET-type) k-space trajectories to increase SNR efficiency, combined with regularization-by-denoising (RED) implementation in the iterative image reconstruction process (19, 20) for increasing SNR furthermore, as well as deblurring the ^{23}Na data.

In conclusion, we developed the MNF method to generate seven whole-brain maps related to morphology (*i.e.* tissue structure from three ^1H MRF maps) and physiology (*i.e.* sodium homeostasis from four ^{23}Na MRF maps), all acquired simultaneously with exact co-registration, and identical spatial and temporal resolutions. Thus far, the MNF data can be acquired over the whole brain in 13 min at 7 T with a final spatial resolution of $1.5 \times 1.5 \times 5 \text{ mm}^3$. We expect that MNF could prove useful for two purposes: (1) as a clinical tool to monitor the evolution of brain pathologies and their responses to therapy, or (2) as a basic research imaging tool to study conjointly brain morphology and physiology *in vivo*, and their interaction in healthy brain or in pathologies. This proof-of-concept for MNF was first implemented in brain, but it can also be adapted to other parts of the body.

Methods

Hardware

The experiments were performed at 7 T (MAGNETOM, Siemens, Erlangen, Germany) using a 16-channel transmit/receive (8 ^1H channels and 8 ^{23}Na channels) dual-tuned $^1\text{H}/^{23}\text{Na}$ RF head coil developed in-house (12). The scanner was modified to allow simultaneous acquisition of both ^1H and ^{23}Na signals by inserting an external frequency generator in the RF cabinet of the system to demodulate the ^{23}Na signal with a proper local oscillator (13, 17).

Brain imaging protocol

MNF brain images were acquired on seven healthy volunteers (4 females, mean age = 27 ± 3 years) after informed consent, in accordance with the New York University Grossman School of Medicine institutional review board and national guidelines. All volunteers were scanned with the simultaneous 3D $^1\text{H}/^{23}\text{Na}$ MRF acquisition, and their ^{23}Na MNF LR maps were then post-processed with the super-resolution algorithm to generate ^{23}Na MNF HR maps that match the resolution of the ^1H MNF HR maps. In addition, two subjects (#5 and #6) participated in a second session where standard measurements of T_1 using multi-TR ^{23}Na FLORET saturation-recovery (SR) experiments, and of $T_{2,\text{short}}$ and $T_{2,\text{long}}$ using multi-TE ^{23}Na FLORET experiments, were acquired for comparison with the MNF results.

MNF data acquisition

Simultaneous 3D $^1\text{H}/^{23}\text{Na}$ MRF

We developed the new simultaneous 3D $^1\text{H}/^{23}\text{Na}$ MRF pulse sequence based on our previous work on simultaneous ^1H MRF/ ^{23}Na MRI with a stack-of-star k-space trajectory (13–15). It was optimized to generate low resolution (LR, $2.85 \times 2.85 \times 5 \text{ mm}^3$) ^{23}Na maps, and high resolution (HR, $1.5 \times 1.5 \times 5 \text{ mm}^3$) ^1H maps in the whole brain at 7 T in about 13 min. In this pulse sequence, the nuclear spins are sequentially excited every inter-pulse delay τ for ^1H , and every inter-pulse delay 2τ for ^{23}Na (delay between the start of each pulse), using non-selective RF pulses followed by one simultaneous ADC readout for both nuclei. The partition phase-encoding gradient moments were distributed such that images from both nuclei had the same slice thickness. The frequency-encoding gradient moments were distributed such that a full radial trajectory for ^1H and a center-out radial trajectory for ^{23}Na were obtained in k-space, leading to a ratio of approximately 1.9 for in-plane resolution between the ^1H and ^{23}Na images, which corresponds to half of the ratio of their respective gyromagnetic ratios (14). Fig. 5 shows a schematic diagram of the simultaneous 3D $^1\text{H}/^{23}\text{Na}$ MRF pulse sequence.

^1H RF pulse train

The ^1H 500-pulse train is the same as the one introduced by Yu. et al (14). It starts with an adiabatic inversion pulse (21), followed by 275 rectangular RF pulses with variable flip angle (FA) and constant pulse duration of 1 ms, distributed in different segments, and some extra delays between the segments (225 pulses with FA = 0°). All pulses are separated by a delay τ . This pulse train contains both fast imaging with steady precession (FISP) and fast low angle shot (FLASH) segments to help differentiate T_1 , T_2 , and B_1^+ effects (11). The first seg-

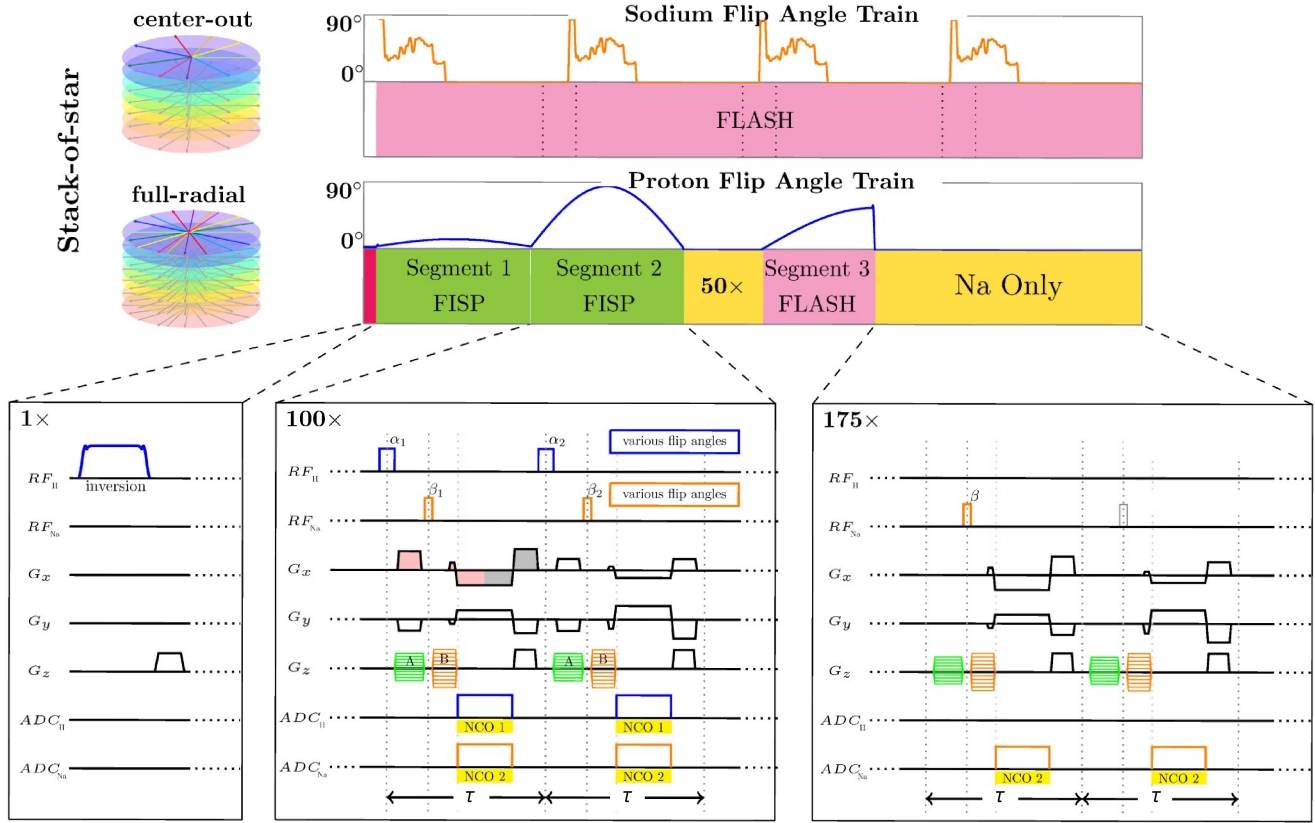


Figure 5. The simultaneous $^1\text{H}/^{23}\text{Na}$ MRF pulse sequence. Magnetic resonance fingerprinting (MRF) data is acquired simultaneously for proton (^1H) using a full-radial stack-of-stars k-space trajectory and for sodium (^{23}Na) using a center-out stack-of-stars trajectory. The ^1H flip angle (FA) train is made up of 500 RF pulses α applied every delay τ of 7.5 ms, and that includes 27 variable pulses (for data acquisition) and 225 pulses with FA = 0° (no data acquisition). The ^{23}Na FA train is made up of 22 variable RF pulses β applied every 2τ (with following pulses set to zero), applied 4 times per shot. Slice encoding gradients A (green) and B (orange) are used to encode the same slice for different nuclei. TR per shot was 3.75 s. *Abbreviations:* FISP = Fast Imaging with Steady-state Free Precession; FLASH = Fast Low Angle Shot; NCO N = Numerical Oscillator event N.

ment (FISP, pulses 1–100) includes flip angles up to 20° . The second segment (FISP, pulses 101–200) contains higher flip angles (up to 90°) to help encode T_2 . A $50\text{-}\tau$ delay corresponding to pulses 201–250 with FA = 0° was inserted to recover some magnetization before the third segment with flip angles up to 60° (FLASH, pulses 251–325), which was RF-spoiled to help encode B_1^+ . A final $175\text{-}\tau$ delay corresponding to pulses 326–500 with with FA = 0° was added at the end of the pulse train to allow T_1 recovery for the ^1H magnetization before the next inversion pulse and pulse train acquisition, resulting in a repetition time (TR) of 3.75 s per "shot" (one set of 275 data acquisitions from the 275-pulse variable train and including the 225-pulse train with FA = 0°).

^{23}Na RF pulse train

The ^{23}Na pulse train consists of 22 rectangular RF pulses of duration 0.6 ms and separated by a delay of 2τ . The 22 flip angles were optimized by a genetic algorithm to minimize the Pearson correlation coefficient between

signals of GM and WM matter based on the simulated signal evolution for ^{23}Na nuclear spins, and using average ^{23}Na relaxation times for GM and WM from the literature, similarly to the method described in O'Donnell et al. (22, 23). Note that in O'Donnell et al. (22, 23), a 23-pulse train was optimized for ^{23}Na MRF-only acquisition, and which included a composite $90^\circ\text{-}180^\circ\text{-}90^\circ$ inversion block at the beginning of the pulse train. After multiple experiments with the 23-pulse train, and in order to significantly reduce specific absorption rate (SAR) from our simultaneous $^1\text{H}/^{23}\text{Na}$ MRF sequence, we decided to remove the 180° RF pulse from the composite inversion block, and resimulate the ^{23}Na MRF dictionary with the resulting 22-pulse train. Modelization of the ^{23}Na nuclear spin $\frac{3}{2}$ dynamics under this 22-pulse train was performed using the irreducible spherical tensor operator (ISTO) formalism (5) in Matlab (The MathWorks Inc, Natick, MA, USA). The resulting 22 ^{23}Na FA excitations were: $90^\circ, 90^\circ, 39^\circ, 32^\circ, 35^\circ, 38^\circ, 35^\circ, 49^\circ, 42^\circ, 52^\circ, 62^\circ, 45^\circ, 61^\circ, 63^\circ, 60^\circ, 55^\circ, 52^\circ, 53^\circ, 30^\circ, 27^\circ, 27^\circ, 28^\circ$.

All RF pulse phases were equal to zero. A final delay of 600 ms was then applied at the end of the pulse train to allow full T_1 recovery for the ^{23}Na magnetization before the next pulse train acquisition, and such that this ^{23}Na pulse train can be applied 4 times per shot ($\text{TR} = 3.75$ s).

Acquisition parameters

The simultaneous 3D $^1\text{H}/^{23}\text{Na}$ MRF data was acquired in brain with the following parameters: Field-of-view (FOV) = $240 \times 240 \times 175$ mm³, in-plane sagittal resolution = 1.5×1.5 mm² for ^1H and 2.85×2.85 mm² for ^{23}Na , inter-pulse delay $\tau = 7.5$ ms for ^1H and $2\tau = 15$ ms for ^{23}Na , echo time (TE) = 2 ms for ^1H and 1.2 ms for ^{23}Na , 1 slab of 35 slices, sagittal slice thickness = 5 mm for both ^1H and ^{23}Na , 3 shots per slab, $\text{TR} = 3.75$ s/shot, 2 acquisitions averaged together, total scan time = 13 min.

MNF data reconstruction

^1H MRF

Image reconstruction: For the ^1H MRF data, all individual images acquired after each RF pulse were reconstructed using conjugate gradient sensitivity encoding (CG-SENSE) (24) to reduce the radial artifacts. The radial samples from the 275 data acquisitions were reconstructed with an 11-acquisition sliding window (25). In total, 265 image frames were therefore reconstructed by sliding this 11-acquisition window in increments of 1 acquisition. The fingerprint dictionary was grouped and averaged with the same sliding window as the CG-SENSE reconstruction along the time domain (11).

Fingerprint dictionary: The ^1H fingerprint dictionary was computed using the extended phase graph formalism (11, 26) implemented in C++, with different step sizes: T_1 ranged from 150 to 4347 ms, and T_2 ranged from 15 to 435 ms, both incremented in steps of 5%; B_1^+ ranged from 10° to 130° , in steps of 1° (14).

Matching: Matching between the acquired signal and the fingerprint dictionary was performed voxel by voxel. The final T_1 , T_2 and B_1^+ maps were obtained from the maximum correlation between the dictionary and pixel signal evolution, where the correlation was defined as the matrix product between them (14).

^{23}Na MRF

Image reconstruction: For ^{23}Na MRF, all individual images acquired after each RF pulse were reconstructed using compressed-sensing (CS) using total-generalized-variation regularization to maximize SNR and minimize radial artifacts (27). As the radial spokes were acquired with golden angle increment, the radial samples from the 4 pulse trains from each shot were reconstructed altogether. The radial samples from 22 acquisitions per

pulse train were reconstructed with a 5-acquisition circular sliding window to increase SNR. In total, 22 image frames were then reconstructed by sliding this window in increments of 1 acquisition. The fingerprint dictionary was grouped and averaged with the same sliding window as the CS reconstruction (11).

Fingerprint dictionary: The spin $\frac{3}{2}$ dynamics simulation to generate the ^{23}Na fingerprint dictionary was performed in Matlab R2020b. Signals were simulated starting from thermal equilibrium and propagated under the optimized 22-pulse train using the irreducible spherical tensor operators (ISTO) framework (5, 23, 28). Parameter ranges to build the dictionary were T_1 from 20 ms to 74 ms (steps of 2 ms), $T_{2,\text{long}}$ from 10 ms to 66 ms (steps of 2 ms), $T_{2,\text{short}}$ from 0.5 to 66 ms (steps of 0.5 ms for $T_{2,\text{short}}$ from 0.5 to 2 ms, then steps of 2 ms), ΔB_1^+ factor from 0.7 to 1.3 (applied as a multiplying factor to the RF amplitude, steps of 0.1), and Δf_0 from -60 Hz to 60 Hz (steps of 10 Hz). Parameter combinations where $T_{2,\text{long}} > T_1$ and $T_{2,\text{short}} > T_{2,\text{long}}$ were omitted from the computation.

Matching: Matching between the acquired signal and the fingerprint dictionary was performed voxel by voxel. The brain was first segmented into two compartments (WM+GM and EYE+CSF) using the masks from the segmentation processing described in section "Brain segmentation" below. For EYE+CSF, the following matching constraints were implemented: T_1 in range [49-74] ms, $T_{2,\text{long}}$ in range [42-66] ms and $T_{2,\text{short}} = T_{2,\text{long}} \equiv T_2$. For GM+WM, T_1 was in range [20-48] ms, $T_{2,\text{long}}$ in range [10-40] ms and $T_{2,\text{short}}$ in range [0.5-20] ms. These ranges were chosen in accordance with the expected values in these tissues from the literature (23). The fingerprint dictionary (size = 113,880 entries for GM+WM and 5,187 for EYE+CSF) was matched voxelwise to the ^{23}Na signals using Pearson correlation.

Correlation weighting: Because of the dictionary size and due to the low intrinsic SNR of the ^{23}Na images, and thus noisy ^{23}Na signal evolution over the ^{23}Na RF pulse train, it was therefore possible that more than fingerprint could generate a high correlation for a single voxel signal evolution. To account for this and to increase robustness of the matching process, we included matches for a subset of the top correlation coefficients for each voxel v , and constructed the final ^{23}Na LR maps by calculating the correlation-weighted parameter X_v from the dictionary of values $X_{v,i}$, and corresponding to the matching correlation coefficient $W_{v,i}$ according to (23):

$$X_v = \frac{\sum_{i=1}^k W_{v,i} X_{v,i}}{\sum_{i=1}^k W_{v,i}}, \quad (1)$$

where k was the maximum number of correlation coefficients used for weighting, and X_v and $X_{v,i}$ correspond to the metrics T_1 , $T_{2,\text{short}}$, $T_{2,\text{long}}$, ΔB_1^+ factor or Δf_0 .

The number k of highest correlation coefficients used for the weighting was determined empirically considering the number of dictionary entries and the SNR of the ^{23}Na data, after testing a wide range of values for k ($k = 1$ to 1,000), and chosen to be $k = 50$ for EYE+CSF ($\sim 1\%$ of the total number of correlation coefficients calculated from all dictionary entries for these tissues) and $k = 500$ for GM+WM ($\sim 0.5\%$ of the total number of correlation coefficients calculated from all dictionary entries for these tissues).

Brain segmentation

The MNF brain data from each volunteer was segmented into four ROIs using SMP12 (UCL, London, UK) in Matlab (29): vitreous humor from the eyes (EYE), grey matter (GM), white matter (WM), and cerebrospinal fluid (CSF). Tissue segmentation was performed using the PD, T_1 , and T_2 maps from the ^1H MNF HR data as input images. Note that SPM12 generate five probability maps by default: GM, WM, CSF, SKULL, and OTHER tissues excluding the eyes. The eye segmentation was generated by calculating $\text{EYE} = 1 - [\text{CSF} + \text{GM} + \text{WM} + \text{SKULL} + \text{OTHER}]$ probabilities. The EYE, GM, WM and CSF probability maps were then normalized and binarized with a threshold of 0.90 to minimize the number of voxels with multiple tissue components to generate non-overlapping EYE, GM, WM, and CSF HR masks. LR masks were also calculated by resizing the HR masks in Matlab using the function *imresize3* with *nearest* option.

PD and TSC quantification

Proton density (PD): Initial non-normalized PD maps were calculated voxelwise as the mean value of the division between the signal evolution and the optimal fingerprint from dictionary matching. The bias field from these initial maps was corrected by bias regularization in SPM12 (29, 30) during the segmentation process for generating different tissues masks. The resulting images were then normalized by the mean value measured in the vitreous humor of the eyes, accounting for a reference PD in the eyes of 0.98 (31, 32) to generate truly quantitative final PD maps in the brain. In order to make the final PD measurements more accurate and more robust against potential local map inhomogeneities with the reference ROI, as well as PVE from the edges of the reference ROI, PD quantification was performed 20 times by using the mean reference value from only the N_{REF} % highest voxel values of the reference ROI (EYE), with $N_{\text{REF}} = 5\%$ to 100% by steps of 5% (20 N_{REF} values). The mean PD values over these 20

PD maps can then be measured, as explained in more details in subsection "Statistical analysis".

Tissue sodium concentration (TSC): Multiple sodium density (SD) maps were first calculated as the mean value of the division between the absolute value of the ^{23}Na signal evolution for each voxel v and the k optimal fingerprints from dictionary matching. Correlation-weighting was then performed according to Equation 1, where $X_{v,i}$ was the unweighted SD and W_v was the weighted SD. The resulting correlation-weighted SD map was then corrected for B_1^- inhomogeneities (coil sensitivities) (33): The map was divided by the normalized magnitude ^{23}Na image of a uniform phantom previously acquired with the same RF coil. The phantom was a PET screw cap bottle with diameter = 28 cm, height = 50 cm, and volume = 22.7 L (which filled most of the coil volume), and filled with an aqueous solution with 150 mM NaCl. The phantom uniform image was acquired with FLORET with the following parameters: 4 acquisitions averaged together, FOV = 320 mm isotropic, resolution = 10 mm isotropic, TE = 1 ms, TR = 100 ms, 32 averages/acquisition, 3 hubs at 45° , 100 interleaves/hub, flip angle = 80° , RF pulse duration = 2000 μs , total acquisition time = 16 min/acquisition. All 4 complex images were reconstructed as described in section " ^{23}Na FLORET data reconstruction", and averaged together. The magnitude of the final averaged phantom image was then normalized by its maximum value, and its inverse image was used to correct the brain SD map.

The B_1^- -corrected SD map was then normalized by the mean value over the vitreous humor of the eyes from the EYE mask (accounting for a water content of 0.98) and then multiplied by a reference TSC value for the eyes of 145 mM (34–36) to generate the TSC map. Similarly to PD, in order to make the final TSC measurements more accurate and more robust against potential local map inhomogeneities with the reference ROI, as well as PVE from the edges of the reference ROI, TSC quantification was performed 20 times by using the mean reference value from the N_{REF} % highest voxel values of the reference ROI (EYE), with $N_{\text{REF}} = 5\%$ to 100% by steps of 5% (20 N_{REF} values). The mean TSC values over these 20 TSC maps can then be measured, as explained in more details in subsection "Statistical analysis".

Super-resolution (SR) post-processing

Finally, a super-resolution algorithm based on partial least square (PLS) regression (9, 16) between the ^1H HR maps and the ^{23}Na LR maps acquired with simultaneous $^1\text{H}/^{23}\text{Na}$ MRF was applied to generate ^{23}Na HR maps with the same resolution as the ^1H HR maps. The algorithm is described in details in Rodriguez et al. (9), and was simply adapted here to operate with all seven maps

as inputs (3 HR ^1H maps + 4 LR ^{23}Na maps), instead of four images (3 HR ^1H maps + 1 LR ^{23}Na image). In summary, the goal of the algorithm is to link all ^{23}Na metrics from the LR maps to a combination of ^1H -based metrics from the HR maps by modeling the distribution of co-registered measurements from both types of images using PLS regression. An iterative loop, including deconvolution/convolution with point spread functions and image resizing between LR and HR with a fast Fourier transform approach, were included in the algorithm to generate the final HR ^{23}Na maps without losing features from the LR ^{23}Na maps. The average processing time was 5.1 s per slice on a computer with 6-core CPU, 3.4 GHz, 32 GB RAM. The output for this SR postprocessing was four ^{23}Na HR maps.

^{23}Na FLORET data acquisition

Acquisition parameters

For comparison with MNF results, ^{23}Na data was also acquired in two subjects (#5 and #6) in different scanning sessions, with the Fermat looped, orthogonally encoded trajectories (FLORET) sequence (37) with the following parameters: 3 hubs at 45° with 240 interleaves per hub, with different TR and TE values for relaxation fitting (see below), 4 averages, 3.75 mm isotropic resolution, FOV = $240 \times 240 \times 240 \text{ mm}^3$, 64 slices, rectangular RF excitation pulses with FA = 90° and pulse duration = 0.8 ms.

Multi-TR acquisitions

We measured ^{23}Na T_1 using a multi-TR saturation recovery reference experiment that consisted of a series of five FLORET scans with different TR = [50, 80, 140, 200, 400] ms and fixed TE = 1 ms. Respective times of acquisition (TA) were [2:24, 3:50, 6:43, 9:36, 19:12] min.

Multi-TE acquisitions

We measured ^{23}Na $T_{2,\text{short}}$ and $T_{2,\text{long}}$ using a multi-TE reference experiment that consisted of a series of nine FLORET scans with different TE = [0.1, 0.5, 1, 2, 5, 10, 20, 50, 90] ms, fixed TR = 200 ms, and TA = 9:36 min for each acquisition.

MPRAGE for brain segmentation

During the ^{23}Na FLORET scanning session, an additional ^1H Magnetization-Prepared Rapid Gradient Echo (MPRAGE) image was acquired with the following parameters: TR = 2300 ms, TE = 2.77 ms, FOV = $240 \times 240 \text{ mm}^2$, slice thickness = 1 mm, 176 slices/slab, GRAPPA acceleration factor 2, 1 average, total acquisition time = 3:33 min.

^{23}Na FLORET data reconstruction

Image reconstruction

For each channel, the raw k-space data was filtered with a Hamming kernel and then reconstructed using standard gridding (37, 38) after sampling density compensation (39). The images from the 8 channels were combined using image-based coil sensitivity profiles as described by Bydder et al. (40).

Brain segmentation

Brain segmentation was processed in Matlab with SPM12 as for the MNF data, but from the MPRAGE data acquired along the ^{23}Na FLORET data, to generate four ROIs (masks): EYE, CSF, GM and WM. These masks were then applied to the ^{23}Na FLORET data to quantify mean and standard deviation values of TSC, T_1 , $T_{2,\text{long}}$ and $T_{2,\text{short}}$ for comparison with the MNF data

T_1 fitting

For T_1 mapping, a mono-exponential fitting was performed voxelwise on the multi-TR FLORET data using the *fit* function in Matlab (Curve Fitting Toolbox) with a nonlinear least square method. The fitting function was $S_v(\text{TR}) = \alpha(1 - e^{-\text{TR}/T_1}) + \beta$, with S_v the magnitude of ^{23}Na signal evolution in voxel v at different TRs, α and β fitting variables to adjust data magnitude and baseline offset, respectively. Using the masks from the MPRAGE brain segmentation, T_1 ranges were defined as [49-74] ms for EYE+CSF, and [20-48] ms for GM+WM. These ranges times were chosen to coincide with the ranges used for ^{23}Na MRF dictionary matching.

$T_{2,\text{short}}$ and $T_{2,\text{long}}$ fitting

For $T_{2,\text{short}}$ and $T_{2,\text{long}}$ mapping, a bi-exponential fitting was performed voxelwise on the multi-TE FLORET data using the *fit* function in Matlab (Curve Fitting Toolbox) with a nonlinear least square method. The fitting function was $S_v(\text{TE}) = \alpha e^{-\text{TE}/T_{2,\text{short}}} + (1 - \alpha)e^{-\text{TE}/T_{2,\text{long}}} + \beta$, with S_v the magnitude of ^{23}Na signal evolution in voxel v at different TEs, α and β fitting variables to adjust data magnitude related to the bi-exponential components and baseline offset, respectively. Using the masks from the MPRAGE brain segmentation, $T_{2,\text{short}}$ and $T_{2,\text{long}}$ were forced to be equal to mono-exponential T_2 for EYE+CSF (vitreous humor and liquids) in range [49-74] ms. For GM+WM, $T_{2,\text{short}}$ and $T_{2,\text{long}}$ ranges were defined as [0.5-20] and [10-40], respectively. These ranges times were chosen to coincide with the ranges used for ^{23}Na MRF dictionary matching.

TSC quantification: The ^{23}Na FLORET image with shorter TE = 0.1 ms and longer TR = 200 ms was used to quantify TSC with the same process as for the MNF

data: B_1 correction, normalization, and quantification from the EYE reference. See section "MNF data reconstruction\Tissue sodium concentration (TSC)".

Statistical analysis

Data types to analyze

In summary, data types to be analyzed after simultaneous $^1\text{H}/^{23}\text{Na}$ MRF acquisition and SR post-processing have been performed (where $\text{MNF} = ^1\text{H}/^{23}\text{Na}$ MRF + SR) were denominated as follows:

- 4 datasets: ^1H MNF HR (from ^1H MRF), ^{23}Na MNF LR (from ^{23}Na MRF), ^{23}Na MNF HR (from ^{23}Na MRF + SR), and ^{23}Na FLORET.
- 4 ROIs: EYE, CSE, GM, and WM.
- 7 metrics: PD, T_1 and T_2 from ^1H MNF HR, and TSC, T_1 , $T_{2,\text{short}}$ and $T_{2,\text{long}}$ from ^{23}Na MNF LR, ^{23}Na MNF HR and ^{23}Na FLORET.

Data measurements to analyze

Measurements from all ROIs, datasets and metrics described above consist of:

- Reference measurements for both PD and TSC quantification were performed 20 times using the $N_{\text{REF}}\%$ highest voxel values of the reference ROI (EYE) for both metric, with $N_{\text{REF}} = 5\%$ to 100% by steps of 5% (20 N_{REF} values).
- ROI measurements of the mean and standard deviation (std) values of all MNF and ^{23}Na FLORET metrics were performed 20 times in each ROI using the $N_{\text{ROI}}\%$ highest voxel values of the ROI, with $N_{\text{ROI}} = 5\%$ to 100% by steps of 5% (20 N_{ROI} values). The ROI measurements therefore consist of distributions of:
 - $N = 400$ mean PD and TSC values measured in all ROIs in each subject, from 20 $N_{\text{ROI}} \times 20 N_{\text{REF}}$ values.
 - $N = 20$ mean ^1H and ^{23}Na relaxation times values measured in all ROIs in each subject, from 20 N_{ROI} values.

Mean & standard deviation

The mean and std values of each distribution of *mean* values for each metric in each ROI were calculated using three statistical methods, and according to the two following steps:

Step 1: Final mean \pm std for each subject. For each metric and each ROI, we measured the final mean and std using the standard statistical method, jackknife resampling and bootstrap resampling methods. Jackknife and bootstrap resampling are usually used to reduce bias and variance in the estimation of statistical parameters (mean and std in our case).

1. **Standard:** The standard mean \pm std was calculated over all mean values in each dataset (or distribution) of size $N = 20$ or 400 (depending on the metric), resulting in a *final mean* and *std*.
2. **Jackknife:** Jackknife resampling (41, 42) consisted of the following two steps for each subject:
 - (a) Calculate the mean value of each possible leave-one-out subsample of size $(N - 1)$ of the full dataset of size $N = 20$ or 400 mean values (depending on the metric), resulting in a new dataset of N mean values from N subsamples.
 - (b) Calculate the *final mean* and *std* of this new dataset of N mean values from N subsamples.
3. **Bootstrap:** Bootstrap resampling (or bootstrapping) with replacement (41, 42) consisted of the following four steps for each subject:
 - (a) Randomly and separately select N values from the full dataset of size $N = 20$ or 400 mean values (depending on the metric)—which means that some values can be selected multiple times, hence the term "replacement"—to generate a new dataset of N mean values (1 bootstrap).
 - (b) Calculate the mean value of this new bootstrap dataset of N values.
 - (c) Repeat steps (a) and (b) $N_{\text{btsp}} = 1000$ times.
 - (d) Calculate the *final mean* and *std* of the N_{btsp} mean values for each subject.

Step 2: Overall mean \pm std over all subjects. For each method, the *overall mean* \pm one std of both the *final mean* values and the *final std* values from each subject was calculated over all subjects.

Wilcoxon rank-sum test

The Wilcoxon rank-sum statistical test was applied between the *final mean* values from the *standard* method between all metrics from ^{23}Na MNF HR, LR and FLORET over all subjects in each ROI. Bonferroni correction (BC) was applied to the p values in order to take into account the number of tests ($N_{\text{meas}} = 3$) of each metric for each tissue: $p_{\text{BC}} = N_{\text{meas}} \cdot p$. Statistically significant differences between measurements, without and with BC, were therefore defined as p and $p_{\text{BC}} \leq 0.05$.

Data and Code Availability

Simultaneous $^1\text{H}/^{23}\text{Na}$ MRF sequence: The binary files and/or C++ code of the Siemens IDEA sequence (VB17A) and the MATLAB code for image reconstruction are available upon request to the corresponding author, within the Siemens C2P framework

Super-resolution algorithm: The MATLAB code of the SR algorithm (9) is freely available on Github at the following address: <https://github.com/gonggr/Super-Resolution-Sodium-MRI>.

MNF data and statistical analysis: The MNF and FLORET brain data, and the MATLAB code used for statistical analysis and for generating all the histograms and boxplots shown in Supplementary Information and in the main article, are freely available on the UltraViolet repository of New York University at the following address: <https://doi.org/10.58153/m8qj0-v1936>.

Acknowledgements

The authors want to thank Liz Aguilera for recruiting the subjects.

Author Contributions

G.M. and M.C. conceived, designed and supervised the study. M.C. and Z.Y. designed and wrote the pulse sequence code for the Siemens MR scanner, and contributed to the design and optimization of the RF pulse train for ^1H MRF. L.O., G.G.R. and G.M. contributed to the design and optimization of the RF pulse train for ^{23}Na MRF. G.G.R. and G.M. contributed to the design and optimization of the super-resolution algorithm, and design of the experiments. G.G.R. carried out the experiments. G.M. wrote the manuscript, and all authors contributed to revisions of the manuscript.

Funding

This project was supported by grant R01EB026456 from the National Institute of Biomedical Imaging and Bioengineering (NIBIB) at National Institutes of Health (NIH), and was also performed under the rubric of the Center for Advanced Imaging Innovation and Research (CAI2R), a NIBIB Biomedical Technology Resource Center (P41EB017183).

Competing interests

The authors declare no competing interests.

Supplementary Information

Supplementary information is available for this article in Appendix.

References

1. Erecinska, M. & Silver, I. A. Ions and energy in mammalian brain. *Progress in Neurobiology* **43**, 37–71 (1994).
2. Lodish, H. *et al.* *Molecular Cell Biology* (WH Freeman, 2000).
3. Ames III, A. CNS energy metabolism as related to function. *Brain Research Reviews* **34**, 42–68 (2000).
4. Madelin, G. *X-Nuclei Magnetic Resonance Imaging* (Jenny Stanford Publishing; 1st edition (March 15, 2022) & CRC Press, Singapore, 2022).
5. Madelin, G., Lee, J.-S., Regatte, R. R. & Jerschow, A. Sodium MRI: Methods and applications. *Progress in Nuclear Magnetic Resonance Spectroscopy* **79**, 14–47 (2014).
6. Gast, L. V., Platt, T., Nagel, A. M. & Gerhalter, T. Recent technical developments and clinical research-applications of sodium (^{23}Na) MRI. *Progress in Nuclear Magnetic Resonance Spectroscopy* **138–139**, 51 (2023).
7. Song, Y., Yin, Y., Chen, Q., Marchetti, A. & Kong, X. ^{23}Na relaxometry: An overview of theory and applications. *Magnetic Resonance Letters* **3**, 150–174 (2023).
8. Madelin, G. & Regatte, R. R. Biomedical applications of sodium MRI in vivo. *Journal of Magnetic Resonance Imaging* **38**, 511–529 (2013).
9. Rodriguez, G. G. *et al.* Super-resolution of sodium images from simultaneous ^1H MRF/ ^{23}Na MRI acquisition. *NMR in Biomedicine* e4959 (2023).
10. Ma, D. *et al.* Magnetic resonance fingerprinting. *Nature* **495**, 187–192 (2013).
11. Cloos, M. A. *et al.* Multiparametric imaging with heterogeneous radiofrequency fields. *Nature Communications* **7**, 12445 (2016).
12. Wang, B. *et al.* A radially interleaved sodium and proton coil array for brain MRI at 7 T. *NMR in Biomedicine* **34**, e4608 (2021).
13. Yu, Z., Madelin, G., Sodickson, D. K. & Cloos, M. A. Simultaneous proton magnetic resonance fingerprinting and sodium MRI. *Magnetic Resonance in Medicine* **83**, 2232–2242 (2020).
14. Yu, Z. *et al.* Simultaneous 3D acquisition of ^1H MRF and ^{23}Na MRI. *Magnetic Resonance in Medicine* **87**, 2299–2312 (2022).
15. Rodriguez, G. G. *et al.* Repeatability of simultaneous 3D ^1H MRF/ ^{23}Na MRI in brain at 7 T. *Scientific Reports* **12**, 14156 (2022).
16. Van de Plas, R., Yang, J., Spraggins, J. & Caprioli, R. M. Image fusion of mass spectrometry and microscopy: A multimodality paradigm for molecular tissue mapping. *Nature Methods* **12**, 366–372 (2015).
17. Meyerspeer, M. *et al.* Simultaneous and interleaved acquisition of NMR signals from different nuclei with a clinical MRI scanner. *Magnetic Resonance in Medicine* **76**, 1636–1641 (2016).
18. Lopez Kolkovsky, A. L., Carlier, P. G., Marty, B. & Meyerspeer, M. Interleaved and simultaneous multi-nuclear magnetic resonance in vivo. Review of principles, applications and potential. *NMR in Biomedicine* **35**, e4735 (2022).
19. Romano, Y., Elad, M. & Milanfar, P. The little engine that could: Regularization by denoising (RED). *SIAM Journal on*

- Imaging Sciences* **10**, 1804–1844 (2017).
20. Qiusheng, L., Xiaoyu, F., Baoshun, S. & Xiaohua, Z. Compressed sensing MRI based on the hybrid regularization by denoising and the epigraph projection. *Signal Processing* **170**, 107444 (2020).
 21. Ordidge, R. J., Wylezinska, M., Hugg, J. W., Butterworth, E. & Franconi, F. Frequency offset corrected inversion (FOCI) pulses for use in localized spectroscopy. *Magnetic Resonance in Medicine* **36**, 562–566 (1996).
 22. O'Donnell, L. *et al.* Mapping sodium relaxation parameters in brain using magnetic resonance fingerprinting at 7T. In *Proceedings of the Annual Meeting of the ISMRM*, 3306 (2023).
 23. O'Donnell, L. F. *et al.* Correlation-weighted ^{23}Na magnetic resonance fingerprinting in the brain. *NMR in Biomedicine* **38**, e70150 (2025).
 24. Pruessmann, K. P., Weiger, M., Börnert, P. & Boesiger, P. Advances in sensitivity encoding with arbitrary k-space trajectories. *Magnetic Resonance in Medicine* **46**, 638–651 (2001).
 25. Cao, X. *et al.* Robust sliding-window reconstruction for accelerating the acquisition of MR fingerprinting. *Magnetic Resonance in Medicine* **78**, 1579–1588 (2017).
 26. Weigel, M. Extended phase graphs: dephasing, RF pulses, and echoes-pure and simple. *Journal of Magnetic Resonance Imaging* **41**, 266–295 (2015).
 27. Knoll, F., Bredies, K., Pock, T. & Stollberger, R. Second order total generalized variation (TGV) for MRI. *Magnetic Resonance in Medicine* **65**, 480–491 (2011).
 28. Kratzer, F. J. *et al.* 3D sodium (^{23}Na) magnetic resonance fingerprinting for time-efficient relaxometric mapping. *Magnetic Resonance in Medicine* **86**, 2412–2425 (2021).
 29. Ashburner, J. *et al.* SPM12 manual. *Wellcome Trust Centre for Neuroimaging, London, UK* **2464** (2014).
 30. Ashburner, J. & Ridgway, G. R. Symmetric diffeomorphic modeling of longitudinal structural MRI. *Frontiers in Neuroscience* **6**, 197 (2013).
 31. Chau, F. Y. *et al.* Osteogenesis imperfecta and the eye. In *Osteogenesis Imperfecta*, 289–303 (Elsevier, 2014).
 32. Forrester, J. V., Dick, A. D., McMenemy, P. G., Roberts, F. & Pearlman, E. *The eye: basic sciences in practice* (Elsevier Health Sciences, 2015).
 33. Axel, L., Costantini, J. & Listerud, J. Intensity correction in surface-coil MR imaging. *American Journal of Roentgenology* **148**, 418–420 (1987).
 34. Kokavec, J. *et al.* Biochemical analysis of the living human vitreous. *Clinical & Experimental Ophthalmology* **44**, 597–609 (2016).
 35. Winkler, S. S., Thomasson, D. M., Sherwood, K. & Perman, W. H. Regional T2 and sodium concentration estimates in the normal human brain by sodium-23 MR imaging at 1.5 T. *Journal of Computer Assisted Tomography* **13**, 561–566 (1989).
 36. Adlung, A. *et al.* Quantification of tissue sodium concentration in the ischemic stroke: A comparison between external and internal references for ^{23}Na MRI. *Journal of Neuroscience Methods* **382**, 109721 (2022).
 37. Pipe, J. G. *et al.* A new design and rationale for 3D orthogonally oversampled k-space trajectories. *Magnetic Resonance in Medicine* **66**, 1303–1311 (2011).
 38. Fessler, J. A. On NUFFT-based gridding for non-Cartesian MRI. *Journal of Magnetic Resonance* **188**, 191–195 (2007).
 39. Pipe, J. G. & Menon, P. Sampling density compensation in MRI: rationale and an iterative numerical solution. *Magnetic Resonance in Medicine* **41**, 179–186 (1999).
 40. Bydder, M., Larkman, D. J. & Hajnal, J. V. Combination of signals from array coils using image-based estimation of coil sensitivity profiles. *Magnetic Resonance in Medicine* **47**, 539–548 (2002).
 41. Shao, J. & Tu, D. *The jackknife and bootstrap* (Springer Science & Business Media, 2012).
 42. Efron, B. *The jackknife, the bootstrap and other resampling plans* (SIAM, 1982).
 43. Koolstra, K., Beenakker, J.-W. M., Koken, P., Webb, A. & Börnert, P. Cartesian MR fingerprinting in the eye at 7T using compressed sensing and matrix completion-based reconstructions. *Magnetic Resonance in Medicine* **81**, 2551–2565 (2019).
 44. Richdale, K. *et al.* 7 Tesla MR imaging of the human eye in vivo. *Journal of Magnetic Resonance Imaging* **30**, 924–932 (2009).
 45. Rooney, W. D. *et al.* Magnetic field and tissue dependencies of human brain longitudinal $^1\text{H}_2\text{O}$ relaxation in vivo. *Magnetic Resonance in Medicine* **57**, 308–318 (2007).
 46. Marques, J. P. *et al.* MP2RAGE, a self bias-field corrected sequence for improved segmentation and T₁-mapping at high field. *NeuroImage* **49**, 1271–1281 (2010).
 47. Wright, P. *et al.* Water proton T₁ measurements in brain tissue at 7, 3, and 1.5 T using IR-EPI, IR-TSE, and MPRAGE: results and optimization. *Magnetic Resonance Materials in Physics, Biology and Medicine* **21**, 121–130 (2008).
 48. Caan, M. W. *et al.* MP2RAGEME: T₁, T₂^{*}, and QSM mapping in one sequence at 7 tesla. *Human Brain Mapping* **40**, 1786–1798 (2019).
 49. Dieringer, M. A. *et al.* Rapid parametric mapping of the longitudinal relaxation time T₁ using two-dimensional variable flip angle magnetic resonance imaging at 1.5 Tesla, 3 Tesla, and 7 Tesla. *PLoS One* **9**, e91318 (2014).
 50. Leroi, L. *et al.* Simultaneous proton density, T₁, T₂, and flip-angle mapping of the brain at 7 T using multiparametric 3D SSFP imaging and parallel-transmission universal pulses. *Magnetic Resonance in Medicine* **84**, 3286–3299 (2020).
 51. Emmerich, J. *et al.* Rapid and accurate dictionary-based T2 mapping from multi-echo turbo spin echo data at 7 Tesla. *Journal of Magnetic Resonance Imaging* **49**, 1253–1262 (2019).
 52. Sabati, M. & Maudsley, A. A. Fast and high-resolution quantitative mapping of tissue water content with full brain coverage for clinically-driven studies. *Magnetic Resonance Imaging* **31**, 1752–1759 (2013).
 53. Neeb, H., Ermer, V., Stocker, T. & Shah, N. J. Fast quantitative mapping of absolute water content with full brain coverage. *NeuroImage* **42**, 1094–1109 (2008).
 54. Abbas, Z., Gras, V., Möllenhoff, K., Oros-Peusquens, A.-M. & Shah, N. J. Quantitative water content mapping at clinically relevant field strengths: a comparative study at 1.5 T and 3 T. *NeuroImage* **106**, 404–413 (2015).
 55. Volz, S., Nöth, U. & Deichmann, R. Correction of system-

- atic errors in quantitative proton density mapping. *Magnetic Resonance in Medicine* **68**, 74–85 (2012).
56. Mezer, A., Rokem, A., Berman, S., Hastie, T. & Wandell, B. A. Evaluating quantitative proton-density-mapping methods. Tech. Rep., Wiley Online Library (2016).
 57. Tofts, P. S. PD: Proton density of tissue water. *Quantitative MRI of the brain: Measuring changes caused by disease* 83–109 (2003).
 58. Shah, N. J., Abbas, Z., Ridder, D., Zimmermann, M. & Oros-Peusquens, A.-M. A novel MRI-based quantitative water content atlas of the human brain. *NeuroImage* **252**, 119014 (2022).
 59. Mirkes, C. C., Hoffmann, J., Shajan, G., Pohmann, R. & Scheffler, K. High-resolution quantitative sodium imaging at 9.4 Tesla. *Magnetic Resonance in Medicine* **73**, 342–351 (2015).
 60. Worthoff, W. A., Shymanskaya, A. & Shah, N. J. Relaxometry and quantification in simultaneously acquired single and triple quantum filtered sodium MRI. *Magnetic Resonance in Medicine* **81**, 303–315 (2019).
 61. Kolodny, N. *et al.* A feasibility study of ^{23}Na magnetic resonance imaging of human and rabbit vitreal disorders. *Investigative Ophthalmology & Visual Science* **34**, 1917–1922 (1993).
 62. Kohler, S. J. *et al.* Magnetic resonance imaging determination of ^{23}Na visibility and T_2^* in the vitreous body. *Journal of Magnetic Resonance* **82**, 505–517 (1989).
 63. Pettegrew, J. W., Glonek, T., Minshew, N. J. & Woessner, D. E. Sodium-23 NMR of intact bovine lens and vitreous humor. *Journal of Magnetic Resonance* **63**, 439–444 (1985).
 64. Kratzer, F. J. *et al.* Sodium relaxometry using ^{23}Na MR fingerprinting: A proof of concept. *Magnetic Resonance in Medicine* **84**, 2577–2591 (2020).
 65. Lommen, J. M. *et al.* Probing the microscopic environment of ^{23}Na ions in brain tissue by MRI: on the accuracy of different sampling schemes for the determination of rapid, biexponential decay at low signal-to-noise ratio. *Magnetic Resonance in Medicine* **80**, 571–584 (2018).
 66. Fleysher, L., Oesingmann, N., Stoeckel, B., Grossman, R. I. & Inglese, M. Sodium long-component T_2^* mapping in human brain at 7 Tesla. *Magnetic Resonance in Medicine* **62**, 1338–1341 (2009).
 67. Blunck, Y. *et al.* 3D-multi-echo radial imaging of ^{23}Na (3D-MERINA) for time-efficient multi-parameter tissue compartment mapping. *Magnetic Resonance in Medicine* **79**, 1950–1961 (2018).
 68. Niesporek, S. C. *et al.* Improved T_2^* determination in ^{23}Na , ^{35}Cl , and ^{17}O MRI using iterative partial volume correction based on ^1H MRI segmentation. *Magnetic Resonance Materials in Physics, Biology and Medicine* **30**, 519–536 (2017).
 69. Riemer, F., Solanky, B. S., Wheeler-Kingshott, C. A. & Golay, X. Bi-exponential ^{23}Na T_2^* component analysis in the human brain. *NMR in Biomedicine* **31**, e3899 (2018).
 70. Ridley, B. *et al.* Distribution of brain sodium long and short relaxation times and concentrations: a multi-echo ultra-high field ^{23}Na MRI study. *Scientific Reports* **8**, 4357 (2018).
 71. Ridley, B., Morsillo, F., Zaaaraoui, W. & Nonino, F. Variability by region and method in human brain sodium concentrations estimated by ^{23}Na magnetic resonance imaging: A meta-analysis. *Scientific Reports* **13**, 3222 (2023).
 72. Gilles, A., Nagel, A. M. & Madelin, G. Multipulse sodium magnetic resonance imaging for multicompartiment quantification: Proof-of-concept. *Scientific Reports* **7**, 17435 (2017).
 73. Inglese, M. *et al.* Brain tissue sodium concentration in multiple sclerosis: a sodium imaging study at 3 tesla. *Brain* **133**, 847–857 (2010).
 74. Gerhalter, T. *et al.* Global decrease in brain sodium concentration after mild traumatic brain injury. *Brain Communications* **3**, fcab051 (2021).
 75. Meyer, M. M. *et al.* Cerebral sodium (^{23}Na) magnetic resonance imaging in patients with migraine—a case-control study. *European Radiology* **29**, 7055–7062 (2019).
 76. Meyer, M. M. *et al.* Repeatability and reproducibility of cerebral ^{23}Na imaging in healthy subjects. *BMC Medical Imaging* **19**, 1–7 (2019).
 77. Bhatia, A. *et al.* Quantitative Sodium (^{23}Na) MRI in Pediatric Gliomas: Initial Experience. *Diagnostics* **12**, 1223 (2022).
 78. Petracca, M. *et al.* Brain intra-and extracellular sodium concentration in multiple sclerosis: a 7 T MRI study. *Brain* **139**, 795–806 (2016).
 79. Haeger, A. *et al.* 3T sodium MR imaging in Alzheimer's disease shows stage-dependent sodium increase influenced by age and local brain volume. *NeuroImage: Clinical* **36**, 103274 (2022).
 80. Niesporek, S. C. *et al.* Partial volume correction for in vivo ^{23}Na -MRI data of the human brain. *NeuroImage* **112**, 353–363 (2015).
 81. Lu, A., Atkinson, I. C., Claiborne, T. C., Damen, F. C. & Thulborn, K. R. Quantitative sodium imaging with a flexible twisted projection pulse sequence. *Magnetic Resonance in Medicine* **63**, 1583–1593 (2010).
 82. Romanzetti, S. *et al.* Mapping tissue sodium concentration in the human brain: a comparison of MR sequences at 9.4 Tesla. *NeuroImage* **96**, 44–53 (2014).

Table 1. Summary of the mean value measurements from ^1H MNF HR, ^{23}Na MNF HR and ^{23}Na MNF LR in brain at 7 T: Results are presented as the overall mean \pm one standard deviation (std) of the final mean and std values measured in each ROI and in each subject, from 3 statistical methods: (1) Standard mean \pm std; (2) Jackknife; (3) Bootstrap (n = 1000 bootstraps with replacement). For ^{23}Na MNF HR and ^{23}Na MNF LR measurements in the eyes (vitreous humor) and CSF; $T_{2,\text{long}} = T_{2,\text{short}} \equiv T_2$. See Tables S1, S2 and S3 in Supplementary Information for a detailed summary of all the mean measurements in each subject.

Statistical Method	^1H MNF HR			^{23}Na MNF HR			^{23}Na MNF LR		
	Standard	Jackknife	Bootstrap	Standard	Jackknife	Bootstrap	Standard	Jackknife	Bootstrap
Eye (Vitreous Humor)	PD			T_1 [ms]			T_2 [ms]		
	Mean \pm Std of Mean	0.989 \pm 0.003	0.989 \pm 0.003	3913.89 \pm 273.63	3913.89 \pm 273.63	3913.89 \pm 273.63	122.87 \pm 31.25	122.87 \pm 31.25	122.90 \pm 31.29
	Mean \pm Std of Std	0.130 \pm 0.022	0.000 \pm 0.000	230.16 \pm 46.11	0.58 \pm 0.12	11.30 \pm 2.24	31.86 \pm 8.72	0.06 \pm 0.02	1.61 \pm 0.43
	Cerebrospinal Fluid (CSF)	0.821 \pm 0.086	0.821 \pm 0.086	3296.38 \pm 145.47	3296.38 \pm 145.47	3296.37 \pm 145.58	145.40 \pm 17.12	145.40 \pm 17.12	145.35 \pm 17.11
	Mean \pm Std of Std	0.118 \pm 0.017	0.000 \pm 0.000	390.62 \pm 60.17	0.98 \pm 0.15	19.67 \pm 2.95	44.52 \pm 5.78	0.11 \pm 0.01	2.26 \pm 0.31
Gray Matter (GM)	0.739 \pm 0.080	0.739 \pm 0.080	1688.70 \pm 53.25	1688.70 \pm 53.25	1688.73 \pm 53.40	55.25 \pm 3.58	55.25 \pm 3.58	55.42 \pm 3.37	
	Mean \pm Std of Std	0.083 \pm 0.006	0.000 \pm 0.000	107.93 \pm 5.80	0.27 \pm 0.02	5.42 \pm 0.37	10.84 \pm 2.92	0.03 \pm 0.01	0.55 \pm 0.15
	White Matter (WM)	0.548 \pm 0.062	0.548 \pm 0.062	1027.53 \pm 12.52	1027.53 \pm 12.52	1027.53 \pm 12.45	38.28 \pm 2.97	38.28 \pm 2.97	38.27 \pm 2.98
	Mean \pm Std of Std	0.056 \pm 0.005	0.000 \pm 0.000	46.66 \pm 4.50	0.12 \pm 0.01	2.32 \pm 0.23	4.43 \pm 2.31	0.01 \pm 0.01	0.22 \pm 0.12
	T_2,long [ms]			T_1 [ms]			T_2,short [ms]		
Eye (Vitreous Humor)	TSC [mM]	144.37 \pm 0.78	144.37 \pm 0.78	77.00 \pm 11.52	77.00 \pm 11.52	77.00 \pm 11.52	58.38 \pm 8.51	58.38 \pm 8.51	58.38 \pm 8.51
	Mean \pm Std of Mean	25.51 \pm 4.65	0.06 \pm 0.01	7.96 \pm 1.42	0.02 \pm 0.00	0.40 \pm 0.08	6.11 \pm 1.08	0.02 \pm 0.00	0.30 \pm 0.05
	Mean \pm Std of Std	136.56 \pm 24.12	136.56 \pm 24.12	76.54 \pm 7.70	76.54 \pm 7.70	76.54 \pm 7.71	58.64 \pm 6.19	58.64 \pm 6.20	58.65 \pm 6.20
	Cerebrospinal Fluid (CSF)	24.23 \pm 4.18	0.06 \pm 0.01	9.05 \pm 1.04	0.02 \pm 0.00	0.46 \pm 0.05	7.36 \pm 0.72	0.02 \pm 0.00	0.37 \pm 0.04
	Mean \pm Std of Std	89.91 \pm 16.73	89.91 \pm 16.73	43.86 \pm 4.21	43.86 \pm 4.21	43.86 \pm 4.20	11.58 \pm 4.63	11.58 \pm 4.63	11.58 \pm 4.63
Gray Matter (GM)	14.00 \pm 2.83	0.04 \pm 0.01	3.10 \pm 0.34	0.01 \pm 0.00	0.16 \pm 0.02	2.60 \pm 0.27	2.86 \pm 0.34	2.86 \pm 0.34	2.86 \pm 0.34
	Mean \pm Std of Mean	60.67 \pm 13.05	60.67 \pm 13.05	31.26 \pm 3.01	31.26 \pm 3.01	31.26 \pm 3.01	8.67 \pm 2.54	8.67 \pm 2.54	8.67 \pm 2.54
	Mean \pm Std of Std	8.54 \pm 2.12	0.02 \pm 0.01	1.35 \pm 0.12	0.00 \pm 0.00	0.07 \pm 0.01	1.59 \pm 0.32	0.00 \pm 0.00	0.08 \pm 0.02
	White Matter (WM)								
	T_2,short [ms]			T_1 [ms]			T_2,long [ms]		
Eye (Vitreous Humor)	TSC [mM]	144.03 \pm 1.03	144.03 \pm 1.03	60.22 \pm 5.82	60.22 \pm 5.82	60.22 \pm 5.82	50.34 \pm 5.37	50.34 \pm 5.37	50.34 \pm 5.37
	Mean \pm Std of Mean	23.11 \pm 6.33	0.06 \pm 0.02	2.03 \pm 1.28	0.01 \pm 0.00	0.10 \pm 0.06	1.62 \pm 1.57	0.00 \pm 0.00	0.08 \pm 0.08
	Mean \pm Std of Std	105.21 \pm 29.81	105.21 \pm 29.81	62.04 \pm 6.32	62.04 \pm 6.32	62.04 \pm 6.32	51.86 \pm 6.14	51.86 \pm 6.14	51.86 \pm 6.14
	Cerebrospinal Fluid (CSF)	20.19 \pm 7.76	0.05 \pm 0.02	2.33 \pm 0.26	0.01 \pm 0.00	0.12 \pm 0.02	1.86 \pm 0.66	0.01 \pm 0.00	0.09 \pm 0.03
	Mean \pm Std of Std	62.01 \pm 10.22	62.01 \pm 10.22	37.93 \pm 4.61	37.93 \pm 4.61	37.93 \pm 4.61	8.49 \pm 4.71	8.49 \pm 4.71	8.49 \pm 4.71
Gray Matter (GM)	10.95 \pm 1.33	0.03 \pm 0.00	1.57 \pm 0.06	0.00 \pm 0.00	0.09 \pm 0.00	0.09 \pm 0.00	2.74 \pm 0.19	0.01 \pm 0.00	0.14 \pm 0.01
	Mean \pm Std of Mean	51.45 \pm 10.78	51.45 \pm 10.78	38.17 \pm 4.21	38.17 \pm 4.21	38.17 \pm 4.20	9.63 \pm 4.14	9.63 \pm 4.14	9.63 \pm 4.14
	Mean \pm Std of Std	9.16 \pm 1.35	0.02 \pm 0.00	1.81 \pm 0.18	0.00 \pm 0.00	0.09 \pm 0.01	3.17 \pm 0.35	0.01 \pm 0.00	0.16 \pm 0.02
	White Matter (WM)								
	T_2,short [ms]			T_1 [ms]			T_2,long [ms]		
Eye (Vitreous Humor)	TSC [mM]	144.03 \pm 1.03	144.03 \pm 1.03	60.22 \pm 5.82	60.22 \pm 5.82	60.22 \pm 5.82	50.34 \pm 5.37	50.34 \pm 5.37	50.34 \pm 5.37
	Mean \pm Std of Mean	23.11 \pm 6.33	0.06 \pm 0.02	2.03 \pm 1.28	0.01 \pm 0.00	0.10 \pm 0.06	1.62 \pm 1.57	0.00 \pm 0.00	0.08 \pm 0.08
	Mean \pm Std of Std	105.21 \pm 29.81	105.21 \pm 29.81	62.04 \pm 6.32	62.04 \pm 6.32	62.04 \pm 6.32	51.86 \pm 6.14	51.86 \pm 6.14	51.86 \pm 6.14
	Cerebrospinal Fluid (CSF)	20.19 \pm 7.76	0.05 \pm 0.02	2.33 \pm 0.26	0.01 \pm 0.00	0.12 \pm 0.02	1.86 \pm 0.66	0.01 \pm 0.00	0.09 \pm 0.03
	Mean \pm Std of Std	62.01 \pm 10.22	62.01 \pm 10.22	37.93 \pm 4.61	37.93 \pm 4.61	37.93 \pm 4.61	8.49 \pm 4.71	8.49 \pm 4.71	8.49 \pm 4.71
Gray Matter (GM)	10.95 \pm 1.33	0.03 \pm 0.00	1.57 \pm 0.06	0.00 \pm 0.00	0.09 \pm 0.00	0.09 \pm 0.00	2.74 \pm 0.19	0.01 \pm 0.00	0.14 \pm 0.01
	Mean \pm Std of Mean	51.45 \pm 10.78	51.45 \pm 10.78	38.17 \pm 4.21	38.17 \pm 4.21	38.17 \pm 4.20	9.63 \pm 4.14	9.63 \pm 4.14	9.63 \pm 4.14
	Mean \pm Std of Std	9.16 \pm 1.35	0.02 \pm 0.00	1.81 \pm 0.18	0.00 \pm 0.00	0.09 \pm 0.01	3.17 \pm 0.35	0.01 \pm 0.00	0.16 \pm 0.02
	White Matter (WM)								
	T_2,short [ms]			T_1 [ms]			T_2,long [ms]		
Eye (Vitreous Humor)	TSC [mM]	144.03 \pm 1.03	144.03 \pm 1.03	60.22 \pm 5.82	60.22 \pm 5.82	60.22 \pm 5.82	50.34 \pm 5.37	50.34 \pm 5.37	50.34 \pm 5.37
	Mean \pm Std of Mean	23.11 \pm 6.33	0.06 \pm 0.02	2.03 \pm 1.28	0.01 \pm 0.00	0.10 \pm 0.06	1.62 \pm 1.57	0.00 \pm 0.00	0.08 \pm 0.08
	Mean \pm Std of Std	105.21 \pm 29.81	105.21 \pm 29.81	62.04 \pm 6.32	62.04 \pm 6.32	62.04 \pm 6.32	51.86 \pm 6.14	51.86 \pm 6.14	51.86 \pm 6.14
	Cerebrospinal Fluid (CSF)	20.19 \pm 7.76	0.05 \pm 0.02	2.33 \pm 0.26	0.01 \pm 0.00	0.12 \pm 0.02	1.86 \pm 0.66	0.01 \pm 0.00	0.09 \pm 0.03
	Mean \pm Std of Std	62.01 \pm 10.22	62.01 \pm 10.22	37.93 \pm 4.61	37.93 \pm 4.61	37.93 \pm 4.61	8.49 \pm 4.71	8.49 \pm 4.71	8.49 \pm 4.71
Gray Matter (GM)	10.95 \pm 1.33	0.03 \pm 0.00	1.57 \pm 0.06	0.00 \pm 0.00	0.09 \pm 0.00	0.09 \pm 0.00	2.74 \pm 0.19	0.01 \pm 0.00	0.14 \pm 0.01
	Mean \pm Std of Mean	51.45 \pm 10.78	51.45 \pm 10.78	38.17 \pm 4.21	38.17 \pm 4.21	38.17 \pm 4.20	9.63 \pm 4.14	9.63 \pm 4.14	9.63 \pm 4.14
	Mean \pm Std of Std	9.16 \pm 1.35	0.02 \pm 0.00	1.81 \pm 0.18	0.00 \pm 0.00	0.09 \pm 0.01	3.17 \pm 0.35	0.01 \pm 0.00	0.16 \pm 0.02
	White Matter (WM)								
	T_2,short [ms]			T_1 [ms]			T_2,long [ms]		

Table 3. Mean ^{23}Na relaxation times and total sodium concentration (TSC) measured in vivo in brain at 7 T: Comparison of the overall standard mean values from ^{23}Na MNF HR and LR (see Methods, Table 1 and Tables S2 and S3 in Supplementary Information) with values from the literature. TSC is measured in mM (or mmol/L), with mean TSC in the eyes (vitreous humor) used as internal reference (145 mM). Results are presented as average \pm one standard deviation (std). Since TSC does not depend on the magnetic field, values for comparison were gathered from studies performed at different fields. For eye (vitreous humor) and CSF, $T_{2,\text{long}} = T_{2,\text{short}} \equiv T_2$ (monoexponential relaxation in liquid or quasi-liquid state).

Method	Eye (vitreous humor)			Cerebrospinal Fluid (CSF)			Gray Matter (GM)			White Matter (WM)		
	Reference	TSC [mM]	T_1 [ms]	T_2 [ms]	TSC [mM]	T_1 [ms]	T_2 [ms]	TSC [mM]	T_1 [ms]	$T_{2,\text{long}}$ [ms]	$T_{2,\text{short}}$ [ms]	$T_{2,\text{short}}$ [ms]
Assay	(34)	146.7 \pm 3.3										
Used as reference	(35)	145.0 \pm 0.0										
AWSOS	(59)	134.0 \pm 6.0										
Mean from references within	(60)	139.2 \pm 18.9										
Multi-Echo GRE	(61) ¹	143.0 \pm 0.0		46.0 \pm 2.1								
Multi-Echo GRE	(62) ²			45.8 \pm 3.6								
IR + CPMG MRS	(63) ³		60.9 \pm 0.9	60.3 \pm 4.4								
MRF	(28) ⁴					61.9 \pm 2.8	46.3 \pm 4.5		35.0 \pm 3.2	29.3 \pm 3.8	5.5 \pm 1.3	
MR	(64)					67.1 \pm 6.3	41.5 \pm 3.4					29.3 \pm 3.8
DA-3DPR	(65)						53.6 \pm 3.9					29.2 \pm 4.9
3D GRE	(66)						54.0 \pm 4.0					37.7 \pm 2.4
3D-MERINA	(67)						57.2 \pm 6.6		28.0 \pm 2.0	28.0 \pm 2.0	2.0 \pm 1.7	29.0 \pm 2.0
DA-3DPR	(68)						46.9 \pm 2.1		25.9 \pm 8.3	25.9 \pm 8.3	2.0 \pm 1.7	22.4 \pm 7.8
3D SoS	(69)								36.4 \pm 3.1	36.4 \pm 3.1	5.4 \pm 0.2	23.3 \pm 2.6
DA-3DPR	(70) ⁵								17.2 \pm 2.0	17.2 \pm 2.0	2.9 \pm 0.4	18.8 \pm 3.2
Meta-analysis	(71) ^{5,6}								31.5 \pm 1.8	31.5 \pm 1.8	5.0 \pm 0.4	38.3 \pm 2.5
FLORET + Review	(72) ^{5,7}											38.2 \pm 2.0
3D Radial	(73) ⁵											37.5 \pm 9.8
FLORET	(74) ⁵											42.2 \pm 12.2
DA-3DPR	(75)						84.6 \pm 6.2					19.4 \pm 1.7
DA-3DPR	(76) ⁸						103.2 \pm 22.3					31.6 \pm 1.6
TPI	(77)						126.6 \pm 11.3					32.8 \pm 2.2
3D GRE	(78)						156.0 \pm 27.0					40.9 \pm 5.2
DA-3DPR (Vials)	(36) ⁹											52.5 \pm 4.7
DA-3DPR (CSF)	(36) ⁹											27.9 \pm 2.6
DA-3DPR (VH)	(36) ⁹											53.0 \pm 9.0
DA-3DPR (VH)	(36) ⁹											52.5 \pm 5.1
FLORET VFA (old)	(79) ¹⁰											46.8 \pm 1.9
FLORET VFA (young)	(79) ¹⁰											39.6 \pm 3.8
DA-3DPR	(80)											34.5 \pm 5.0
TPI	(81)											41.0 \pm 3.0
TPI	(82) ⁶											28.7 \pm 1.2
Mean \pm Std	(literature)	141.6 \pm 5.1	60.9 \pm 0.9	50.7 \pm 8.3	113.9 \pm 27.1	64.6 \pm 3.7	49.9 \pm 5.9	46.4 \pm 8.8	35.0 \pm 3.2	28.1 \pm 6.4	4.2 \pm 1.6	28.5 \pm 7.0
Range (min, max)		[134.0, 146.7]	[60.9, 60.9]	[45.8, 60.3]	[84.6, 156.0]	[61.9, 67.1]	[41.5, 57.2]	[30.5, 61.6]	[35.0, 35.0]	[17.2, 36.4]	[2.0, 5.5]	[18.8, 38.3]
^{23}Na MNF HR	(this study)	144.4 \pm 0.8	77.0 \pm 11.5	58.4 \pm 8.5	136.6 \pm 24.1	76.5 \pm 7.7	58.6 \pm 6.2	89.9 \pm 16.7	43.9 \pm 4.2	27.9 \pm 6.5	11.6 \pm 4.6	20.2 \pm 4.3
^{23}Na MNF LR	(this study)	144.0 \pm 1.0	60.2 \pm 5.8	50.3 \pm 5.4	105.2 \pm 29.8	62.0 \pm 6.3	51.9 \pm 6.1	62.0 \pm 10.2	37.9 \pm 4.6	25.3 \pm 6.8	8.3 \pm 4.7	25.7 \pm 6.2

¹Ex vivo human eyes, 4, 7 T.

²Ex vivo bovine eyes, 1, 9 T.

³Ex vivo bovine eyes, 4, 7 T.

⁴In this article, gray and white matters were not differentiated and only whole brain tissue was considered (which comprised both gray and white matters together).

⁵Only data from healthy subjects was included.

⁶Meta-analysis over 22 publications.

⁷Average over 15 studies (including the study from the paper), using values measured in parenchyma (GM+WM).

⁸Std here is the average of the std values measured in this repeatability/reproducibility study (3 scans).

⁹In this study, three quantification methods were compared, using Vials, CSF or vitreous humor (VH) as references. For the vials method, TSC was measured only in normal-appearing GM and WM in 50 stroke patients.

¹⁰In this study, median TSC was measured in old (67 \pm 9.4 years old) and young (29.2 \pm 6.4 years old) healthy controls.

Abbreviations: TSC = Total Sodium Concentration; CSF = Cerebrospinal Fluid; GRE = Gradient-Recalled Echo; DA-3DPR = Density Adapted 3-Dimensional Projection Reconstruction; MRF = Magnetic Resonance Fingerprinting; MNF = Multinuclear Fingerprinting; MRS = Magnetic Resonance Spectroscopy; IR = Inversion Recovery; CPMG = Carr-Purcell-Meitboom-Gill; 3D-MERINA = 3D Multi-Echo Radial Imaging; TPI = Twisted Projection Imaging; flexTPI = Flexible TPI; FLORET = Fermat Looped Orthogonally Encoded Trajectories; SoS = Stack-of-Stars; SISTINA = Simultaneous Single-Quantum and Triple-Quantum-Filtered MRI of ^{23}Na ; VH = Vitreous Humor (eye); VFA = Variable Flip Angle.

Supplementary Information

Multinuclear fingerprinting

Gonzalo G. Rodriguez^{1,2}, Zidan Yu^{1,3,4}, Lauren O'Donnell^{1,5}, Martijn A. Cloos^{1,6}, Guillaume Madelin^{1,3*}

¹ Center for Biomedical Imaging, Department of Radiology, New York University Grossman School of Medicine, New York, NY, USA

² NMR Signal Enhancement, Max Planck Institute for Multidisciplinary Sciences Göttingen, Germany

³ Vilcek Institute of Graduate Biomedical Sciences, New York University Grossman School of Medicine, New York, NY, USA

⁴ Philips, Best, The Netherlands

⁵ JEOL USA, Peabody, MA, USA

⁶ Donders Center for Cognitive Neuroimaging, Radboud University, Nijmegen, The Netherlands

* Corresponding author: guillaume.madelin@nyulangone.org

Abbreviations & Acronyms

¹ H	Hydrogen nucleus (proton)
²³ Na	Sodium nucleus
CSF	Cerebrospinal FLuid
FLORET	Fermat Looped Orthogonally Encoded Trajectories
GM	Gray Matter
HR	High Resolution
LR	Low Resolution
MNF	Multinuclear Fingerprinting
MRF	Magnetic Resonance Fingerprinting
PD	Proton Density
ROI	Region-Of-Interest
STD	Standard Deviation
TSC	Tissue Sodium Concentration
WM	White Matter

April 15, 2026

Contents

References	1
1 FIGURES: Examples of full $^1\text{H}/^{23}\text{Na}$ MRF maps in brain	3
2 FIGURES: Single measurement in brain (1 N_{ROI} & 1 N_{REF} values)	5
2.1 PD & TSC quantification (1 N_{REF})	5
2.2 Histograms (1 N_{ROI} & 1 N_{REF})	5
2.3 Boxplots	5
2.4 Summary of the measurements	5
3 FIGURES: Multiple measurements in brain (20 N_{ROI} & 20 N_{REF} values)	35
3.1 PD & TSC quantification (20 N_{REF})	35
3.2 Histograms (20 N_{ROI} & 20 N_{REF})	35
3.3 Boxplots	35
3.4 Summary of the measurements	35
4 TABLES: Multiple measurements in brain (20 N_{ROI} & 20 N_{REF} values)	64
4.1 Statistics	64
4.1.1 Mean & standard deviation (std)	64
4.1.2 Wilcoxon rank-sum test	64
4.2 Summary of the measurements	65
5 REFERENCES	71

1 FIGURES: Examples of full $^1\text{H}/^{23}\text{Na}$ MRF maps in brain

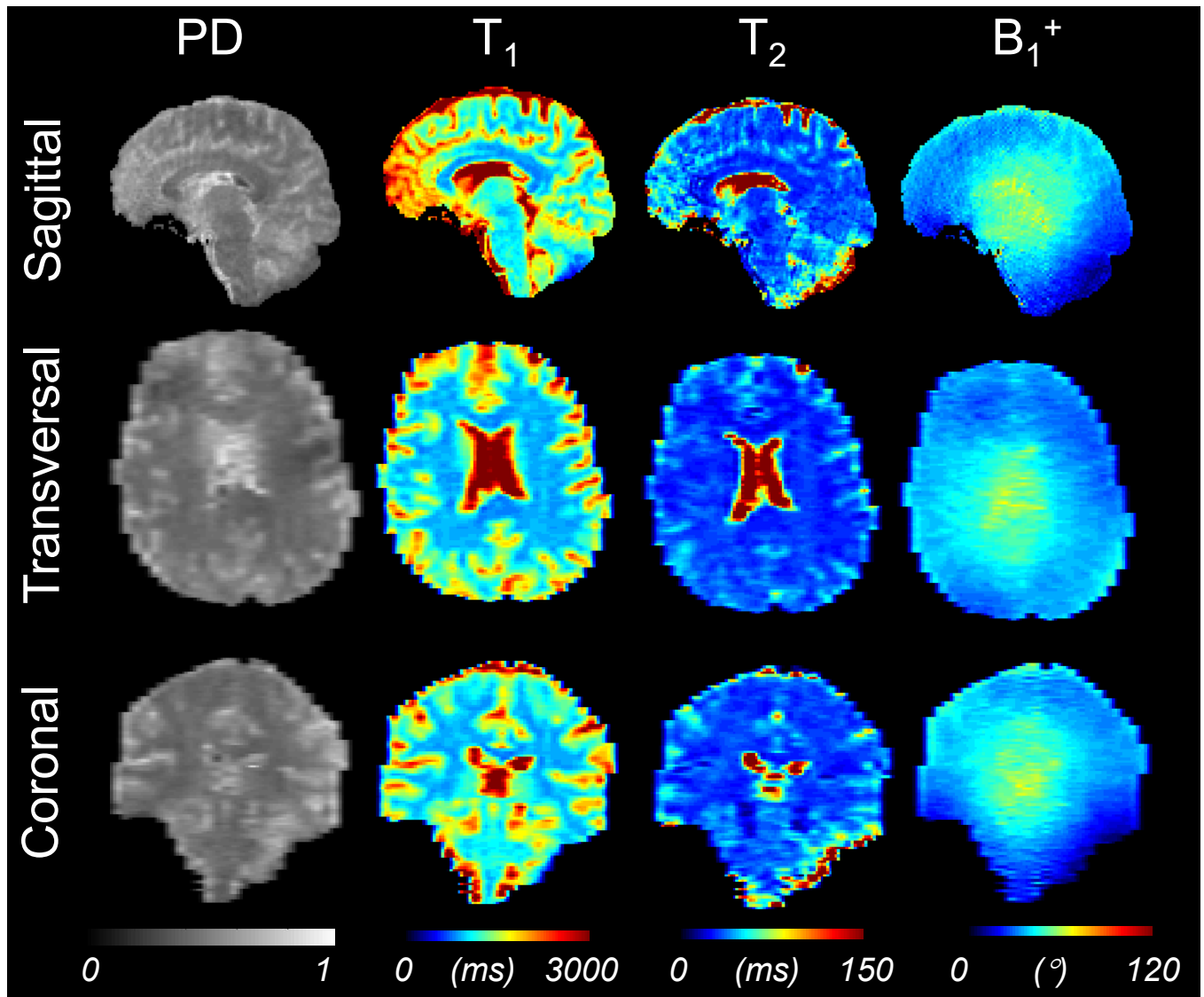


Figure S1. Examples of the four 3D HR maps acquired by the ^1H MRF part of MNF in the whole brain. Representative sagittal, transversal and coronal slices from the 3D HR maps of proton density (PD), T₁, T₂ and B₁⁺ (flip angle variations) in a healthy brain. Resolution = $1.5 \times 1.5 \times 5 \text{ mm}^3$.

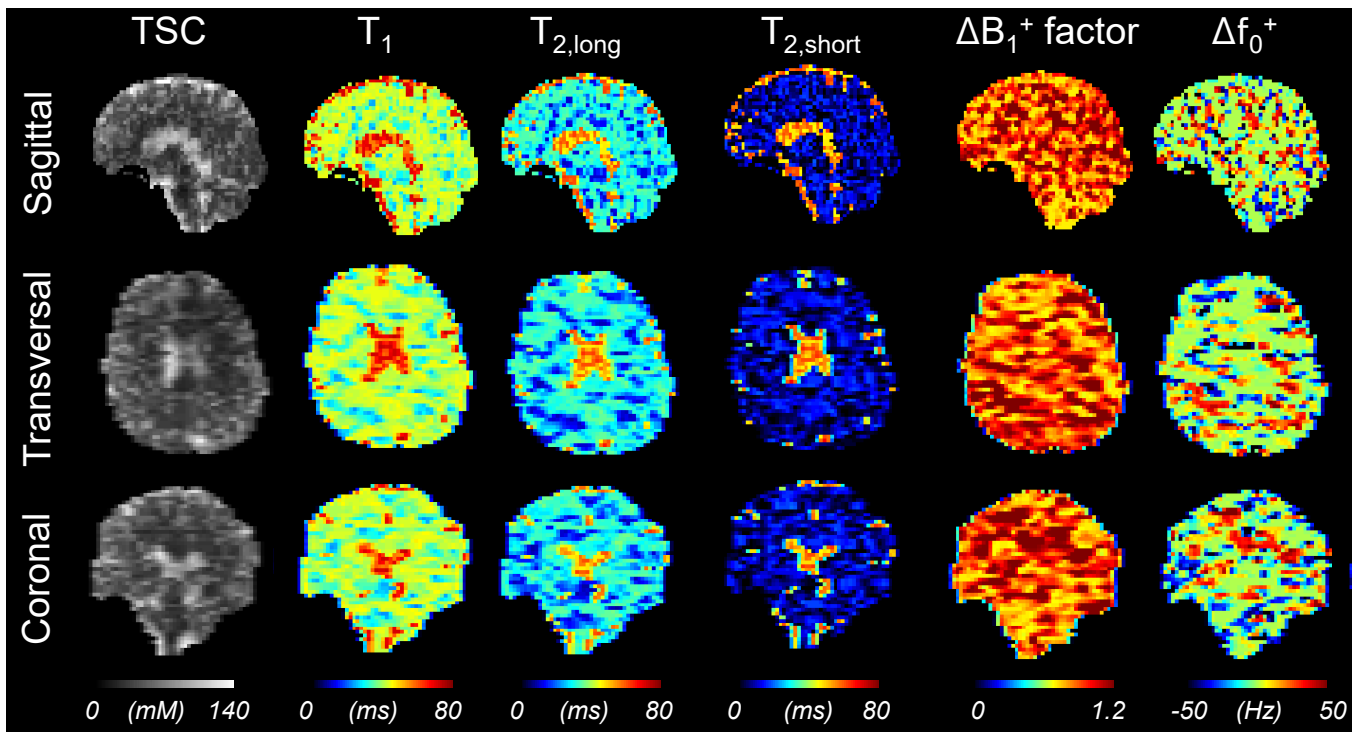


Figure S2. Examples of the six 3D LR maps acquired by the ^{23}Na MRF part of MNF in the whole brain. Representative sagittal, transversal and coronal slices from the quantitative 3D HR maps of tissue sodium concentration (TSC), T_1 , $T_{2,short}$, $T_{2,long}$, ΔB_1^+ factor (applied as a multiplying factor to the flip angles) and Δf_0 (B_0 inhomogeneities) in a healthy brain. Resolution = $2.85 \times 2.85 \times 5 \text{ mm}^3$.

2 FIGURES: Single measurement in brain (1 N_{ROI} & 1 N_{REF} values)

In this supplementary section, we present examples of histograms and boxplots from single measurements (1 N_{ROI} & 1 N_{REF} values only) of all MNF and ^{23}Na FLORET metrics in all subjects ($N = 7$).

2.1 PD & TSC quantification (1 N_{REF})

The mean value of the N_{REF} highest voxel values of the reference ROI (vitreous humor in the EYE) was used as the reference mean value of PD or TSC for generating quantitative PD and TSC maps in the brain, respectively, with $N_{REF} = 80\%$ (1 N_{REF} value in this case), using the following steps:

- 1. PD & TSC:** Normalization of the initial PD and TSC maps (calculated from the matching process in MRF) by the mean value from the N_{REF} measurement and then dividing by 0.98 (considering 98% water content in the vitreous humor of the eye, and assuming that Na^+ is only present in the water compartment).
- 2. TSC only:** Multiply the normalized TSC map by the reference value $\text{TSC}_{\text{EYE}} = 145$ mM.
- 3. Final maps:** This process results in 1 final PD map normalized in arbitrary units (a.u.), and in 1 final TSC map quantified in units of Na^+ concentration in mM (or mmol/L).

2.2 Histograms (1 N_{ROI} & 1 N_{REF})

Histograms show the distributions of the N_{ROI} highest voxel values in each ROI, with $N_{ROI} = 90\%$ (1 N_{ROI} value in this case) for each metric in each subject.

2.3 Boxplots

Boxplots present of the mean values of each histogram distribution from all subjects.

2.4 Summary of the measurements

Data Acquisition	Metrics	N_{REF} (PD & TSC)	N_{ROI} (all metrics)	ROIs	Subjects
^1H MNF HR	PD, T_1 , T_2	80%	90%	EYE, CSF, GM, WM	1-7
^{23}Na MNF HR	TSC, T_1 , $T_{2,\text{short}}$, $T_{2,\text{long}}$	80%	90%	EYE, CSF, GM, WM	1-7
^{23}Na MNF LR	TSC, T_1 , $T_{2,\text{short}}$, $T_{2,\text{long}}$	80%	90%	EYE, CSF, GM, WM	1-7
^{23}Na FLORET	TSC, T_1 , $T_{2,\text{short}}$, $T_{2,\text{long}}$	80%	90%	EYE, CSF, GM, WM	5, 6

Subject 1 - ^1H MNF HR (REF 80%, ROI 90%)

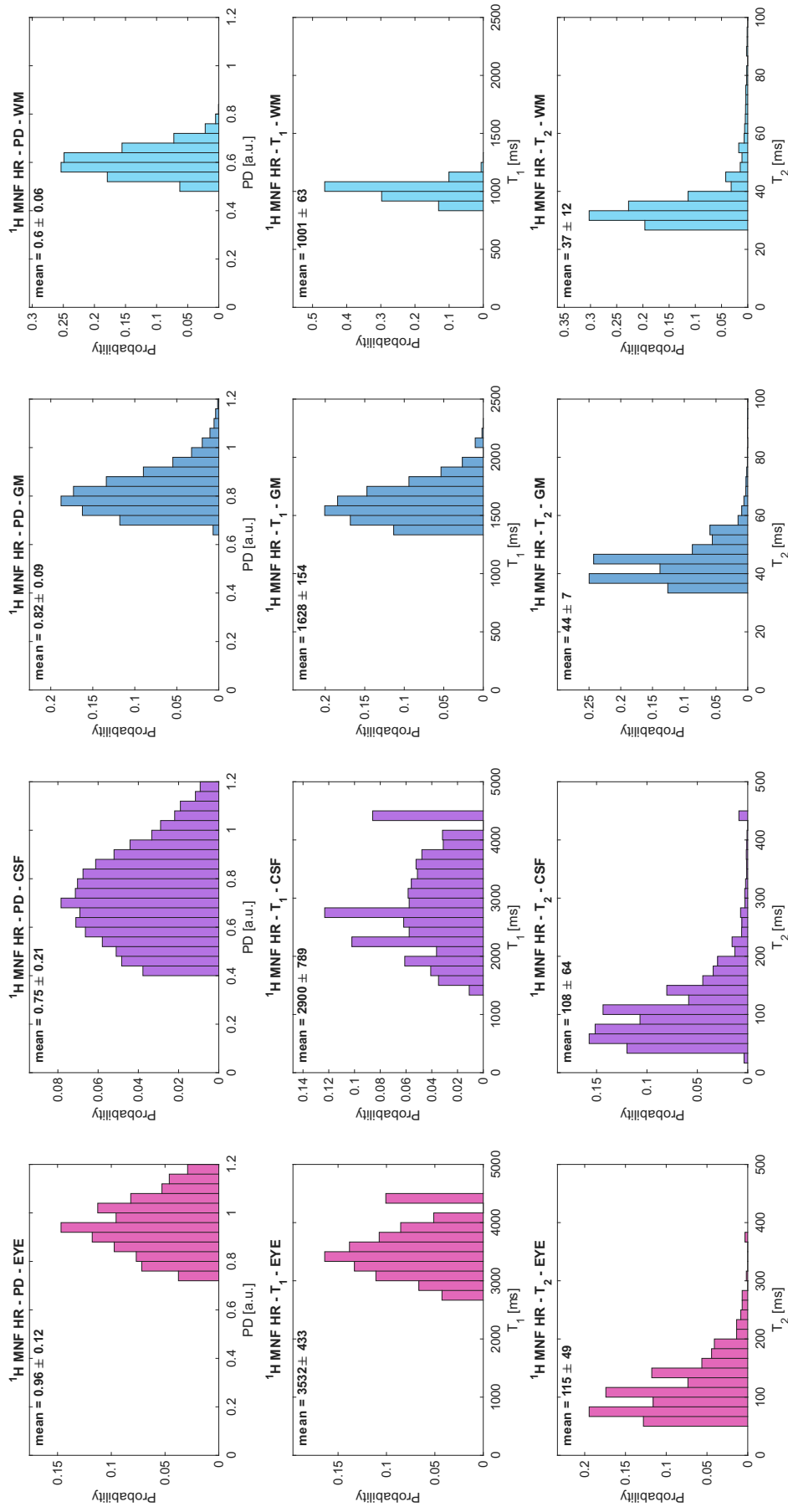


Figure S3. Histograms of the measurements in subject 1, from the ^1H MNF HR data (PD, T_1 , T_2), in the EYE, CSF, GM and WM. PD normalization was calculated using the mean value of the $N_{\text{REF}} = 80\%$ highest values measured in the EYE ROI as a reference (from the eye mask applied to the pre-normalized PD map), considering 98% water content in the vitreous humor of the eye. Histograms represent the $N_{\text{ROI}} = 90\%$ highest values in each ROI.

Subject 2 - ^1H MNF HR (REF 80%, ROI 90%)

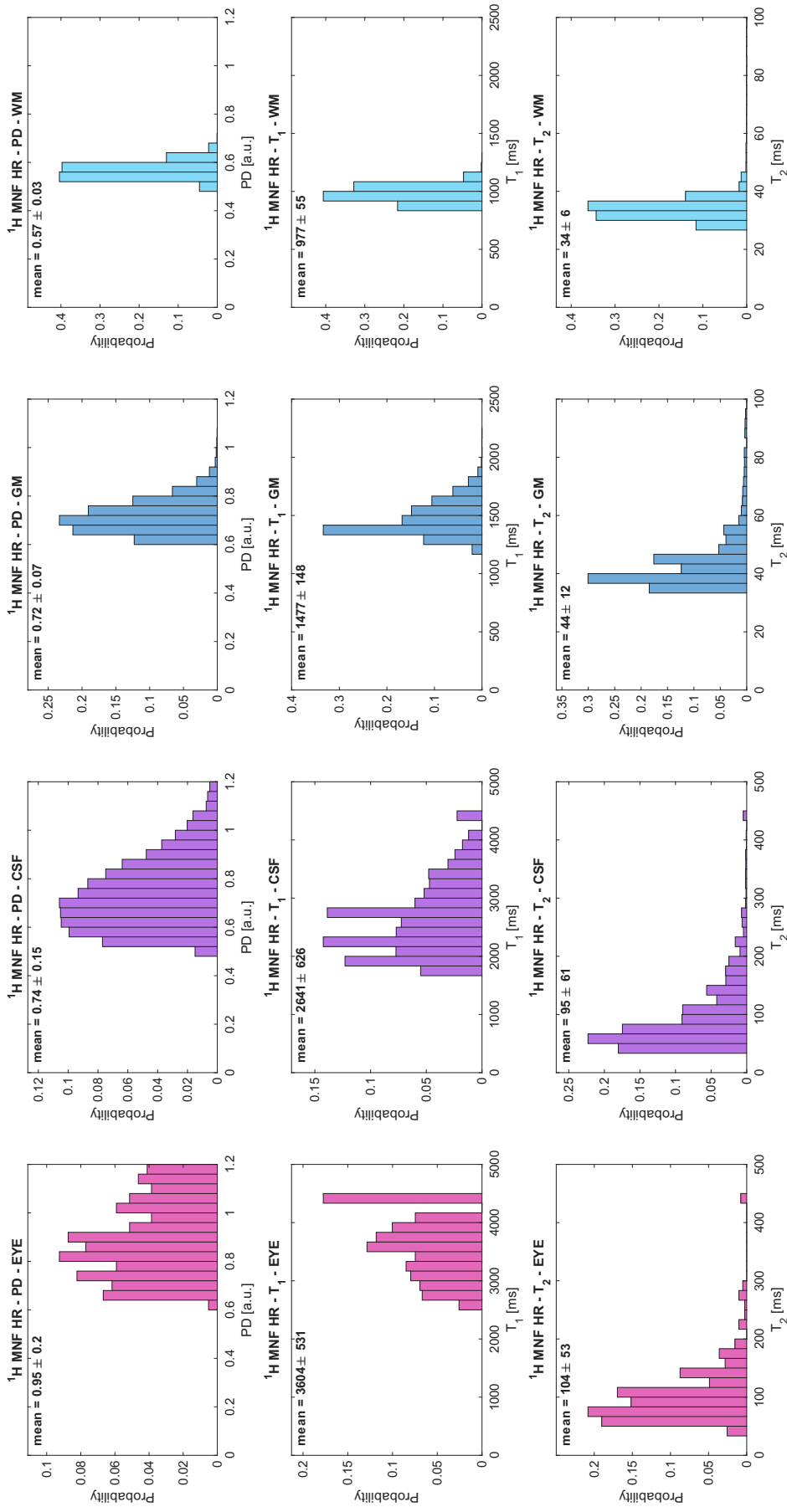


Figure S4. Histograms of the measurements in subject 2, from the ^1H MNF HR data (PD, T_1 , T_2), in the EYE, CSF, GM and WM. PD normalization was calculated using the mean value of the $N_{\text{REF}} = 80\%$ highest values measured in the EYE ROI as a reference (from the eye mask applied to the pre-normalized PD map), considering 98% water content in the vitreous humor of the eye. Histograms represent the $N_{\text{ROI}} = 90\%$ highest values in each ROI.

Subject 3 - ^1H MNF HR (REF 80%, ROI 90%)

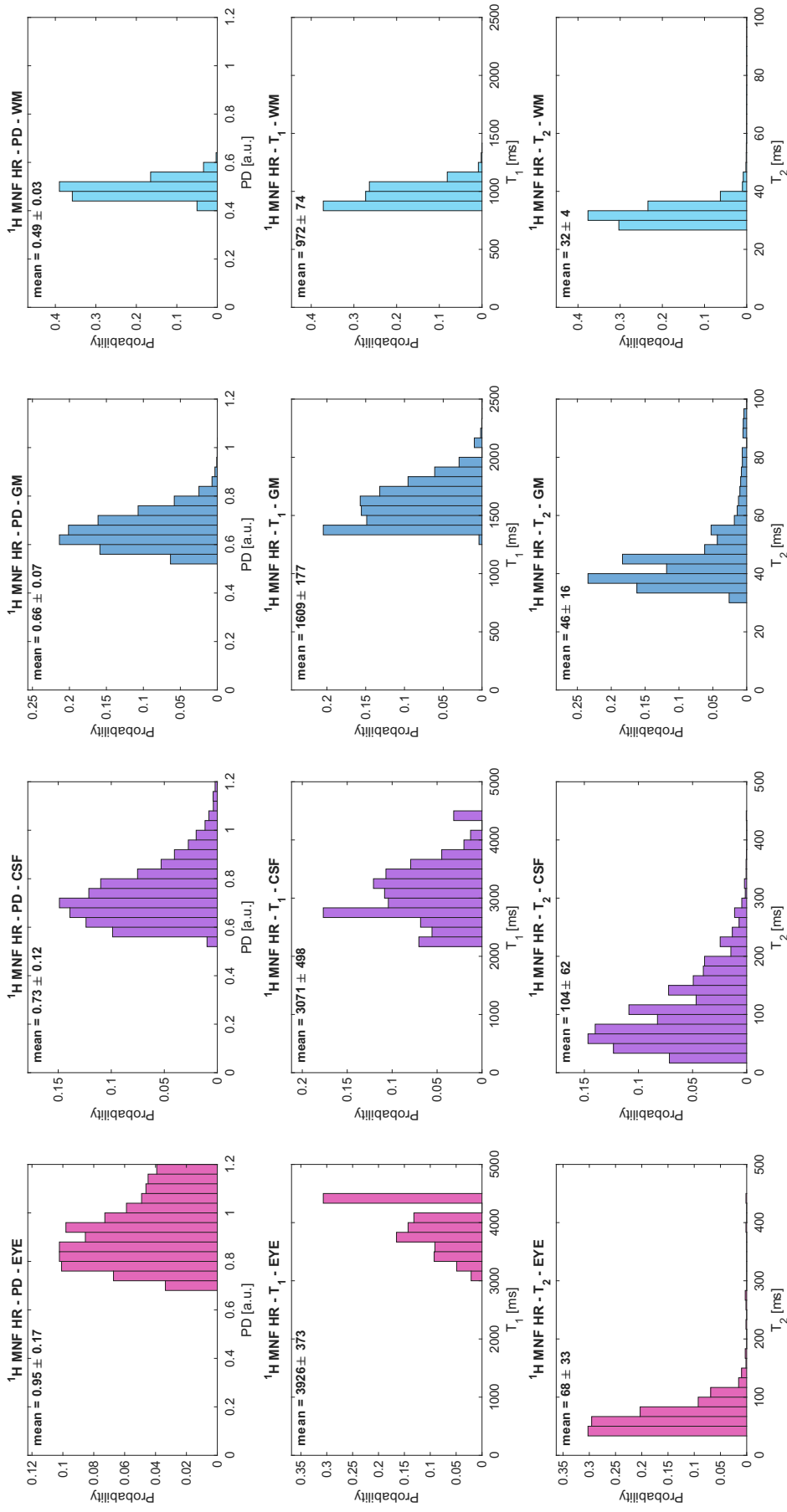


Figure S5. Histograms of the measurements in subject 3, from the ^1H MNF HR data (PD, T_1 , T_2), in the EYE, CSF, GM and WM. PD normalization was calculated using the mean value of the $N_{\text{REF}} = 80\%$ highest values measured in the EYE ROI as a reference (from the eye mask applied to the pre-normalized PD map), considering 98% water content in the vitreous humor of the eye. Histograms represent the $N_{\text{ROI}} = 90\%$ highest values in each ROI.

Subject 4 - ^1H MNF HR (REF 80%, ROI 90%)

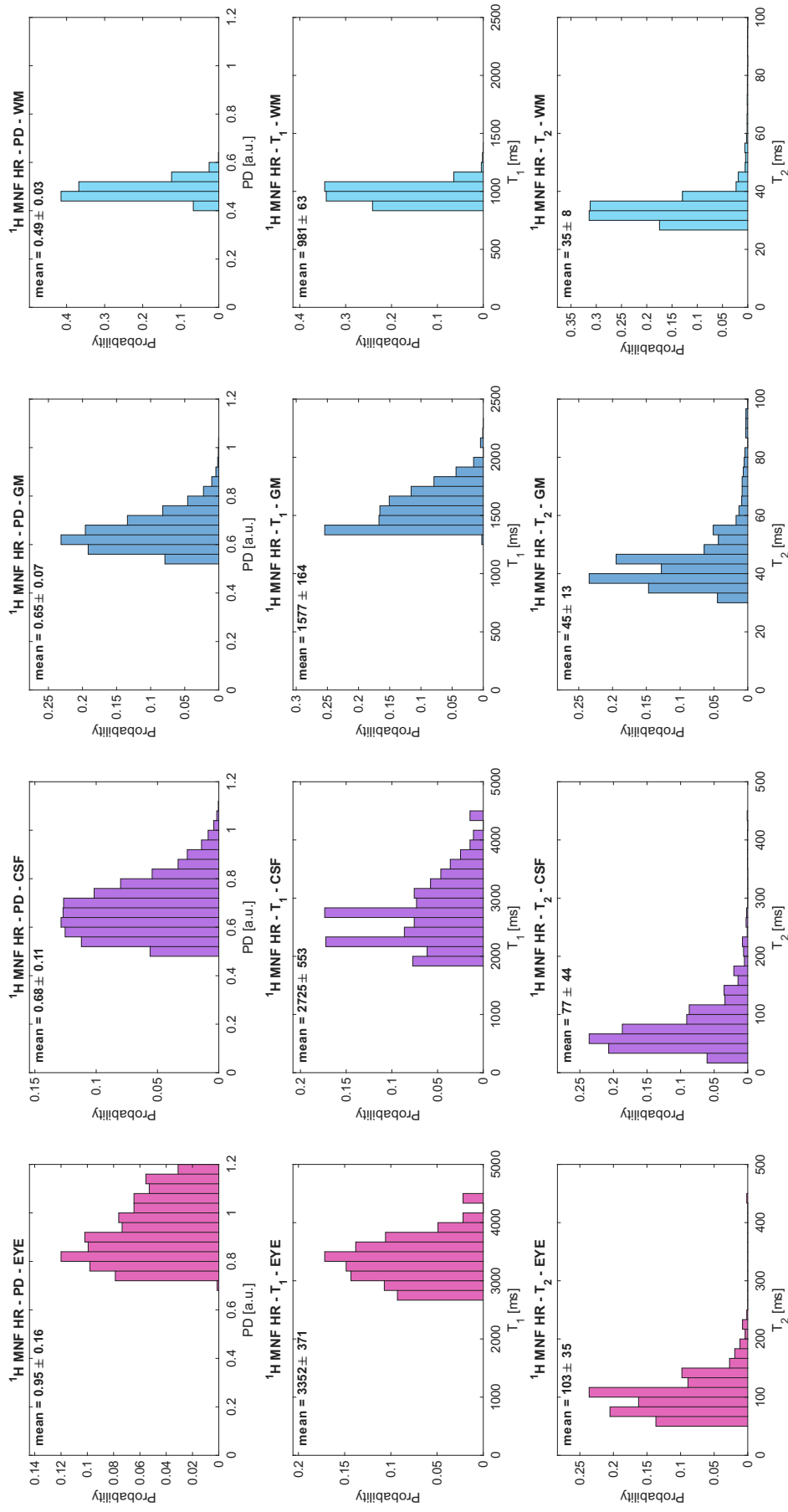


Figure S6. Histograms of the measurements in subject 4, from the ^1H MNF HR data (PD, T_1 , T_2), in the EYE, CSF, GM and WM. PD normalization was calculated using the mean value of the $N_{\text{REF}} = 80\%$ highest values measured in the EYE ROI as a reference (from the eye mask applied to the pre-normalized PD map), considering 98% water content in the vitreous humor of the eye. Histograms represent the $N_{\text{ROI}} = 90\%$ highest values in each ROI.

Subject 5 - ^1H MNF HR (REF 80%, ROI 90%)

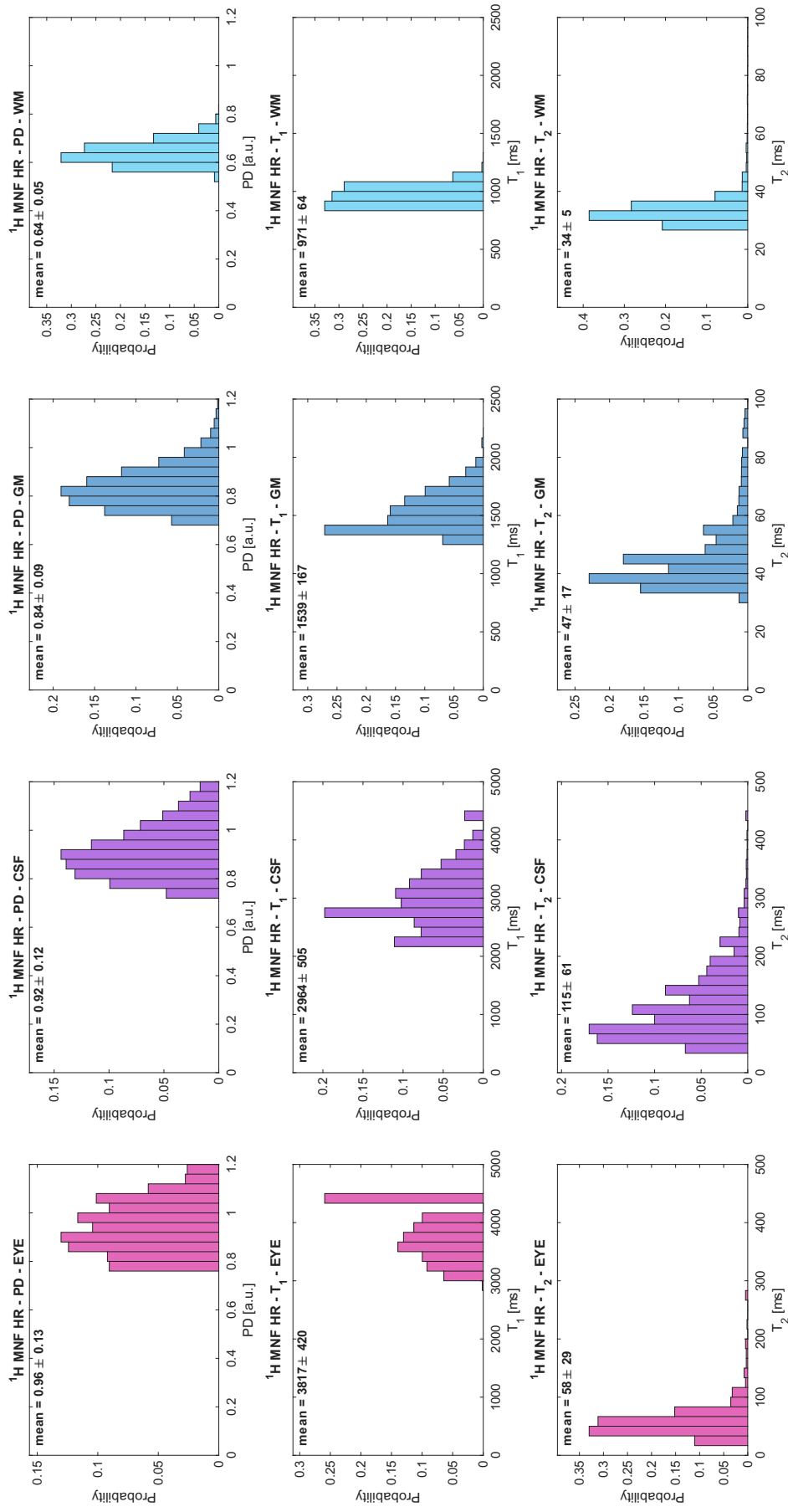


Figure S7. Histograms of the measurements in subject 5, from the ^1H MNF HR data (PD, T_1 , T_2), in the EYE, CSF, GM and WM. PD normalization was calculated using the mean value of the $N_{\text{REF}} = 80\%$ highest values measured in the EYE ROI as a reference (from the eye mask applied to the pre-normalized PD map), considering 98% water content in the vitreous humor of the eye. Histograms represent the $N_{\text{ROI}} = 90\%$ highest values in each ROI.

Subject 6 - ^1H MNF HR (REF 80%, ROI 90%)

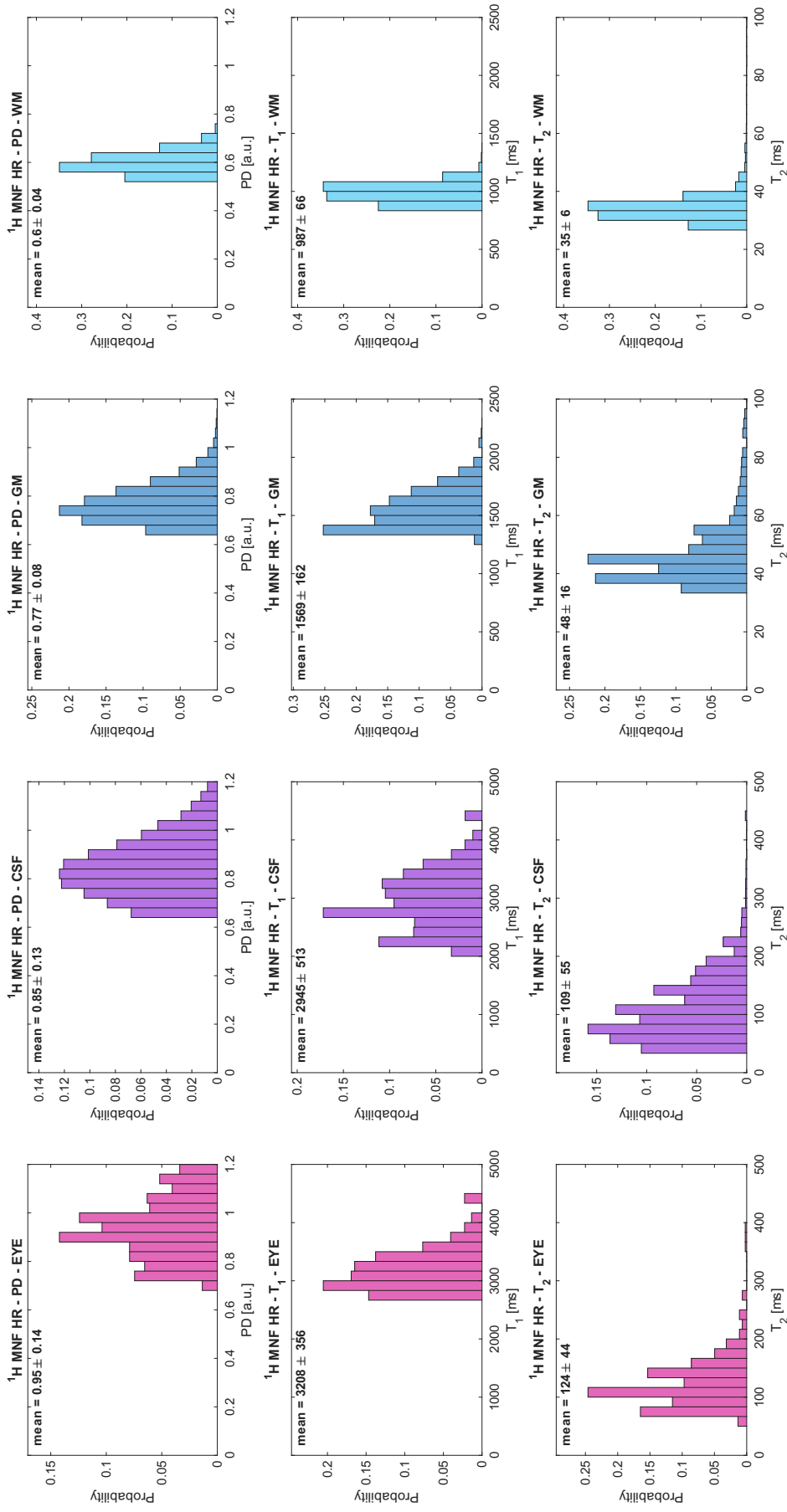


Figure S8. Histograms of the measurements in subject 6, from the ^1H MNF HR data (PD, T_1 , T_2), in the EYE, CSF, GM and WM. PD normalization was calculated using the mean value of the $N_{\text{REF}} = 80\%$ highest values measured in the EYE ROI as a reference (from the eye mask applied to the pre-normalized PD map), considering 98% water content in the vitreous humor of the eye. Histograms represent the $N_{\text{ROI}} = 90\%$ highest values in each ROI.

Subject 7 - ^1H MNF HR (REF 80%, ROI 90%)

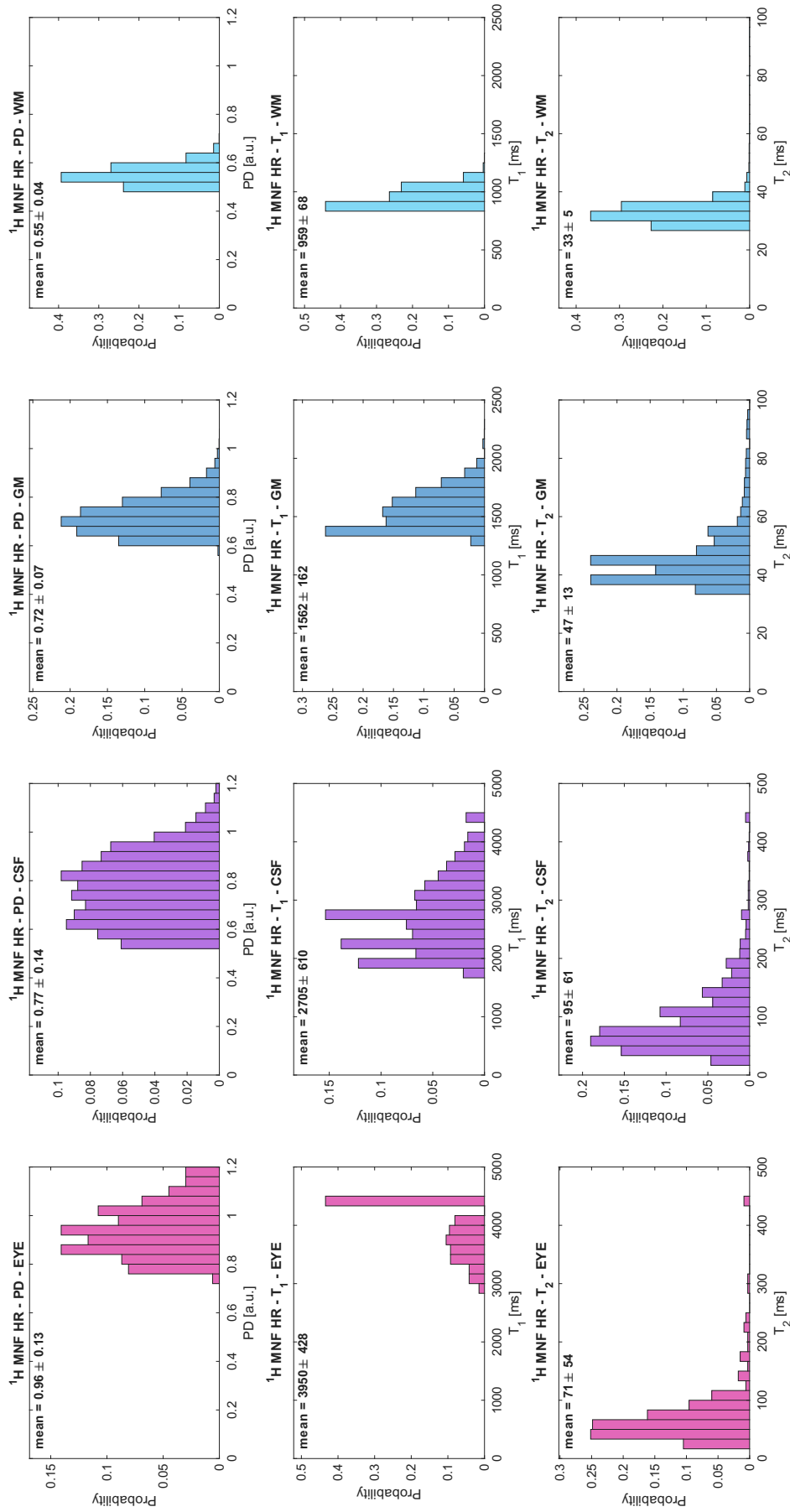


Figure S9. Histograms of the measurements in subject 7, from the ^1H MNF HR data (PD, T_1 , T_2), in the EYE, CSF, GM and WM. PD normalization was calculated using the mean value of the $N_{\text{REF}} = 80\%$ highest values measured in the EYE ROI as a reference (from the eye mask applied to the pre-normalized PD map), considering 98% water content in the vitreous humor of the eye. Histograms represent the $N_{\text{ROI}} = 90\%$ highest values in each ROI.

Subject 1 - ^{23}Na MNF HR (REF 80%, ROI 90%)

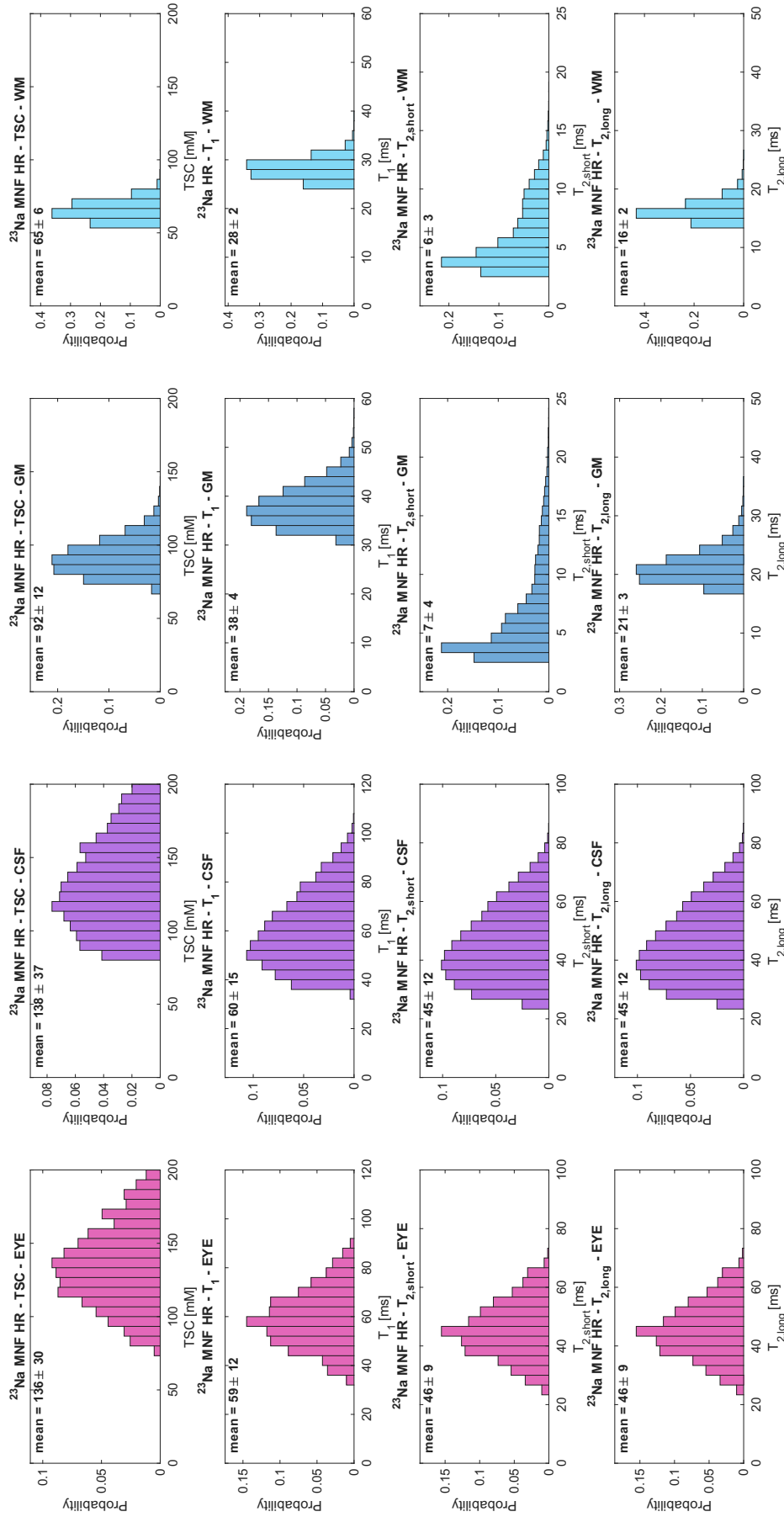


Figure S10. Histograms of the measurements in subject 1, from the ^{23}Na MNF HR data (TSC, T_1 , $T_{2,short}$, $T_{2,long}$), in the EYE, CSF, GM and WM. TSC quantification was calculated using the mean value of the $N_{REF} = 80\%$ highest values measured in the eye ROI as a reference (from the eye mask applied to the pre-normalized TSC map), considering 98% water content and 145 mM NaCl concentration (TSC reference) in the vitreous humor of the eye. Histograms represent the $N_{ROI} = 90\%$ highest values in each ROI.

Subject 2 - ^{23}Na MNF HR (REF 80%, ROI 90%)

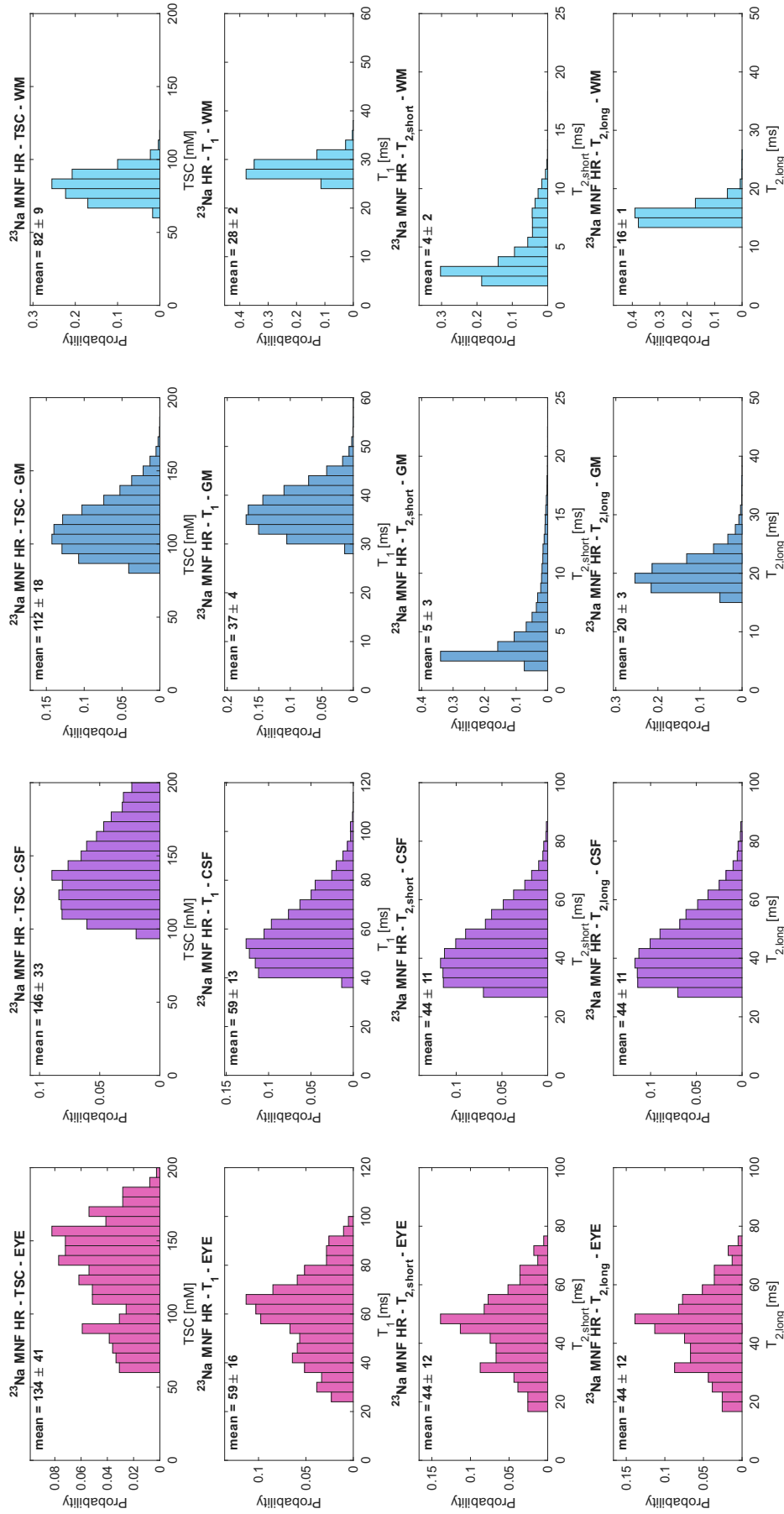


Figure S11. Histograms of the measurements in subject 2, from the ^{23}Na MNF HR data (TSC, T_1 , $T_{2,short}$, $T_{2,long}$), in the EYE, CSF, GM and WM. TSC quantification was calculated using the mean value of the $N_{REF} = 80\%$ highest values measured in the eye ROI as a reference (from the eye mask applied to the pre-normalized TSC map), considering 98% water content and 145 mM NaCl concentration (TSC reference) in the vitreous humor of the eye. Histograms represent the $N_{ROI} = 90\%$ highest values in each ROI.

Subject 3 - ^{23}Na MNF HR (REF 80%, ROI 90%)

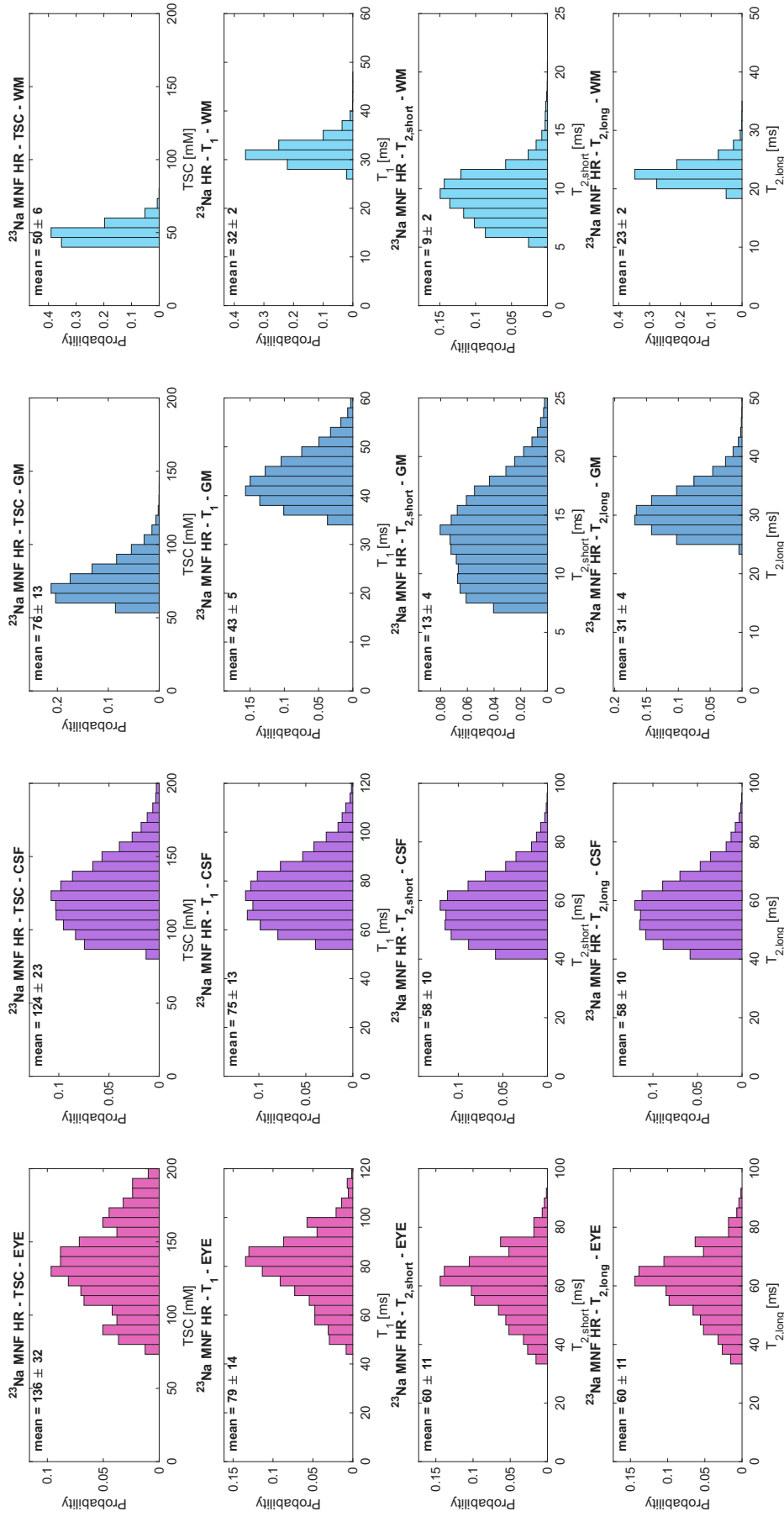


Figure S12. Histograms of the measurements in subject 3, from the ^{23}Na MNF HR data (TSC, T_1 , $T_{2,short}$, $T_{2,long}$), in the EYE, CSF, GM and WM. TSC quantification was calculated using the mean value of the $N_{REF} = 80\%$ highest values measured in the eye ROI as a reference (from the eye mask applied to the pre-normalized TSC map), considering 98% water content and 145 mM NaCl concentration (TSC reference) in the vitreous humor of the eye. Histograms represent the $N_{ROI} = 90\%$ highest values in each ROI.

Subject 4 - ^{23}Na MNF HR (REF 80%, ROI 90%)

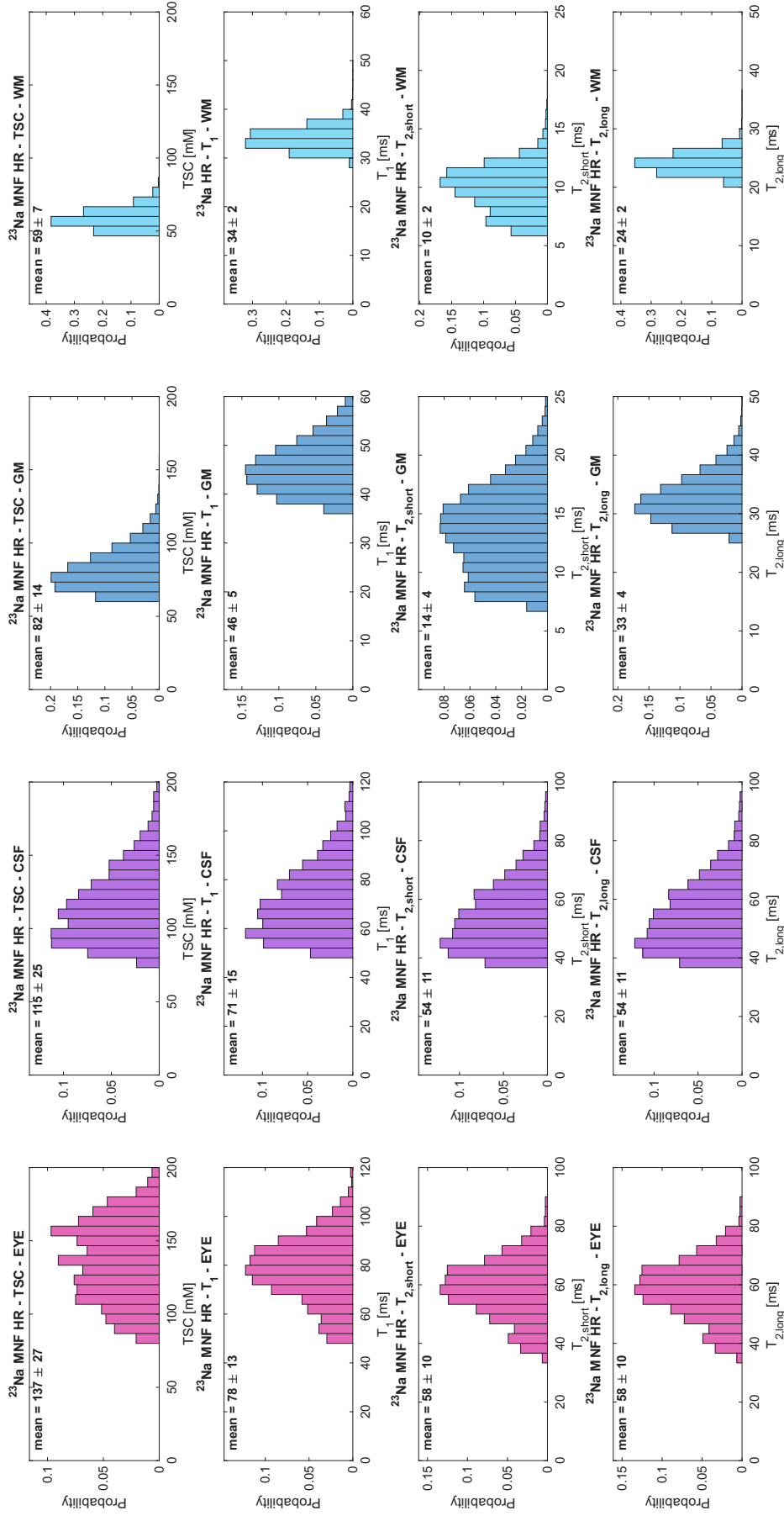


Figure S13. Histograms of the measurements in subject 4, from the ^{23}Na MNF HR data (TSC, T_1 , $T_{2,short}$, $T_{2,long}$), in the EYE, CSF, GM and WM. TSC quantification was calculated using the mean value of the $N_{REF} = 80\%$ highest values measured in the eye ROI as a reference (from the eye mask applied to the pre-normalized TSC map), considering 98% water content and 145 mM NaCl concentration (TSC reference) in the vitreous humor of the eye. Histograms represent the $N_{ROI} = 90\%$ highest values in each ROI.

Subject 5 - ^{23}Na MNF HR (REF 80%, ROI 90%)

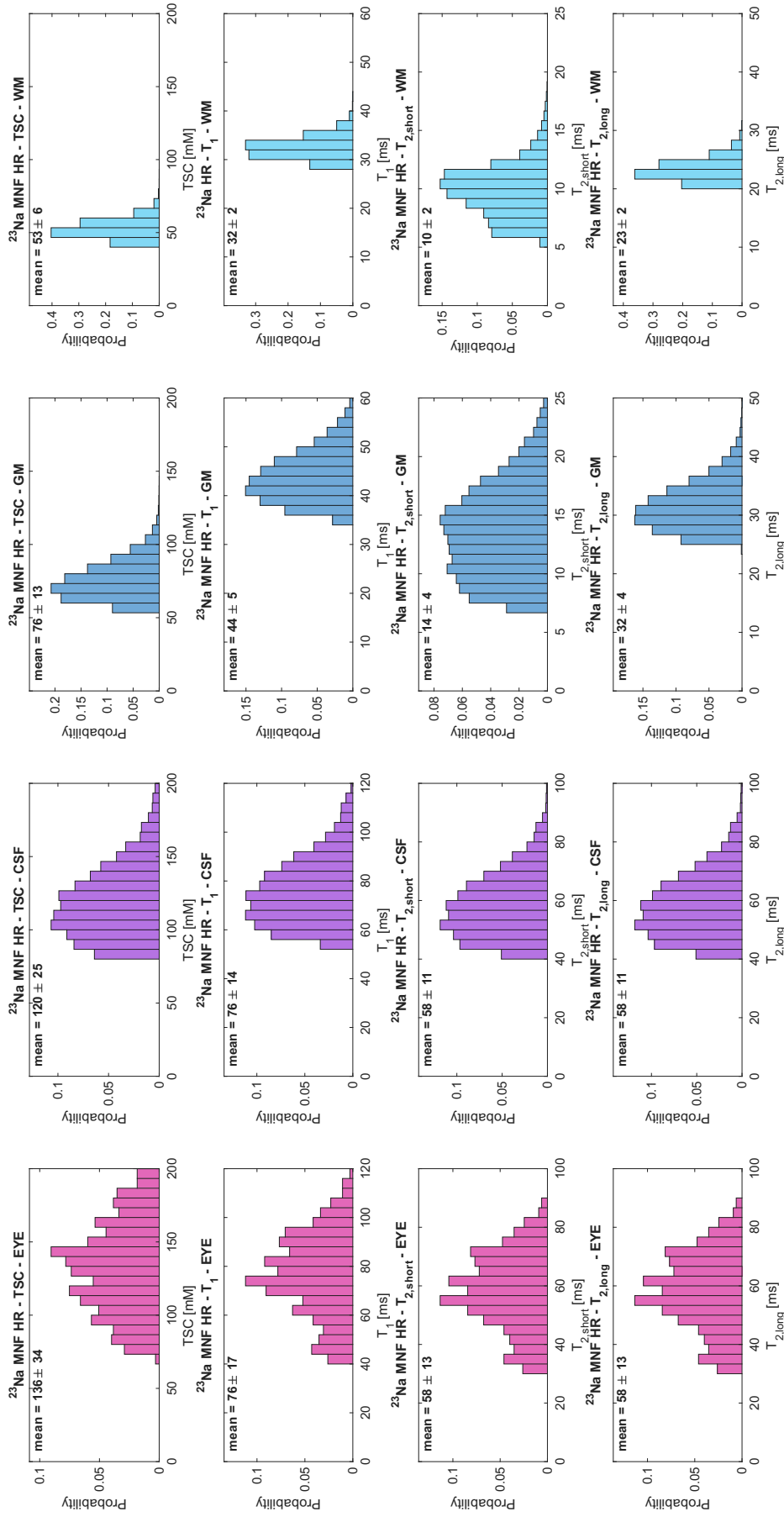


Figure S14. Histograms of the measurements in subject 5, from the ^{23}Na MNF HR data (TSC, T_1 , $T_{2,short}$, $T_{2,long}$), in the EYE, CSF, GM and WM. TSC quantification was calculated using the mean value of the $N_{REF} = 80\%$ highest values measured in the eye ROI as a reference (from the eye mask applied to the pre-normalized TSC map), considering 98% water content and 145 mM NaCl concentration (TSC reference) in the vitreous humor of the eye. Histograms represent the $N_{ROI} = 90\%$ highest values in each ROI.

Subject 6 - ^{23}Na MNF HR (REF 80%, ROI 90%)

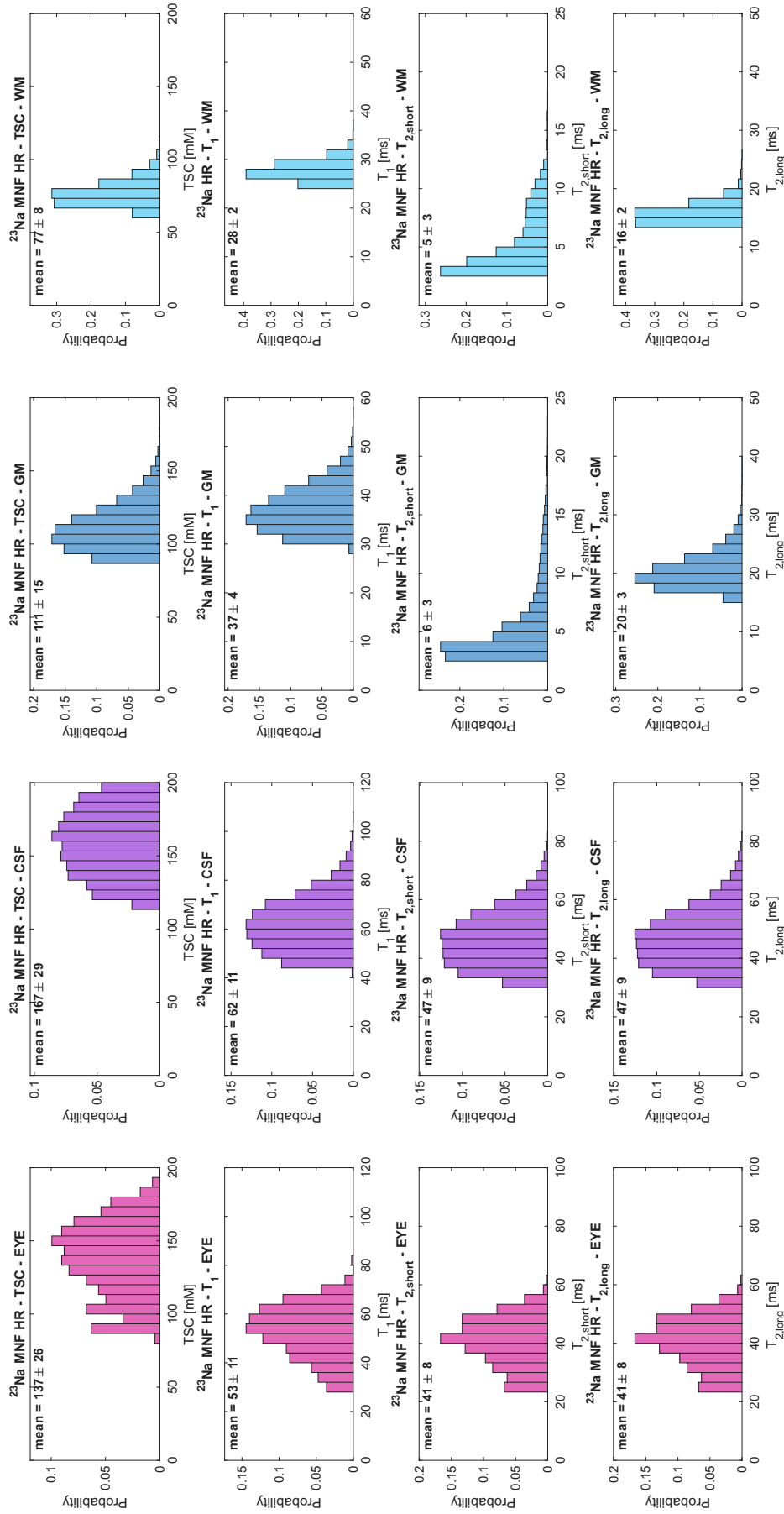


Figure S15. Histograms of the measurements in subject 6, from the ^{23}Na MNF HR data (TSC, T_1 , $T_{2,\text{short}}$, $T_{2,\text{long}}$), in the EYE, CSF, GM and WM. TSC quantification was calculated using the mean value of the $N_{\text{REF}} = 80\%$ highest values measured in the eye ROI as a reference (from the eye mask applied to the pre-normalized TSC map), considering 98% water content and 145 mM NaCl concentration (TSC reference) in the vitreous humor of the eye. Histograms represent the $N_{\text{ROI}} = 90\%$ highest values in each ROI.

Subject 7 - ^{23}Na MNF HR (REF 80%, ROI 90%)

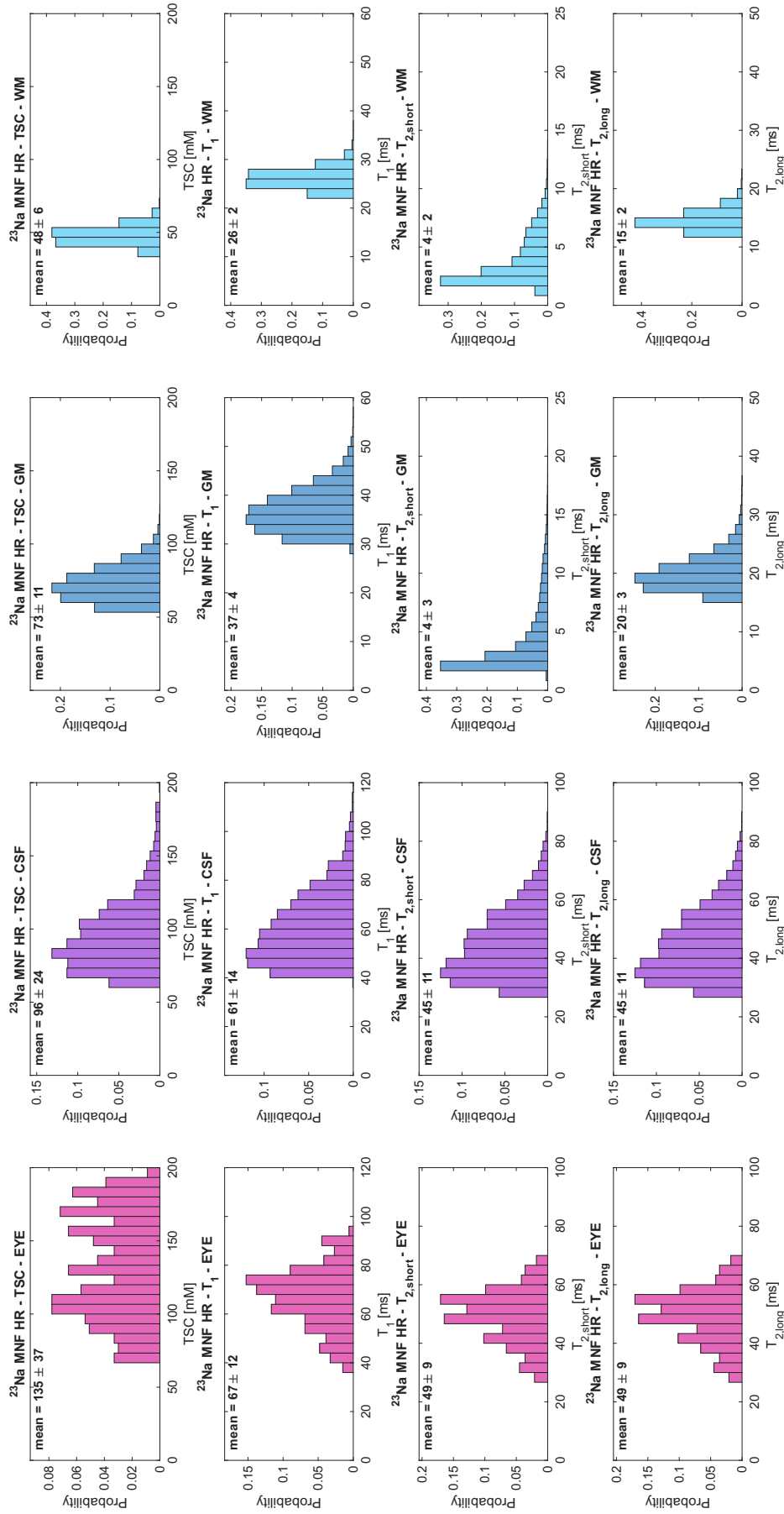


Figure S16. Histograms of the measurements in subject 7, from the ^{23}Na MNF HR data (TSC, T_1 , $T_{2,short}$, $T_{2,long}$), in the EYE, CSF, GM and WM. TSC quantification was calculated using the mean value of the $N_{REF} = 80\%$ highest values measured in the eye ROI as a reference (from the eye mask applied to the pre-normalized TSC map), considering 98% water content and 145 mM NaCl concentration (TSC reference) in the vitreous humor of the eye. Histograms represent the $N_{ROI} = 90\%$ highest values in each ROI.

Subject 1 - ^{23}Na MNF LR (REF 80%, ROI 90%)

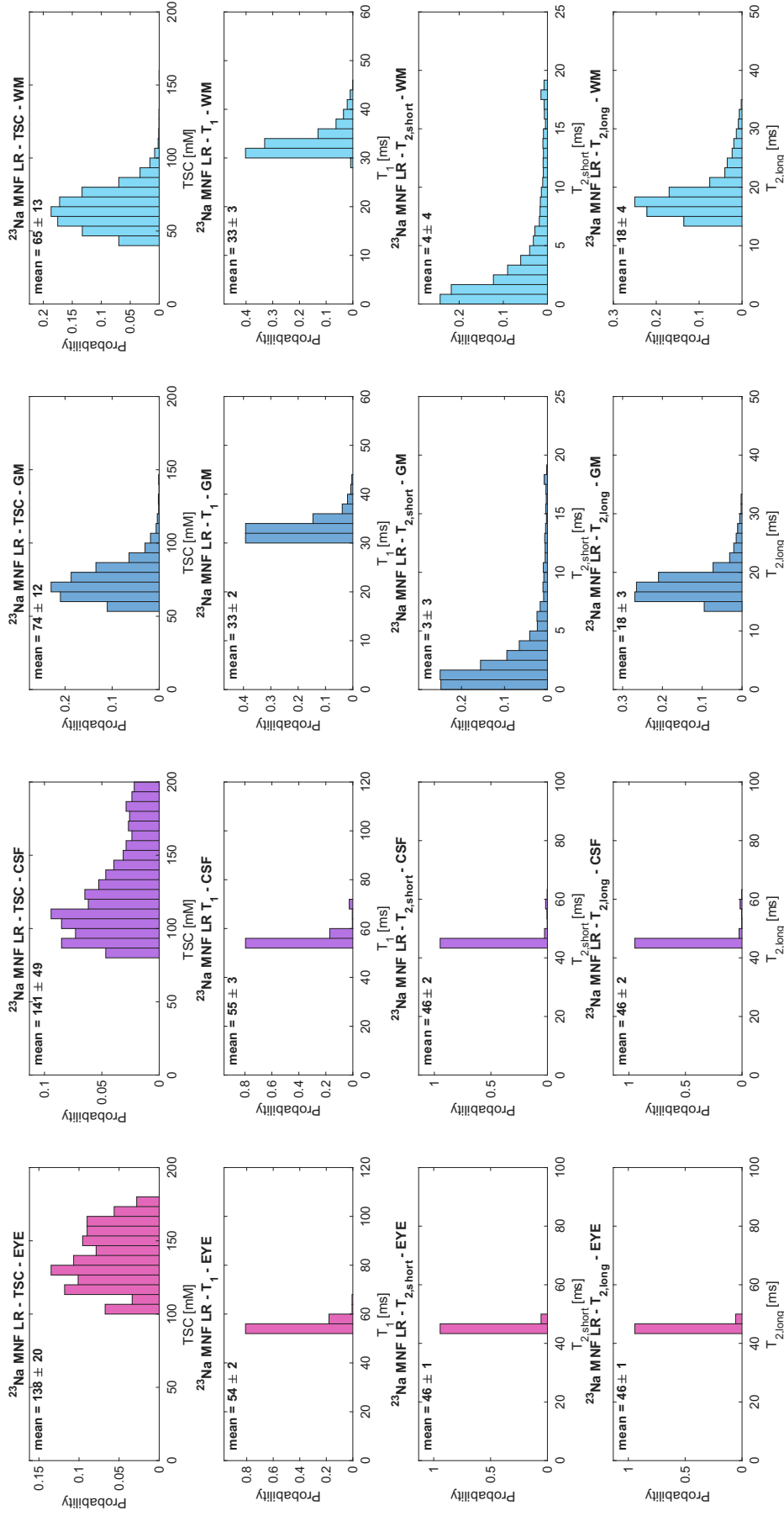


Figure S17. Histograms of the measurements in subject 1, from the ^{23}Na MNF LR data (TSC, T_1 , $T_{2,short}$, $T_{2,long}$), in the EYE, CSF, GM and WM. TSC quantification was calculated using the mean value of the $N_{\text{REF}} = 80\%$ highest values measured in the eye ROI as a reference (from the eye mask applied to the pre-normalized TSC map), considering 98% water content and 145 mM NaCl concentration (TSC reference) in the vitreous humor of the eye. Histograms represent the $N_{\text{ROI}} = 90\%$ highest values in each ROI.

Subject 2 - ^{23}Na MNF LR (REF 80%, ROI 90%)

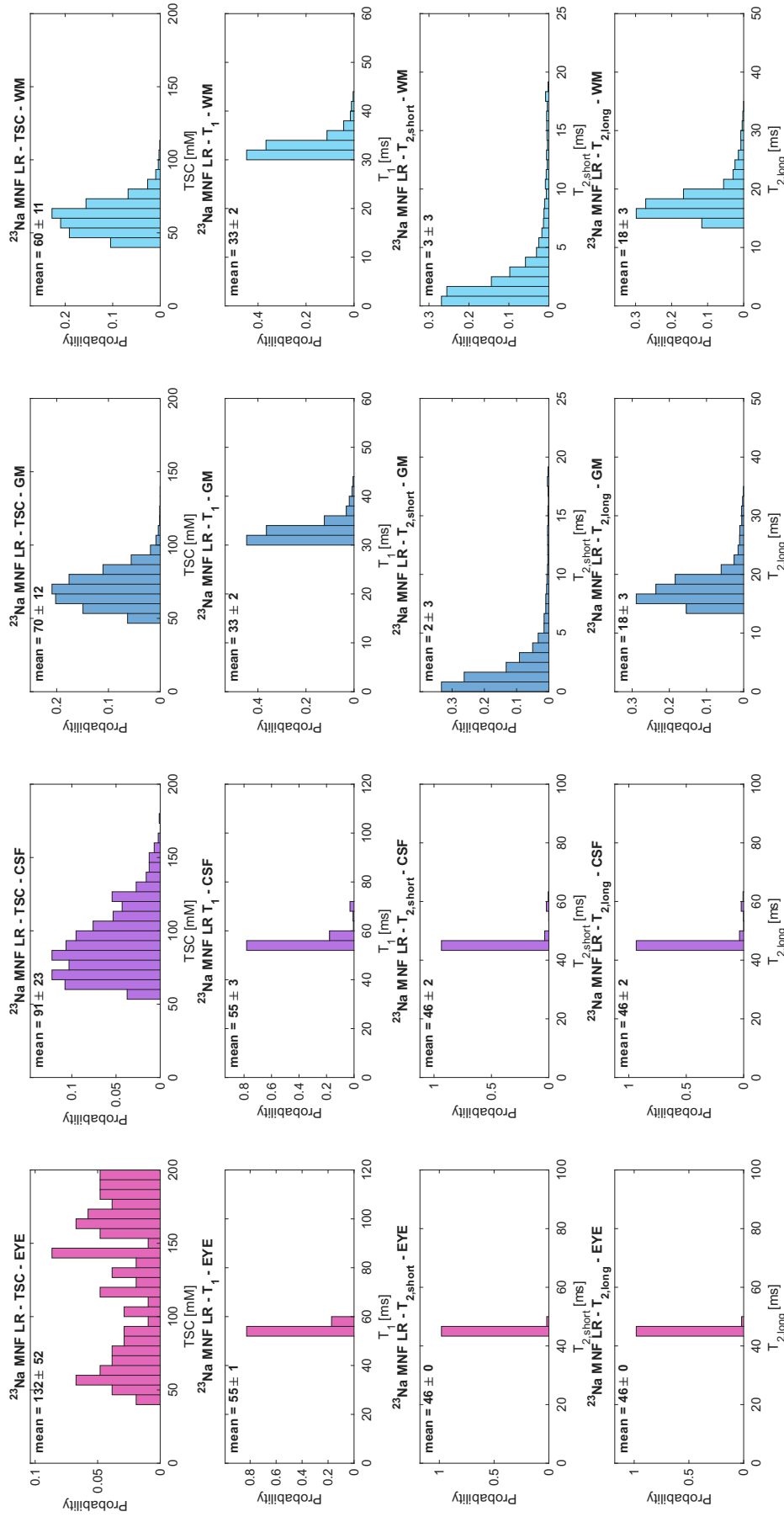


Figure S18. Histograms of the measurements in subject 2, from the ^{23}Na MNF LR data (TSC, T_1 , $T_{2,short}$, $T_{2,long}$), in the EYE, CSF, GM and WM. TSC quantification was calculated using the mean value of the $N_{REF} = 80\%$ highest values measured in the eye ROI as a reference (from the eye mask applied to the pre-normalized TSC map), considering 98% water content and 145 mM NaCl concentration (TSC reference) in the vitreous humor of the eye. Histograms represent the $N_{ROI} = 90\%$ highest values in each ROI.

Subject 3 - ^{23}Na MNF LR (REF 80%, ROI 90%)

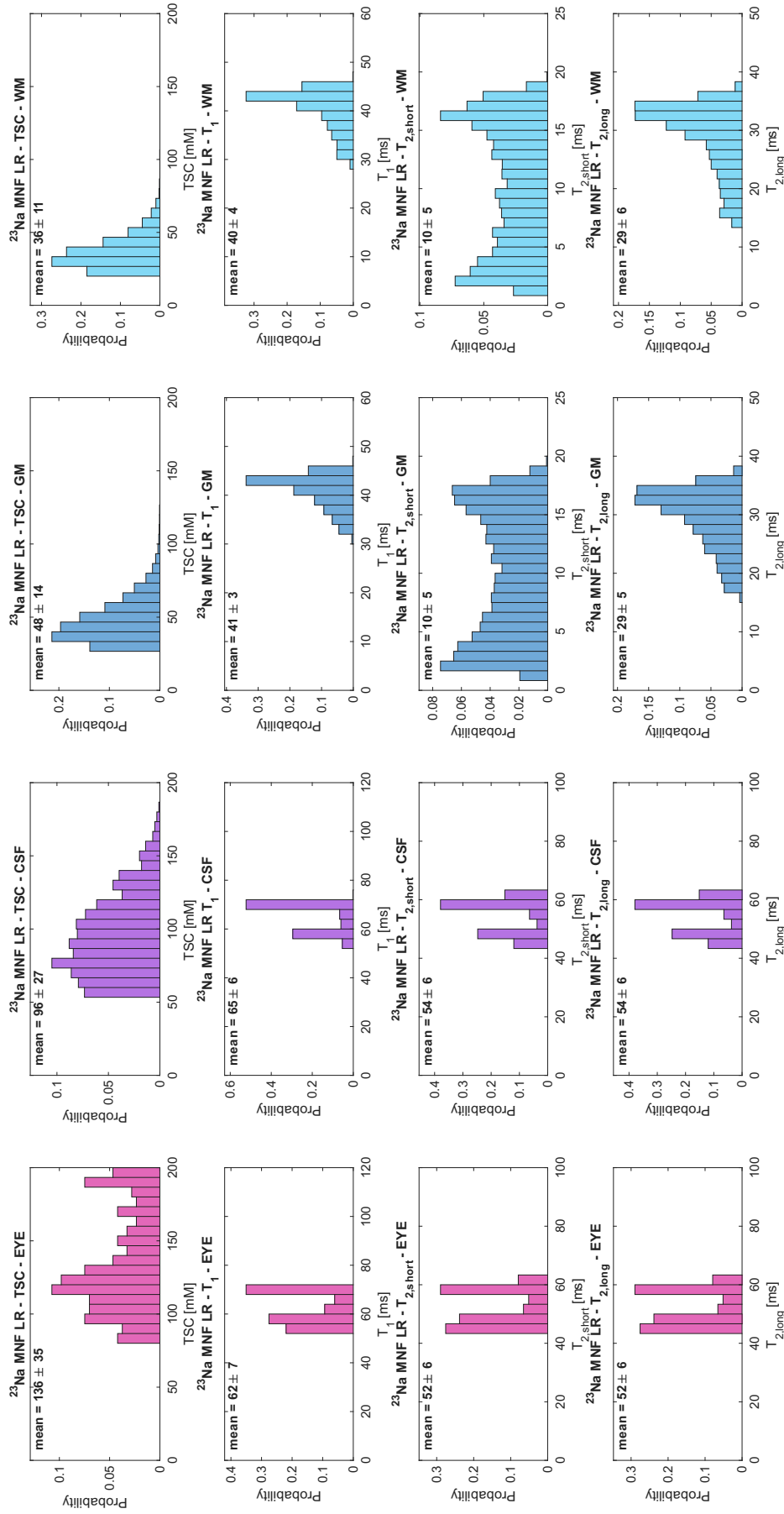


Figure S19. Histograms of the measurements in subject 3, from the ^{23}Na MNF LR data (TSC, T_1 , $T_{2,short}$, $T_{2,long}$), in the EYE, CSF, GM and WM. TSC quantification was calculated using the mean value of the $N_{REF} = 80\%$ highest values measured in the eye ROI as a reference (from the eye mask applied to the pre-normalized TSC map), considering 98% water content and 145 mM NaCl concentration (TSC reference) in the vitreous humor of the eye. Histograms represent the $N_{ROI} = 90\%$ highest values in each ROI.

Subject 4 - ^{23}Na MNF LR (REF 80%, ROI 90%)

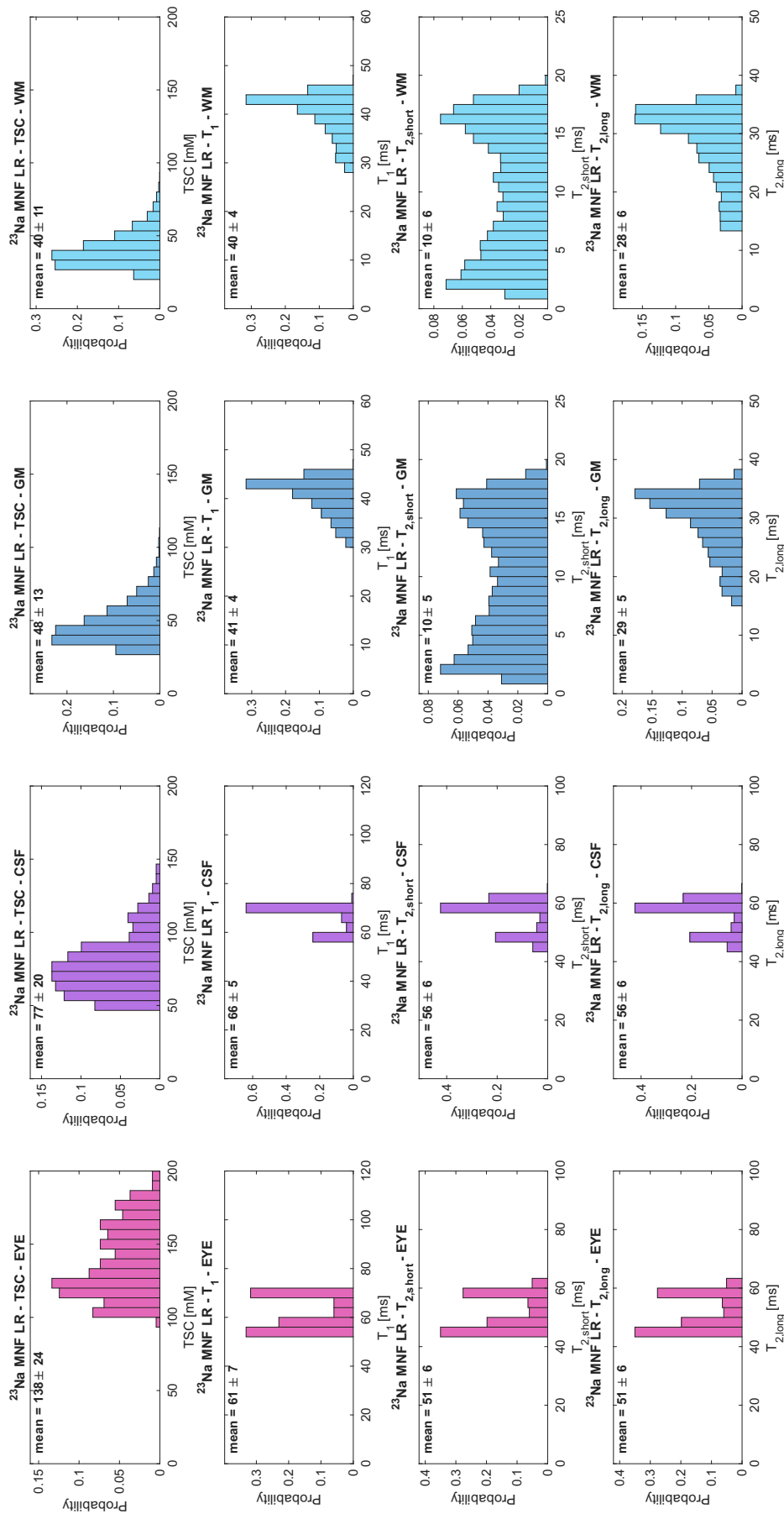


Figure S20. Histograms of the measurements in subject 4, from the ^{23}Na MNF LR data (TSC, T_1 , $T_{2,short}$, $T_{2,long}$), in the EYE, CSF, GM and WM. TSC quantification was calculated using the mean value of the $N_{REF} = 80\%$ highest values measured in the eye ROI as a reference (from the eye mask applied to the pre-normalized TSC map), considering 98% water content and 145 mM NaCl concentration (TSC reference) in the vitreous humor of the eye. Histograms represent the $N_{ROI} = 90\%$ highest values in each ROI.

Subject 5 - ^{23}Na MNF LR (REF 80%, ROI 90%)

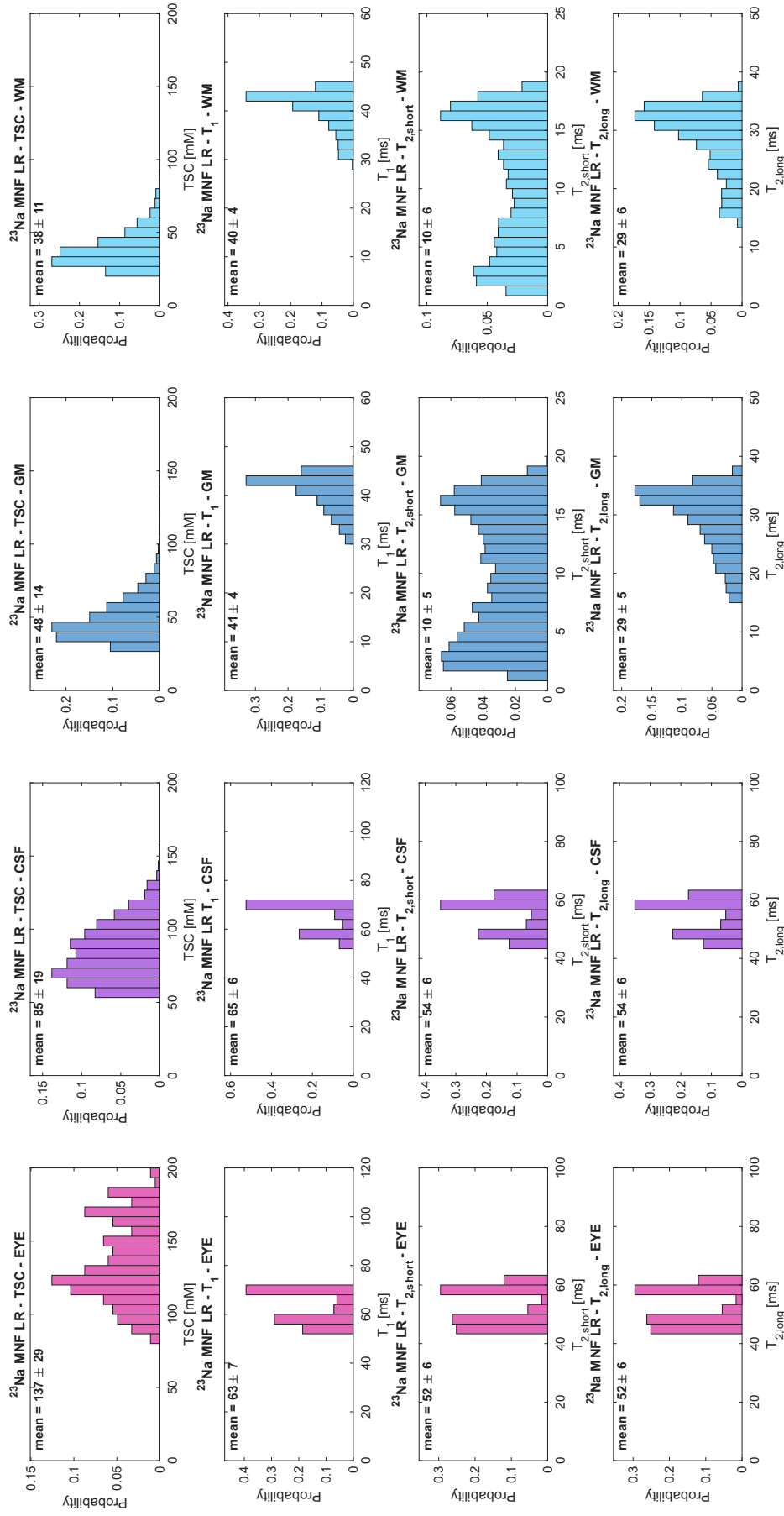


Figure S21. Histograms of the measurements in subject 5, from the ^{23}Na MNF LR data (TSC, T_1 , $T_{2,\text{short}}$, $T_{2,\text{long}}$), in the EYE, CSF, GM and WM. TSC quantification was calculated using the mean value of the $N_{\text{REF}} = 80\%$ highest values measured in the eye ROI as a reference (from the eye mask applied to the pre-normalized TSC map), considering 98% water content and 145 mM NaCl concentration (TSC reference) in the vitreous humor of the eye. Histograms represent the $N_{\text{ROI}} = 90\%$ highest values in each ROI.

Subject 6 - ^{23}Na MNF LR (REF 80%, ROI 90%)

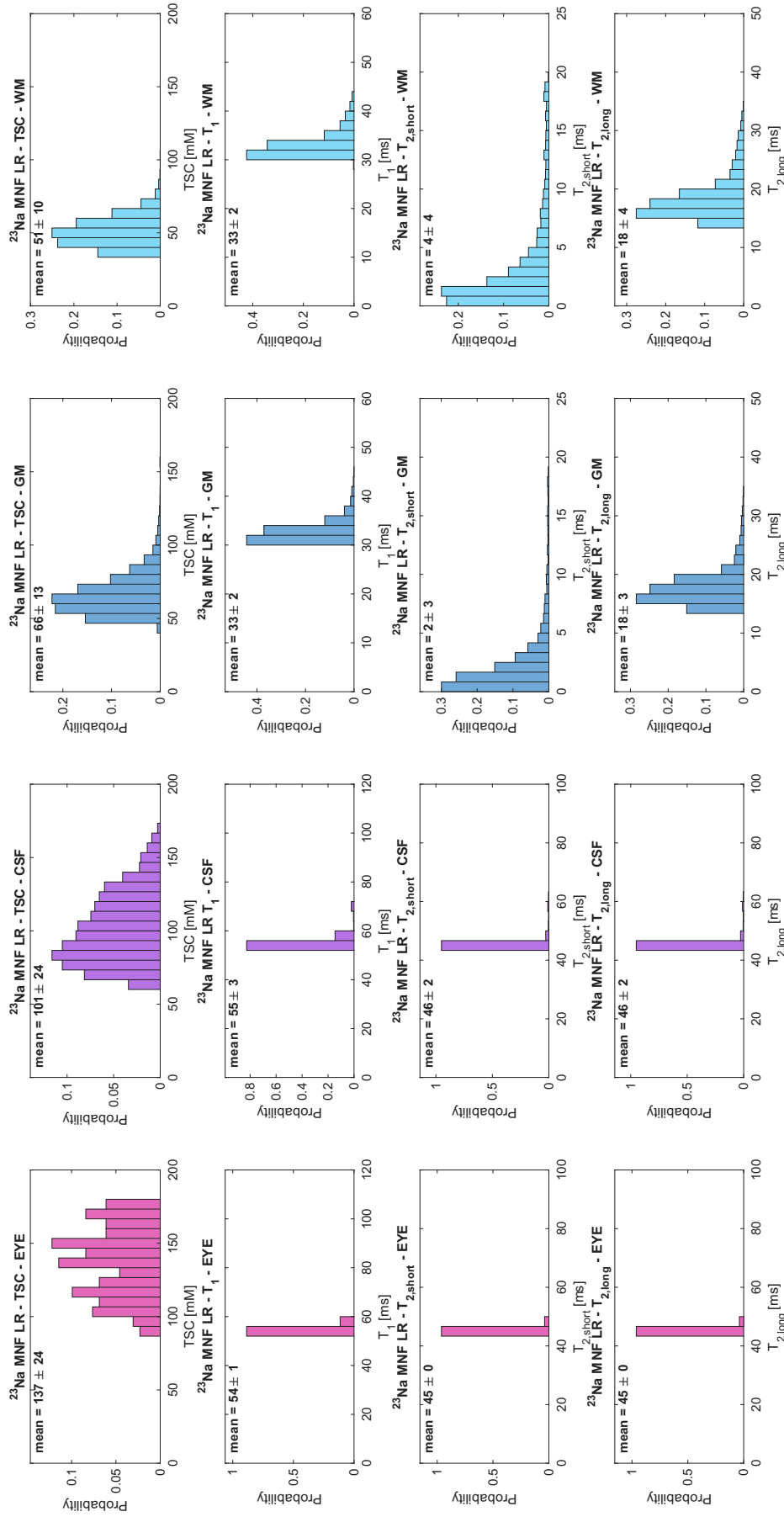


Figure S22. Histograms of the measurements in subject 6, from the ^{23}Na MNF LR data (TSC, T_1 , $T_{2,short}$, $T_{2,long}$), in the EYE, CSF, GM and WM. TSC quantification was calculated using the mean value of the $N_{REF} = 80\%$ highest values measured in the eye ROI as a reference (from the eye mask applied to the pre-normalized TSC map), considering 98% water content and 145 mM NaCl concentration (TSC reference) in the vitreous humor of the eye. Histograms represent the $N_{ROI} = 90\%$ highest values in each ROI.

Subject 7 - ^{23}Na MNF LR (REF 80%, ROI 90%)

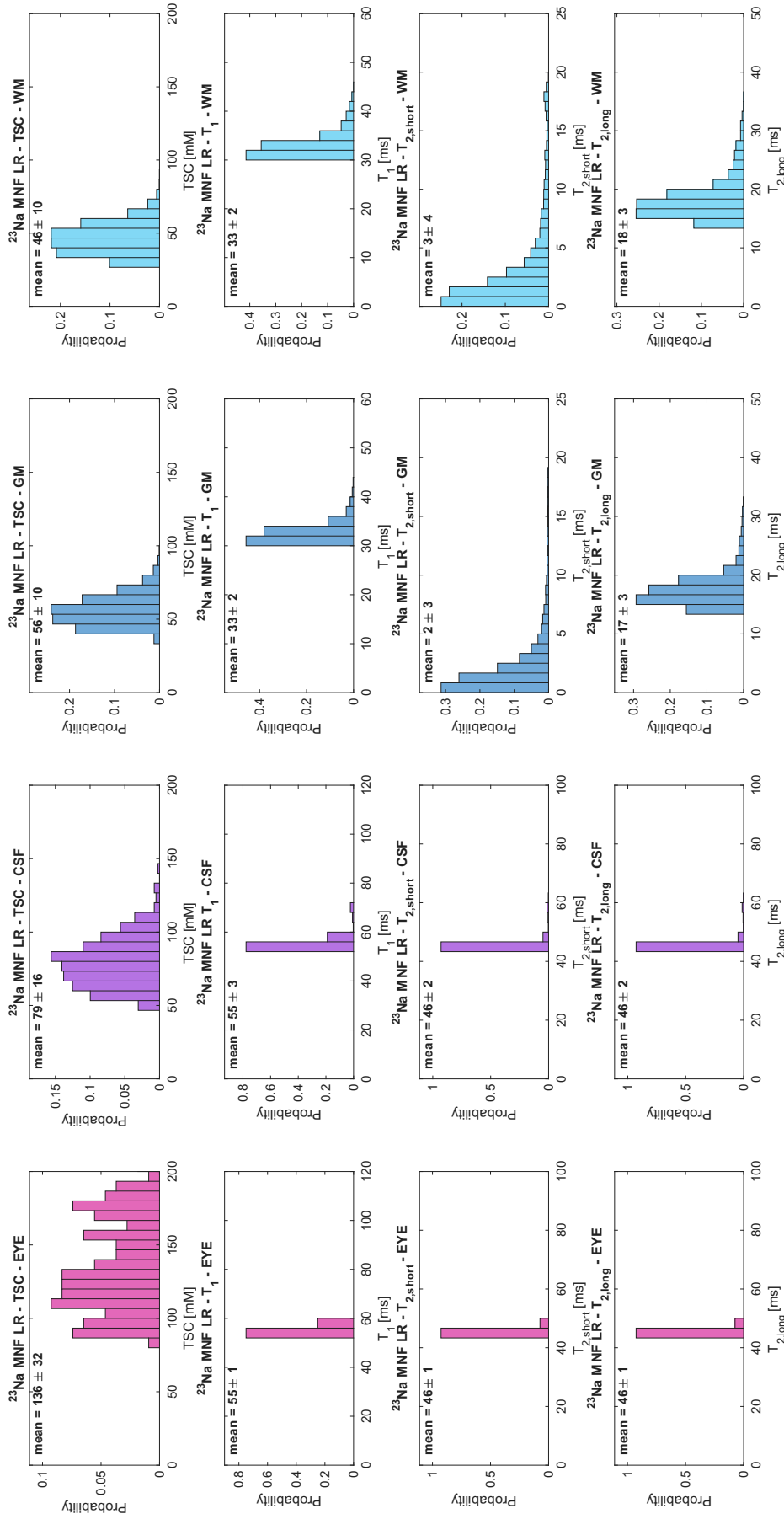


Figure S23. Histograms of the measurements in subject 7, from the ^{23}Na MNF LR data (TSC, T_1 , $T_{2,short}$, $T_{2,long}$), in the EYE, CSF, GM and WM. TSC quantification was calculated using the mean value of the $N_{REF} = 80\%$ highest values measured in the eye ROI as a reference (from the eye mask applied to the pre-normalized TSC map), considering 98% water content and 145 mM NaCl concentration (TSC reference) in the vitreous humor of the eye. Histograms represent the $N_{ROI} = 90\%$ highest values in each ROI.

Subject 5 - ^{23}Na FLORET (REF 80%, ROI 90%)

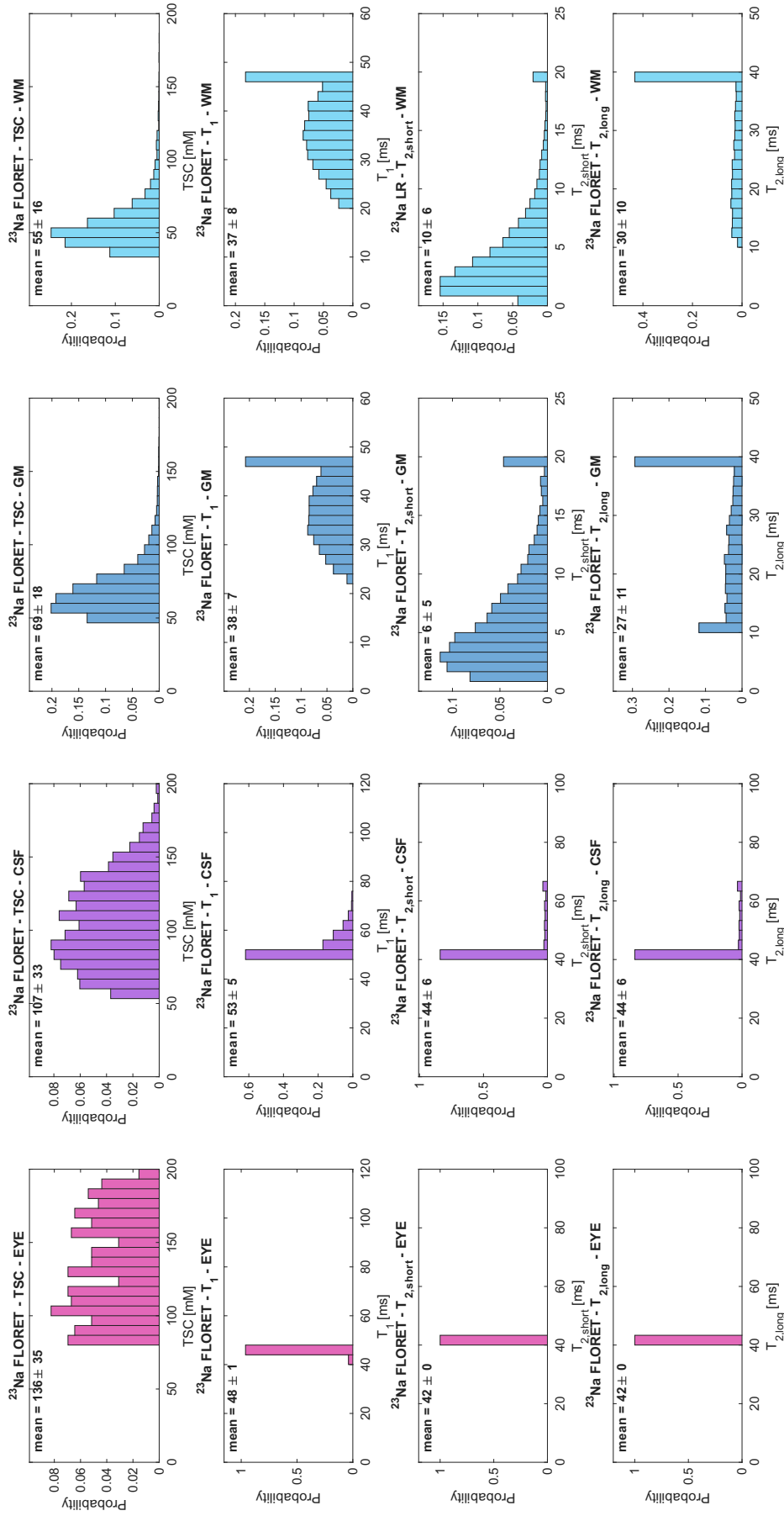


Figure S24. Histograms of the measurements in subject 5, from the ^{23}Na FLORET data (TSC, T_1 , $T_{2,short}$, $T_{2,long}$), in the EYE, CSF, GM and WM. TSC quantification was calculated using the mean value of the $N_{REF} = 80\%$ highest values measured in the eye ROI as a reference (from the eye mask applied to the pre-normalized TSC map), considering 98% water content and 145 mM NaCl concentration (TSC reference) in the vitreous humor of the eye. Histograms represent the $N_{ROI} = 90\%$ highest values in each ROI.

Subject 6 - ^{23}Na FLORET (REF 80%, ROI 90%)

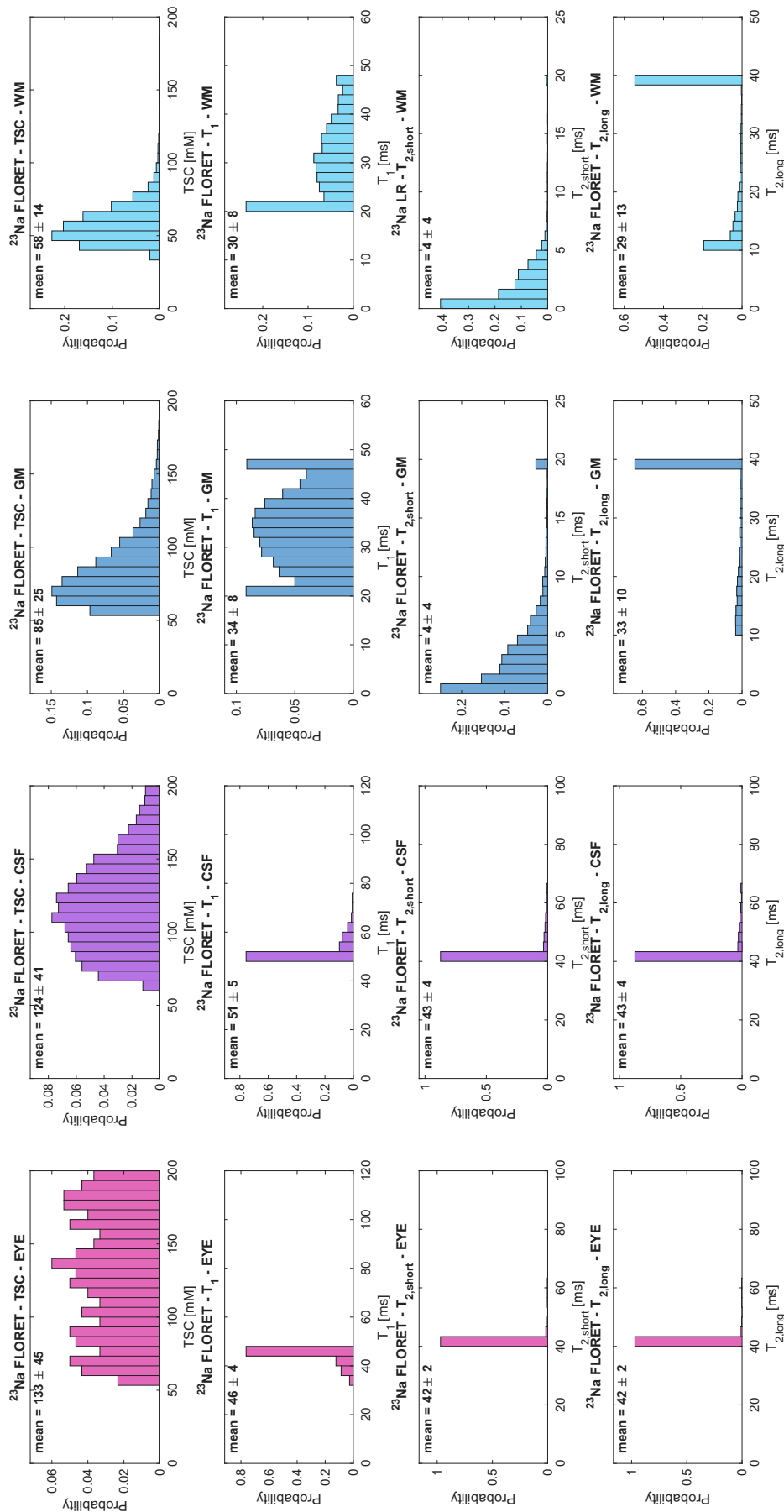


Figure S25. Histograms of the measurements in subject 6, from the ^{23}Na FLORET data (TSC, T_1 , $T_{2,short}$, $T_{2,long}$), in the EYE, CSF, GM and WM. TSC quantification was calculated using the mean value of the $N_{\text{REF}} = 80\%$ highest values measured in the eye ROI as a reference (from the eye mask applied to the pre-normalized TSC map), considering 98% water content and 145 mM NaCl concentration (TSC reference) in the vitreous humor of the eye. Histograms represent the $N_{\text{ROI}} = 90\%$ highest values in each ROI.

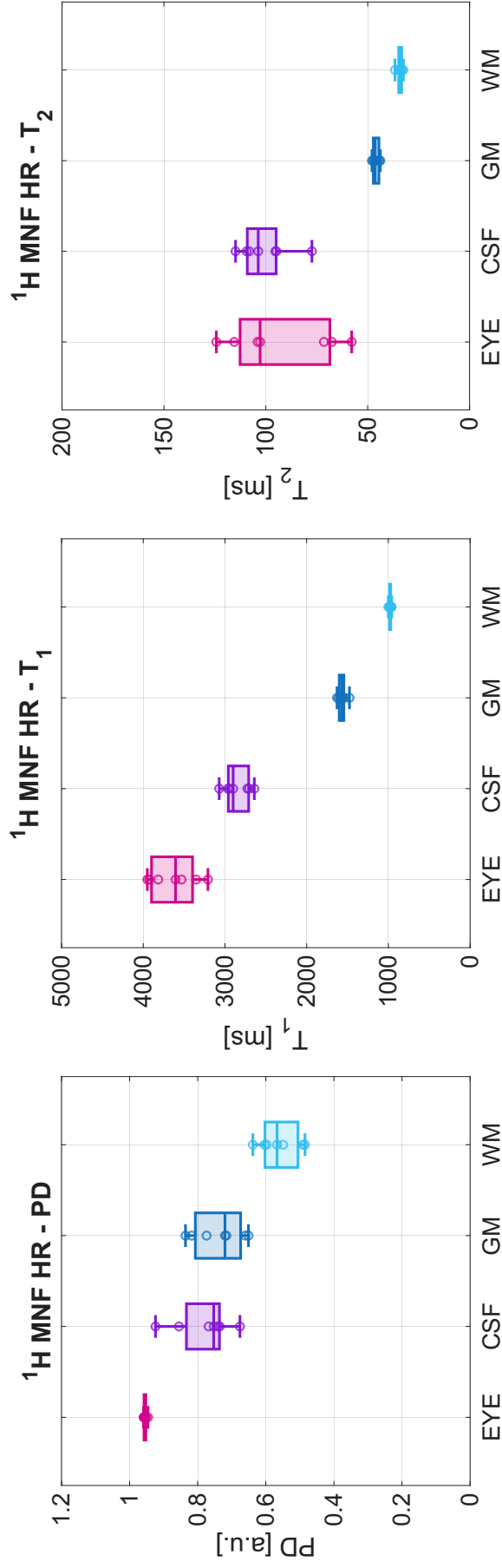


Figure S26. Boxplots of the mean values measured in all 7 subjects, from the ^1H MNF HR data (PD, T_1 , T_2), in the EYE, CSF, GM and WM. PD normalization was calculated using the mean value of the $N_{\text{REF}} = 80\%$ highest values measured in the eye ROI as a reference (from the eye mask applied to the pre-normalized PD map), considering 98% water content in the vitreous humor of the eye. Mean values were calculated over the $N_{\text{ROI}} = 90\%$ highest values in each ROI.

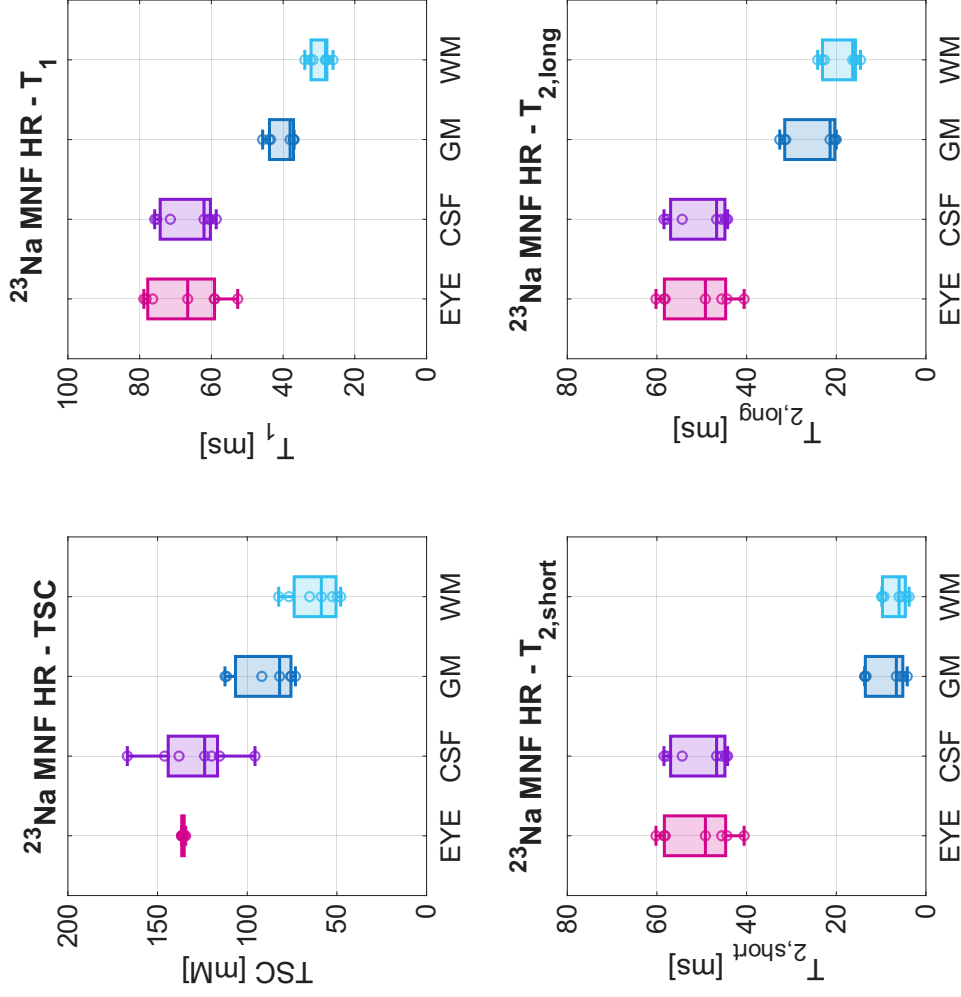


Figure S27. Boxplots of the mean values measured in all 7 subjects, from the ^{23}Na MNF HR data (TSC, T_1 , $T_{2,short}$, $T_{2,long}$), in the EYE, CSF, GM and WM. TSC quantification was calculated using the mean value of the $N_{REF} = 80\%$ highest values measured in the eye ROI as a reference (from the eye mask applied to the pre-normalized TSC map), considering 98% water content and 145 mM NaCl concentration (TSC reference) in the vitreous humor of the eye. Mean values were calculated over the $N_{ROI} = 90\%$ highest values in each ROI.

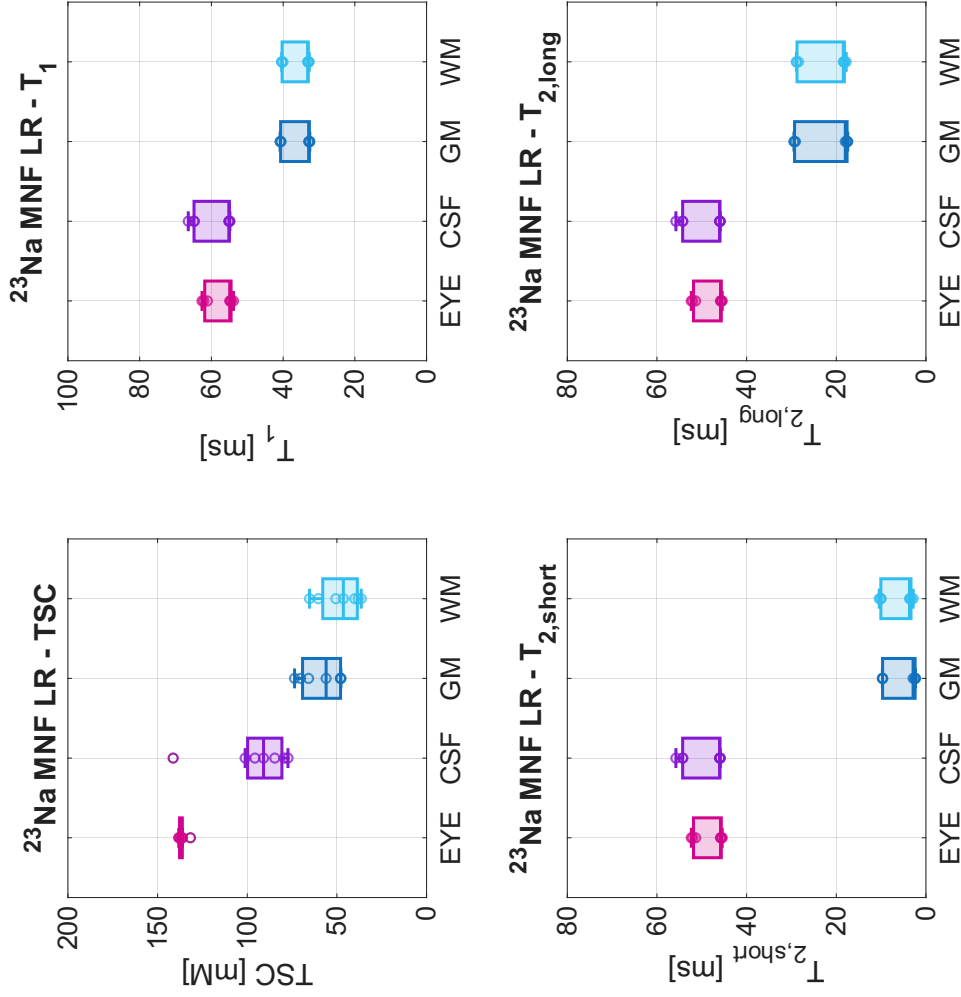


Figure S28. Boxplots of the mean values measured in all 7 subjects, from the ^{23}Na MNF LR data (TSC, T_1 , $T_{2,\text{short}}$, $T_{2,\text{long}}$), in the EYE, CSF, GM and WM. TSC quantification was calculated using the mean value of the $N_{\text{REF}} = 80\%$ highest values measured in the eye ROI as a reference (from the eye mask applied to the pre-normalized TSC map), considering 98% water content and 145 mM NaCl concentration (TSC reference) in the vitreous humor of the eye. Mean values were calculated over the $N_{\text{ROI}} = 90\%$ highest values in each ROI.

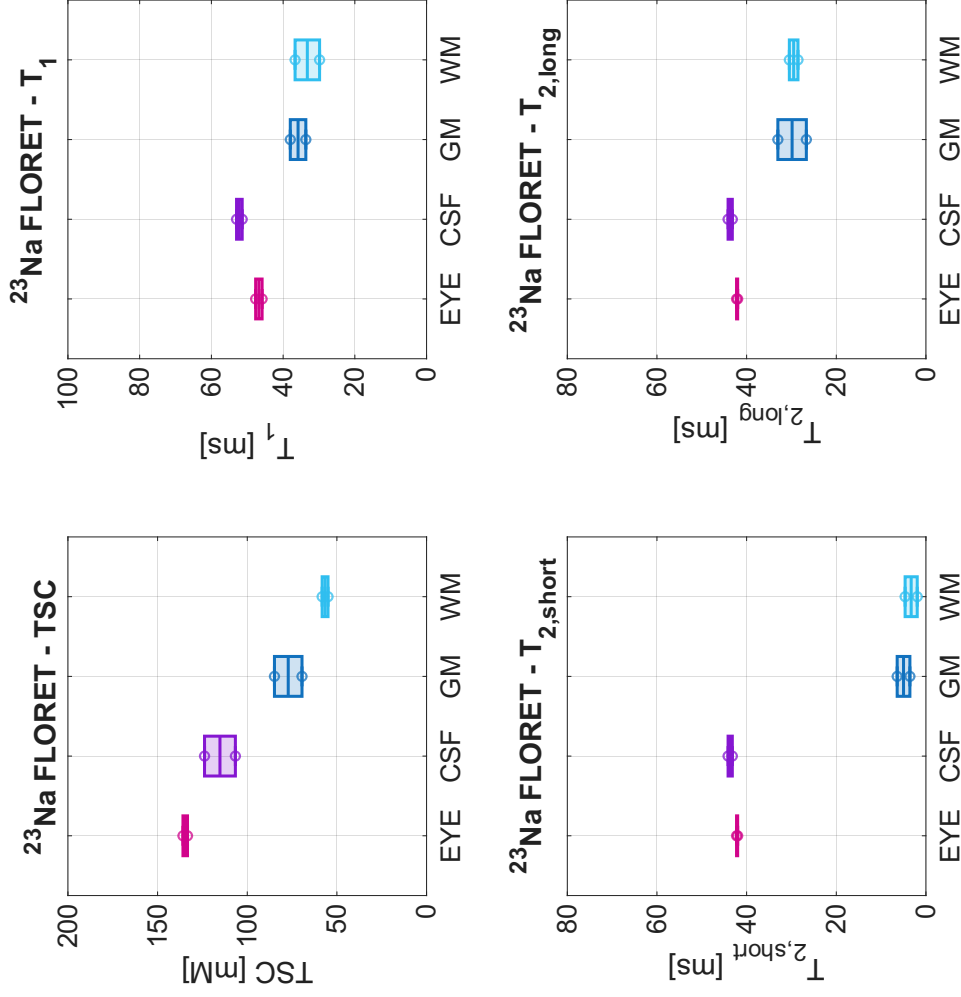


Figure S29. Boxplots of the mean values measured in subjects 5 and 6 only, from the ^{23}Na FLORET data (TSC, T_1 , $T_{2,short}$, $T_{2,long}$), in the EYE, CSF, GM and WM. TSC quantification was calculated using the mean value of the $N_{\text{REF}} = 80\%$ highest values measured in the eye ROI as a reference (from the eye mask applied to the pre-normalized TSC map), considering 98% water content and 145 mM NaCl concentration (TSC reference) in the vitreous humor of the eye. Mean values were calculated over the $N_{\text{ROI}} = 90\%$ highest values in each ROI.

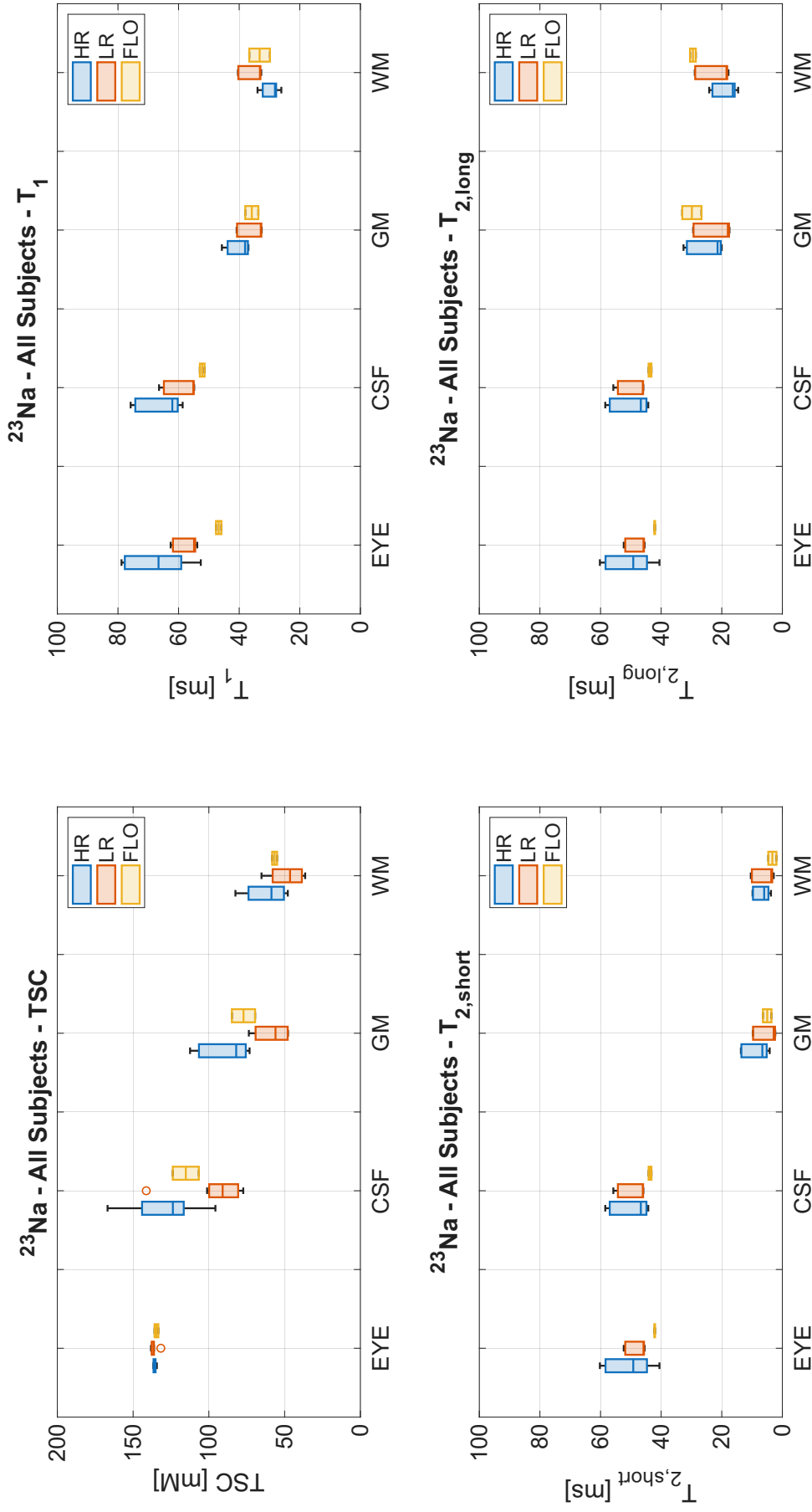


Figure S30. Boxplots for comparison of the mean values measured from the ^{23}Na MNF HR (7 subjects), LR (7 subjects) and FLORET (FLO, 2 subjects: 5 and 6) data (T_{SC} , T_1 , $T_{2,\text{short}}$, $T_{2,\text{long}}$), in the EYE, CSF, GM and WM. TSC quantification was calculated using the mean value of the $N_{\text{REF}} = 80\%$ highest values measured in the eye ROI as a reference (from the eye mask applied to the pre-normalized TSC map), considering 98% water content and 145 mM NaCl concentration (TSC reference) in the vitreous humor of the eye. Mean values were calculated over the $N_{\text{ROI}} = 90\%$ highest values in each ROI.

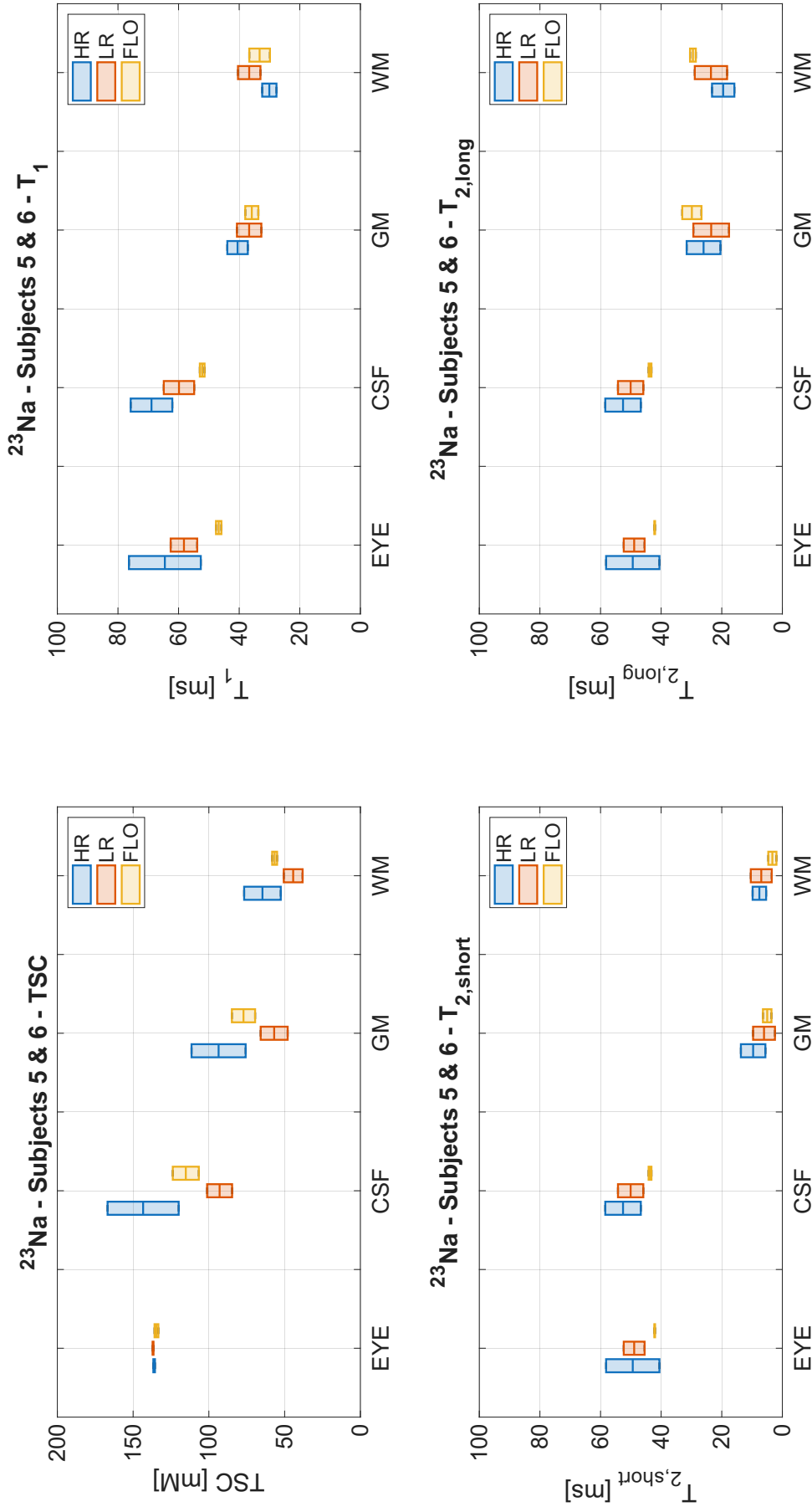


Figure S31. Boxplots for comparison of the mean values measured in subjects 5 and 6 only, from the ^{23}Na MNF HR, LR and FLORET (FLO) data ($T_{2,\text{short}}$, $T_{2,\text{short}}$), in the EYE, CSF, GM and WM. TSC quantification was calculated using the mean value of the $N_{\text{REF}} = 80\%$ highest values measured in the eye ROI as a reference (from the eye mask applied to the pre-normalized TSC map), considering 98% water content and 145 mM NaCl concentration ($T_{2,\text{short}}$ reference) in the vitreous humor of the eye. Mean values were calculated over the $N_{\text{ROI}} = 90\%$ highest values in each ROI.

3 FIGURES: Multiple measurements in brain (20 N_{ROI} & 20 N_{REF} values)

In this supplementary section, we present the histograms and boxplots from multiple measurements (20 N_{ROI} & 20 N_{REF} values) of all MNF and ^{23}Na FLORET metrics in all subjects ($N = 7$).

3.1 PD & TSC quantification (20 N_{REF})

The mean value of the N_{REF} highest voxel values of the reference ROI (vitreous humor in the EYE) was used as the reference mean value of PD or TSC for generating quantitative PD and TSC maps in the brain, respectively, with $N_{REF} = 5\%$ to 100% by steps of 5% (20 N_{REF} values), using the following steps:

1. **PD & TSC:** Normalization of the initial PD and TSC maps (calculated from the matching process in MRF) by the mean value from the N_{REF} measurement and then dividing by 0.98 (considering 98% water content in the vitreous humor of the eye, and assuming that Na^+ is only present in the water compartment).
2. **TSC only:** Multiply the normalized TSC map by the reference value $\text{TSC}_{\text{EYE}} = 145 \text{ mM}$.
3. **Final maps:** This process results in 20 final PD maps normalized in arbitrary units (a.u.), and in 20 final TSC maps quantified in units of Na^+ concentration in mM (or mmol/L).

3.2 Histograms (20 N_{ROI} & 20 N_{REF})

The mean value of each metric was measured using multiple N_{ROI} highest values in each ROI, with $N_{ROI} = 5\%$ to 100% by steps of 5% (20 N_{ROI} values). Histograms show the distributions of the 400 mean PD and TSC values measured in all ROIs in each subject (from 20 $N_{ROI} \times 20 N_{REF}$ values), and of the 20 mean ^1H and ^{23}Na relaxation times values measured in all ROIs in each subject (from 20 N_{ROI} values only, as relaxation times maps do not need quantification from a reference).

3.3 Boxplots

Boxplots present of the mean values of each histogram distribution from all subjects.

3.4 Summary of the measurements

Data Acquisition	Metrics	N_{REF} (PD & TSC)	N_{ROI} (all metrics)	ROIs	Subjects
^1H MNF HR	PD, T_1 , T_2	5:5:100%	5:5:100%	EYE, CSF GM, WM	1-7
^{23}Na MNF HR	TSC, T_1 , $T_{2,\text{short}}$, $T_{2,\text{long}}$	5:5:100%	5:5:100%	EYE, CSF GM, WM	1-7
^{23}Na MNF LR	TSC, T_1 , $T_{2,\text{short}}$, $T_{2,\text{long}}$	5:5:100%	5:5:100%	EYE, CSF GM, WM	1-7
^{23}Na FLORET	TSC, T_1 , $T_{2,\text{short}}$, $T_{2,\text{long}}$	5:5:100%	5:5:100%	EYE, CSF GM, WM	5, 6

For N_{REF} and N_{ROI} , ranges of values are given as begin:step:end.

Subject 1 - ^1H MNF HR - All REF & ROI - MEAN

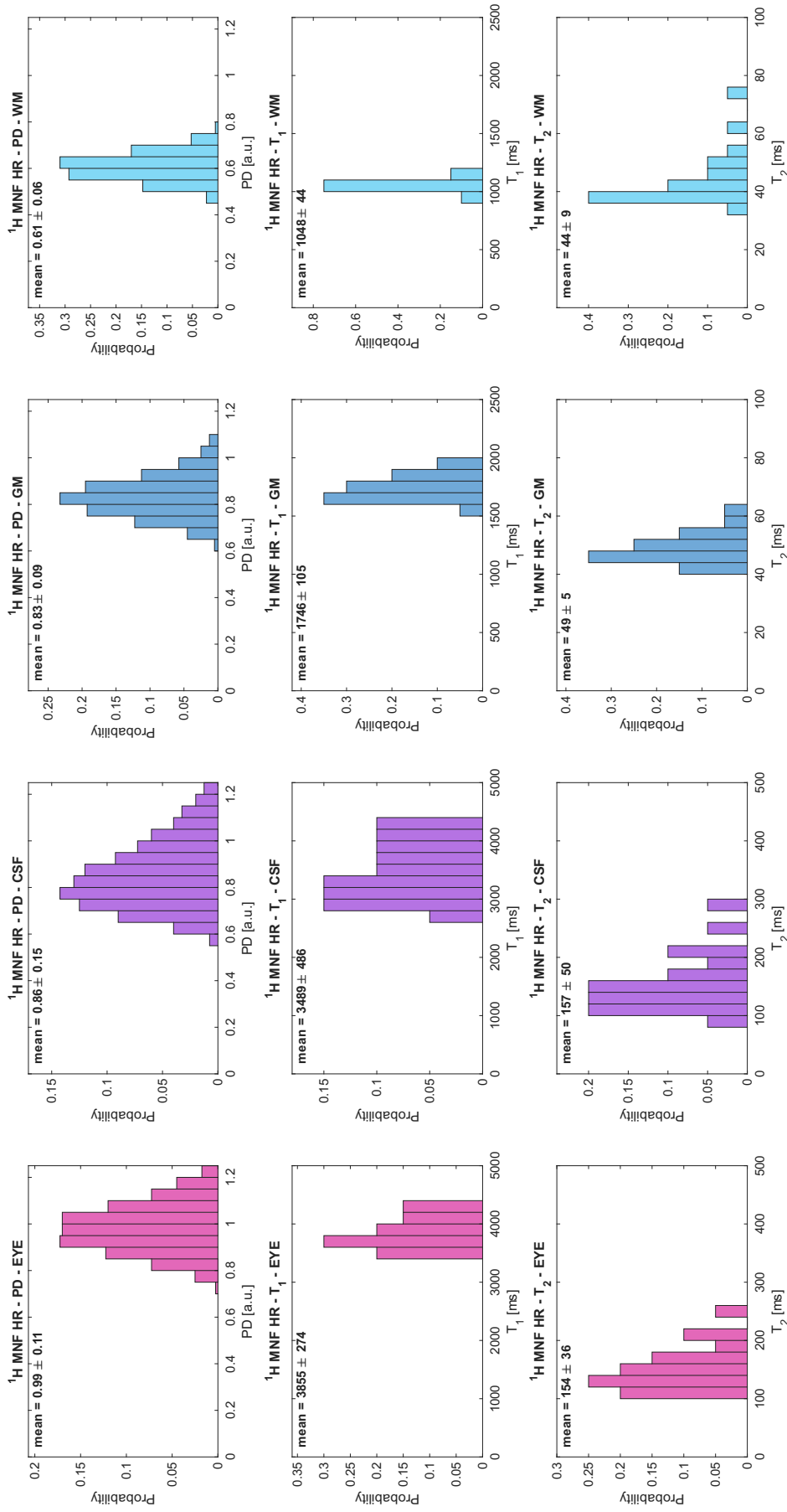


Figure S32. Histograms of the mean values from multiple measurements in subject 1, from the ^1H MNF HR data (PD, T_1 , T_2), in the EYE, CSF, GM and WM. The mean values of each metric were measured multiple times from different N_{ROI} and N_{REF} highest values in all the ROIs and in the reference ROI (eye), respectively, for PD (for a total of 400 measurements), and from different N_{ROI} highest values in all the ROIs for the relaxation times (for a total of 20 measurements). Highest values used: $N_{\text{ROI}} = 5\%$ to 100% by steps of 5% (20 values), $N_{\text{REF}} = 5\%$ to 100% by steps of 5% (20 values).

Subject 2 - ^1H MNF HR - All REF & ROI - MEAN

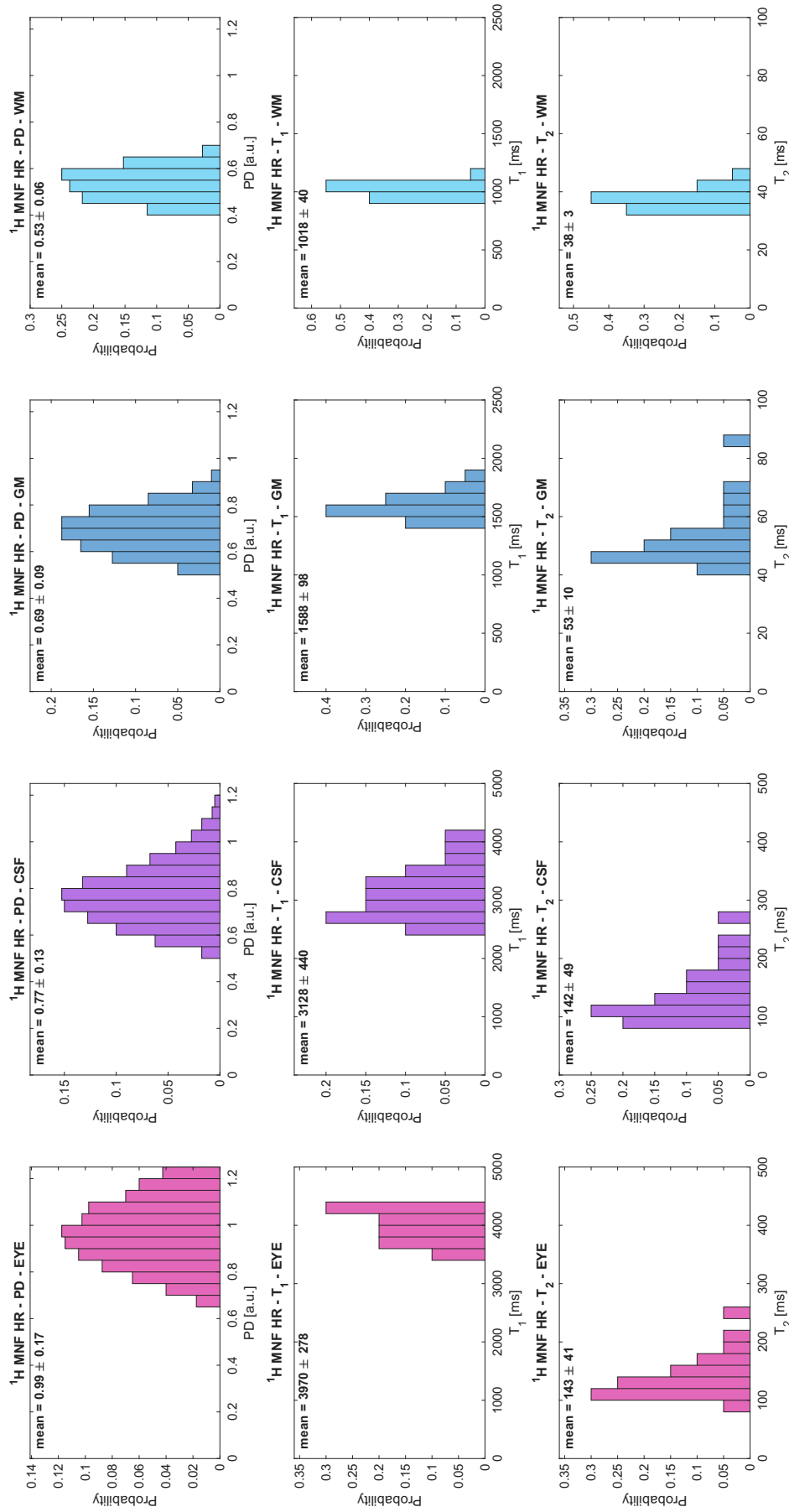


Figure S33. Histograms of the mean values from multiple measurements in subject 2, from the ^1H MNF HR data (PD, T_1 , T_2), in the EYE, CSF, GM and WM. The mean values of each metric were measured multiple times from different N_{ROI} and N_{REF} highest values in all the ROIs and in the reference ROI (eye), respectively, for PD (for a total of 400 measurements), and from different N_{ROI} highest values in all the ROIs for the relaxation times (for a total of 20 measurements). Highest values used: $N_{\text{ROI}} = 5\%$ to 100% by steps of 5%, $N_{\text{REF}} = 5\%$ to 100% by steps of 5% (20 values).

Subject 3 - ^1H MNF HR - All REF & ROI - MEAN

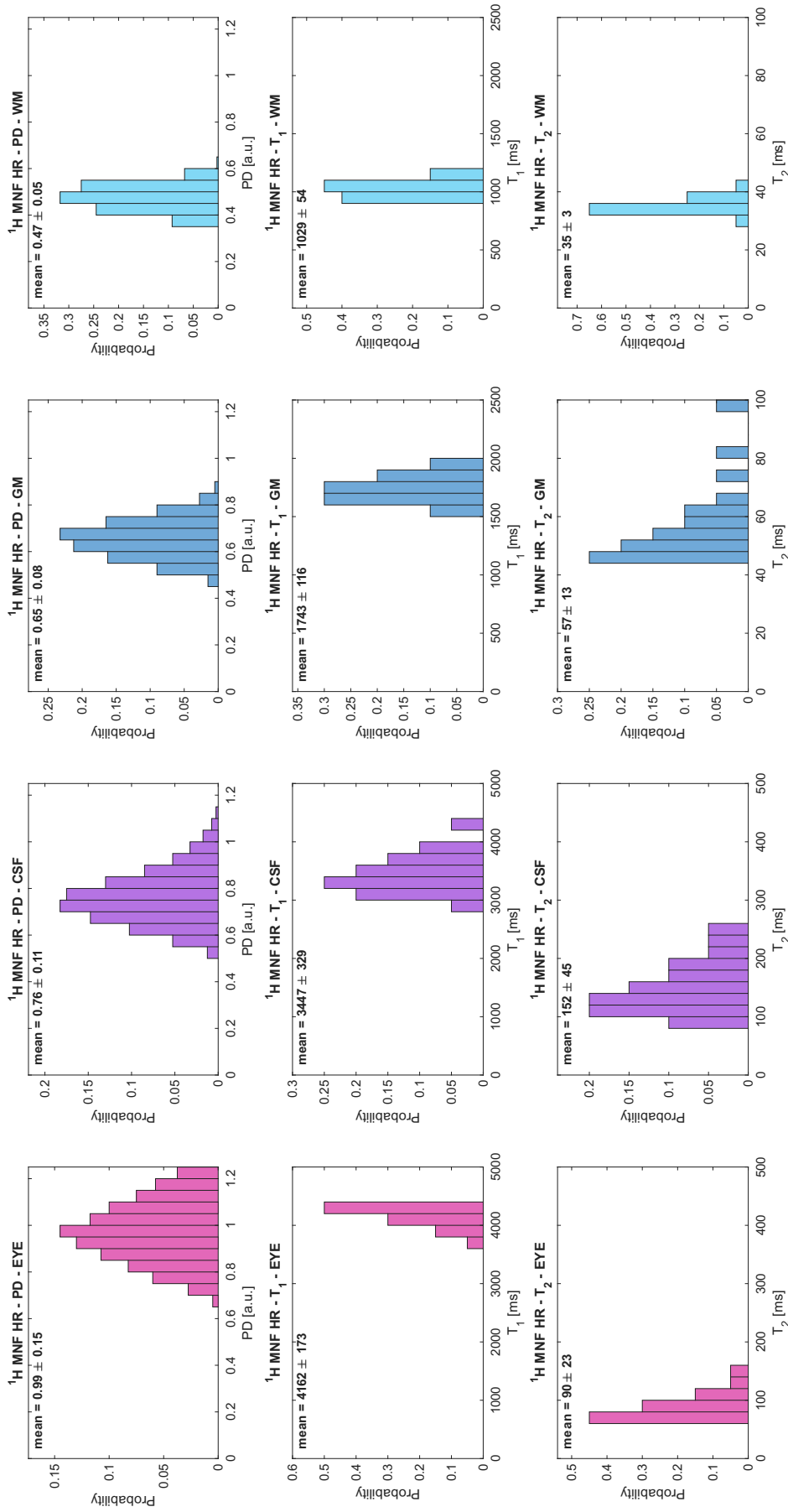


Figure S34. Histograms of the mean values from multiple measurements in subject 3, from the ^1H MNF HR data (PD, T_1 , T_2), in the EYE, CSF, GM and WM. The mean values of each metric were measured multiple times from different N_{ROI} and N_{REF} highest values in all the ROIs and in the reference ROI (eye), respectively, for PD (for a total of 400 measurements), and from different N_{ROI} highest values in all the ROIs for the relaxation times (for a total of 20 measurements). Highest values used: $N_{\text{ROI}} = 5\%$ to 100% by steps of 5% (20 values), $N_{\text{REF}} = 5\%$ to 100% by steps of 5% (20 values).

Subject 4 - ^1H MNF HR - All REF & ROI - MEAN

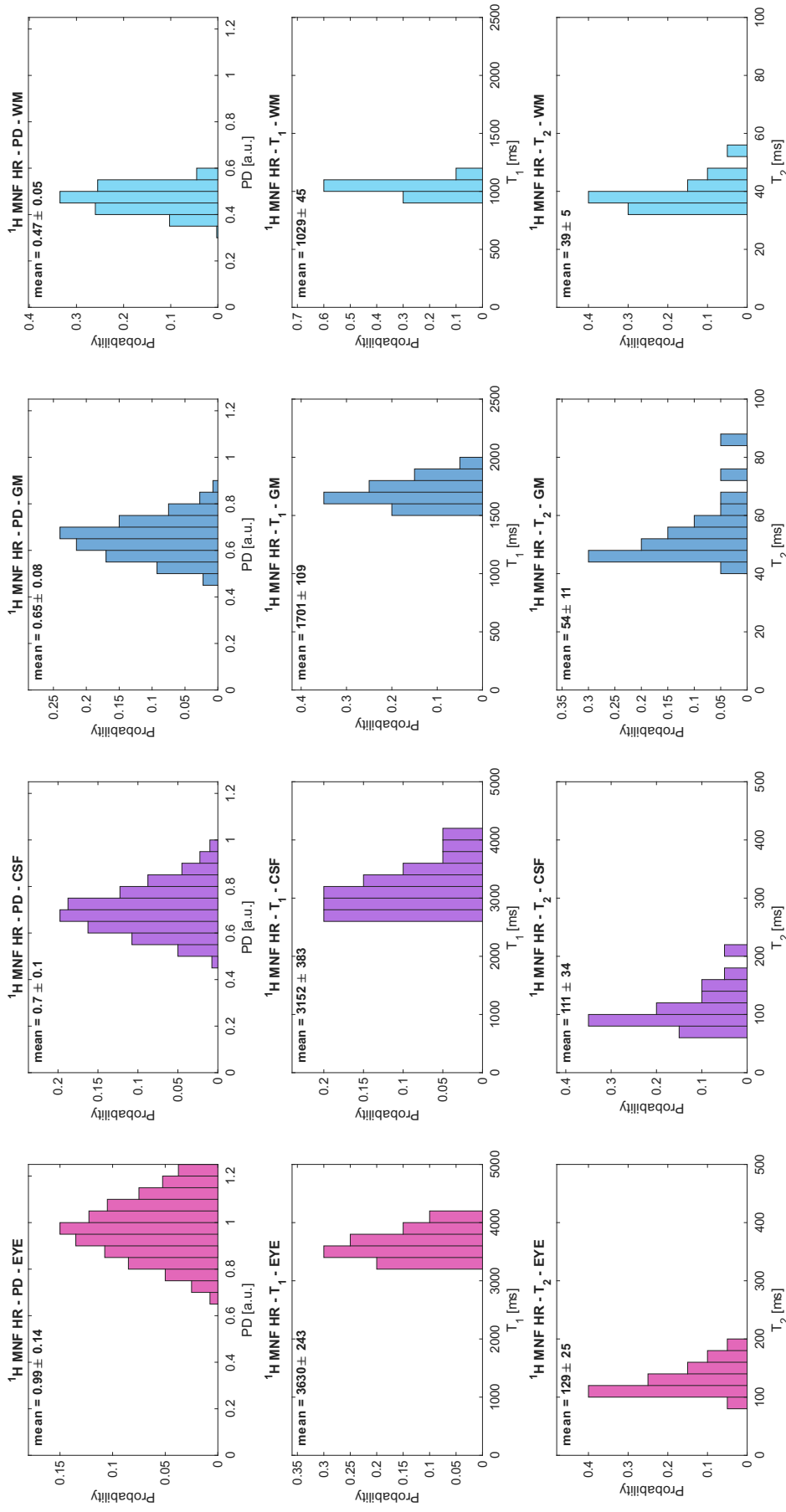


Figure S35. Histograms of the mean values from multiple measurements in subject 4, from the ^1H MNF HR data (PD, T_1 , T_2), in the EYE, CSF, GM and WM. The mean values of each metric were measured multiple times from different N_{ROI} and N_{REF} highest values in all the ROIs and in the reference ROI (eye), respectively, for PD (for a total of 400 measurements), and from different N_{ROI} highest values in all the ROIs for the relaxation times (for a total of 20 measurements). Highest values used: $N_{\text{ROI}} = 5\%$ to 100% by steps of 5%, $N_{\text{REF}} = 5\%$ to 100% by steps of 5% (20 values).

Subject 5 - ^1H MNF HR - All REF & ROI - MEAN

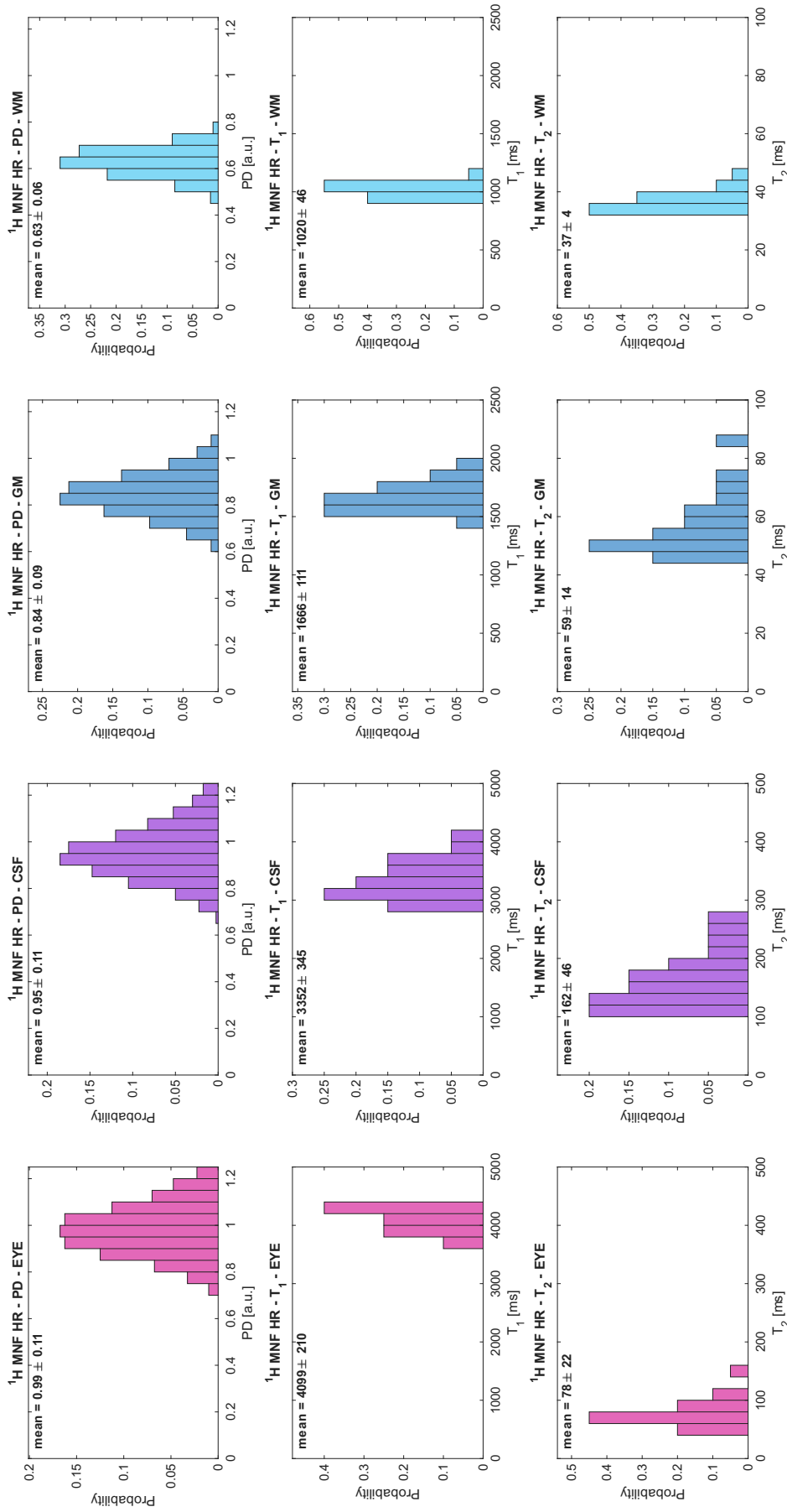


Figure S36. Histograms of the mean values from multiple measurements in subject 5, from the ^1H MNF HR data (PD, T_1 , T_2), in the EYE, CSF, GM and WM. The mean values of each metric were measured multiple times from different N_{ROI} and N_{REF} highest values in all the ROIs and in the reference ROI (eye), respectively, for PD (for a total of 400 measurements), and from different N_{ROI} highest values in all the ROIs for the relaxation times (for a total of 20 measurements). Highest values used: $N_{\text{ROI}} = 5\%$ to 100% by steps of 5% (20 values), $N_{\text{REF}} = 5\%$ to 100% by steps of 5% (20 values).

Subject 6 - ^1H MNF HR - All REF & ROI - MEAN

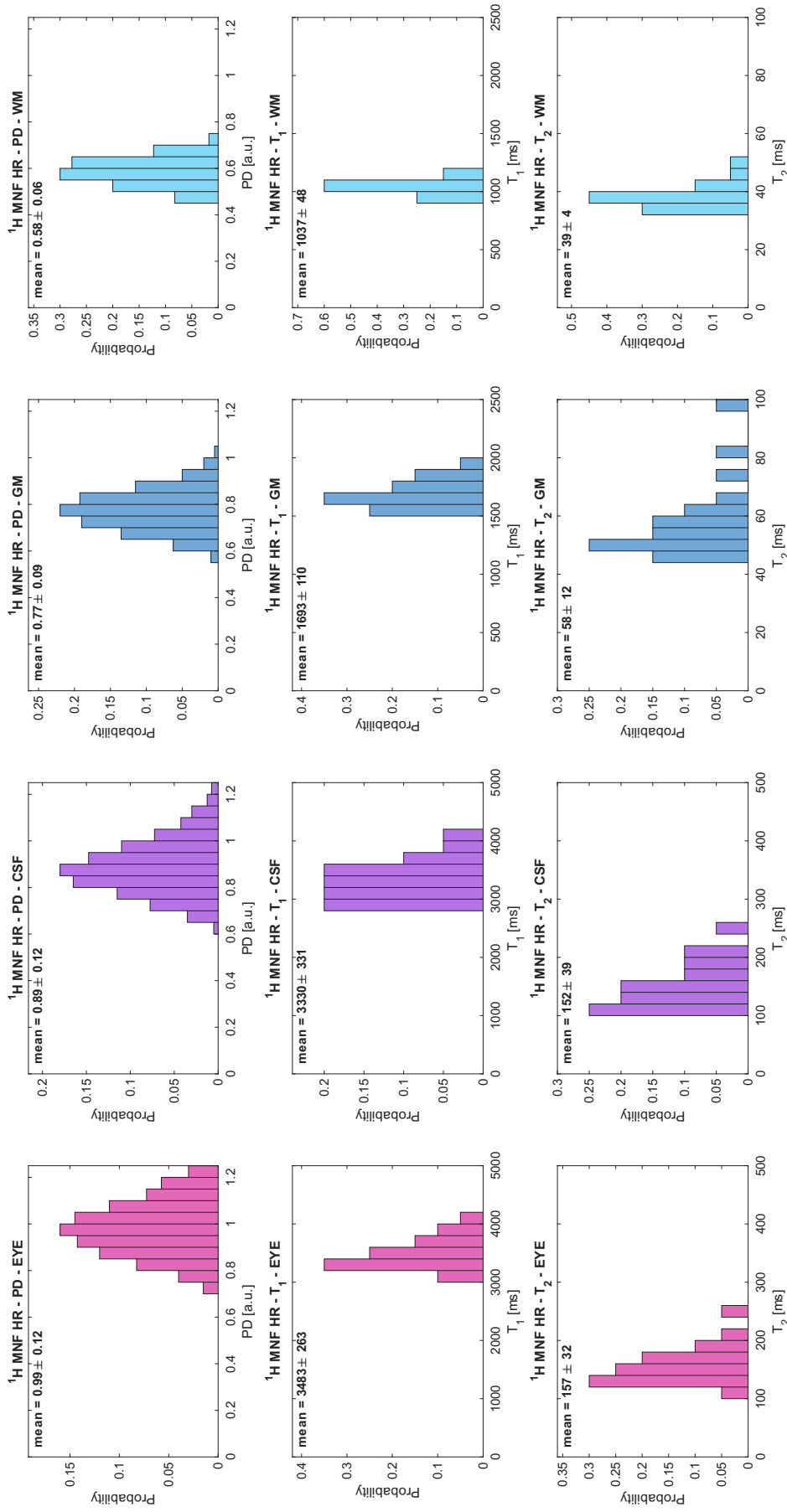


Figure S37. Histograms of the mean values from multiple measurements in subject 6, from the ^1H MNF HR data (PD, T_1 , T_2), in the EYE, CSF, GM and WM. The mean values of each metric were measured multiple times from different N_{ROI} and N_{REF} highest values in all the ROIs and in the reference ROI (eye), respectively, for PD (for a total of 400 measurements), and from different N_{ROI} highest values in all the ROIs for the relaxation times (for a total of 20 measurements). Highest values used: $N_{\text{ROI}} = 5\%$ to 100% by steps of 5% (20 values), $N_{\text{REF}} = 5\%$ to 100% by steps of 5% (20 values).

Subject 7 - ^1H MNF HR - All REF & ROI - MEAN

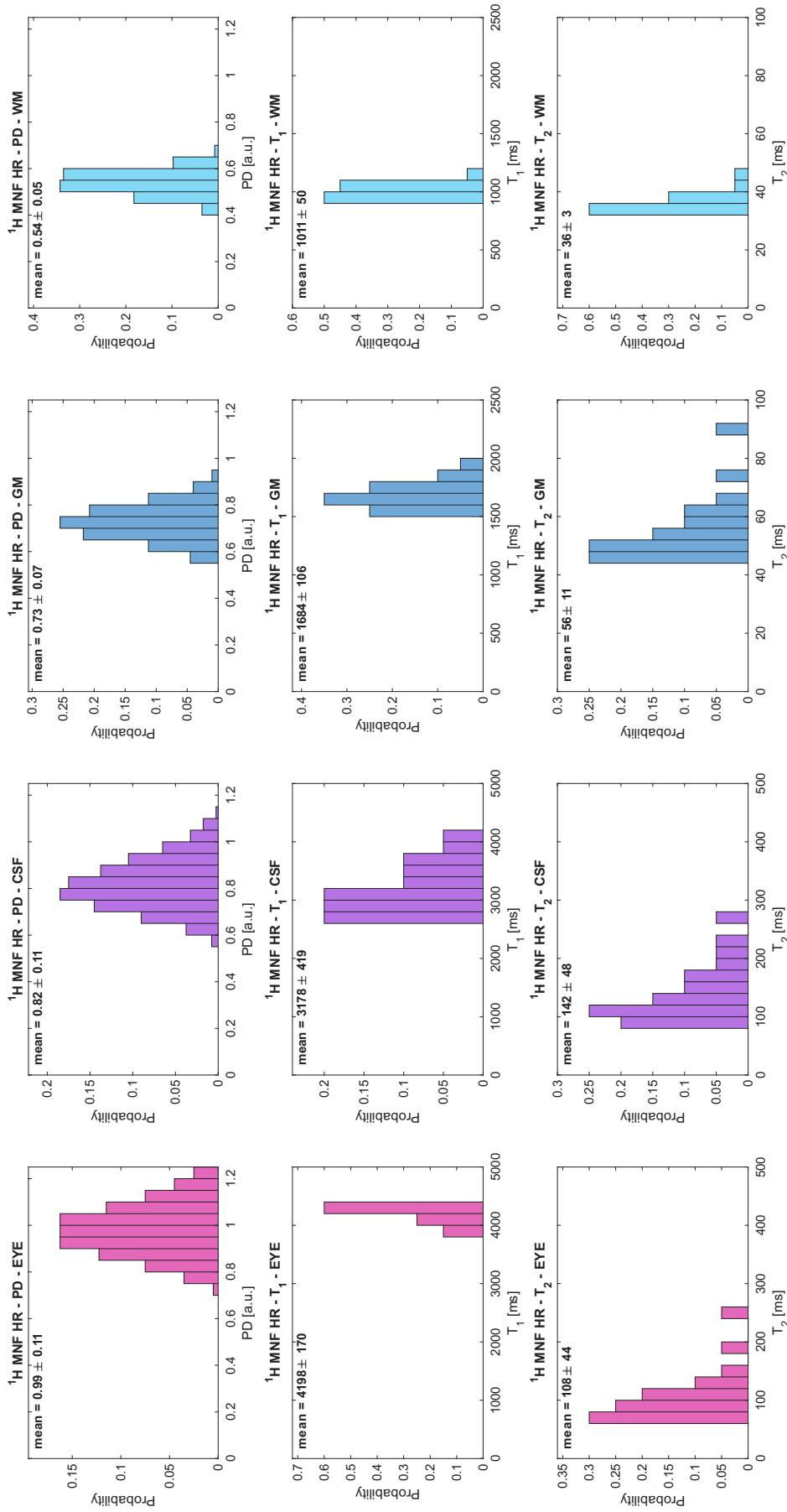


Figure S38. Histograms of the mean values from multiple measurements in subject 7, from the ^1H MNF HR data (PD, T_1 , T_2), in the EYE, CSF, GM and WM. The mean values of each metric were measured multiple times from different N_{ROI} and N_{REF} highest values in all the ROIs and in the reference ROI (eye), respectively, for PD (for a total of 400 measurements), and from different N_{ROI} highest values in all the ROIs for the relaxation times (for a total of 20 measurements). Highest values used: $N_{\text{ROI}} = 5\%$ to 100% by steps of 5% (20 values), $N_{\text{REF}} = 5\%$ to 100% by steps of 5% (20 values).

Subject 1 - ^{23}Na MNF HR - All REF & ROI - MEAN

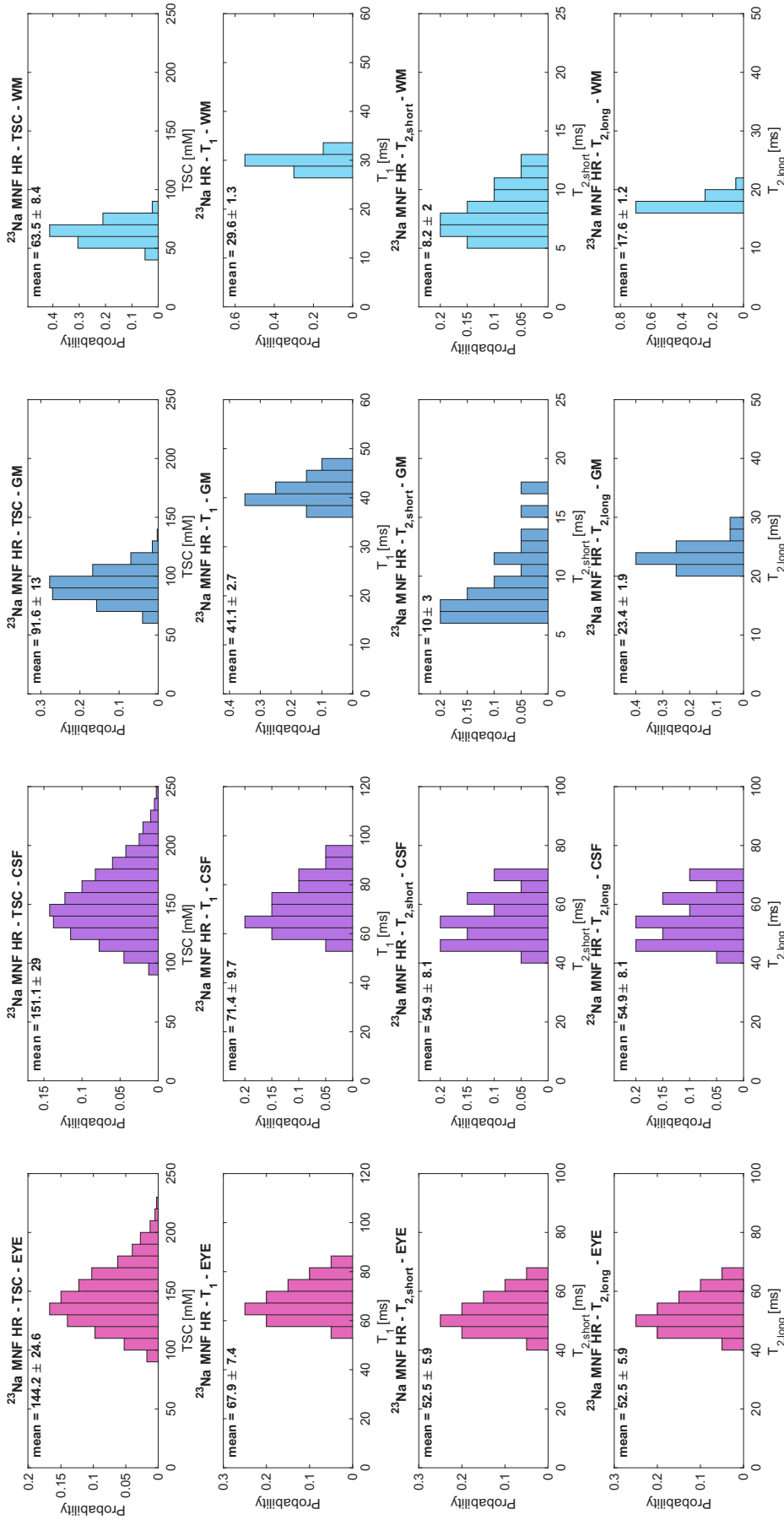


Figure S39. Histograms of the mean values from multiple measurements in subject 1, from the ^{23}Na MNF HR data (TSC, T_1 , $T_{2,short}$, $T_{2,long}$), in the EYE, CSF, GM and WM. The mean values of each metric were measured multiple times from different N_{ROI} and N_{REF} highest values in all the ROIs and in the reference ROI (eye), respectively, for TSC (for a total of 400 measurements), and from different N_{ROI} highest values in all the ROIs for the relaxation times (for a total of 20 measurements). Highest values used: $N_{ROI} = 5\%$ to 100% by steps of 5% (20 values), $N_{REF} = 5\%$ to 100% by steps of 5% (20 values).

Subject 2 - ^{23}Na MNF HR - All REF & ROI - MEAN

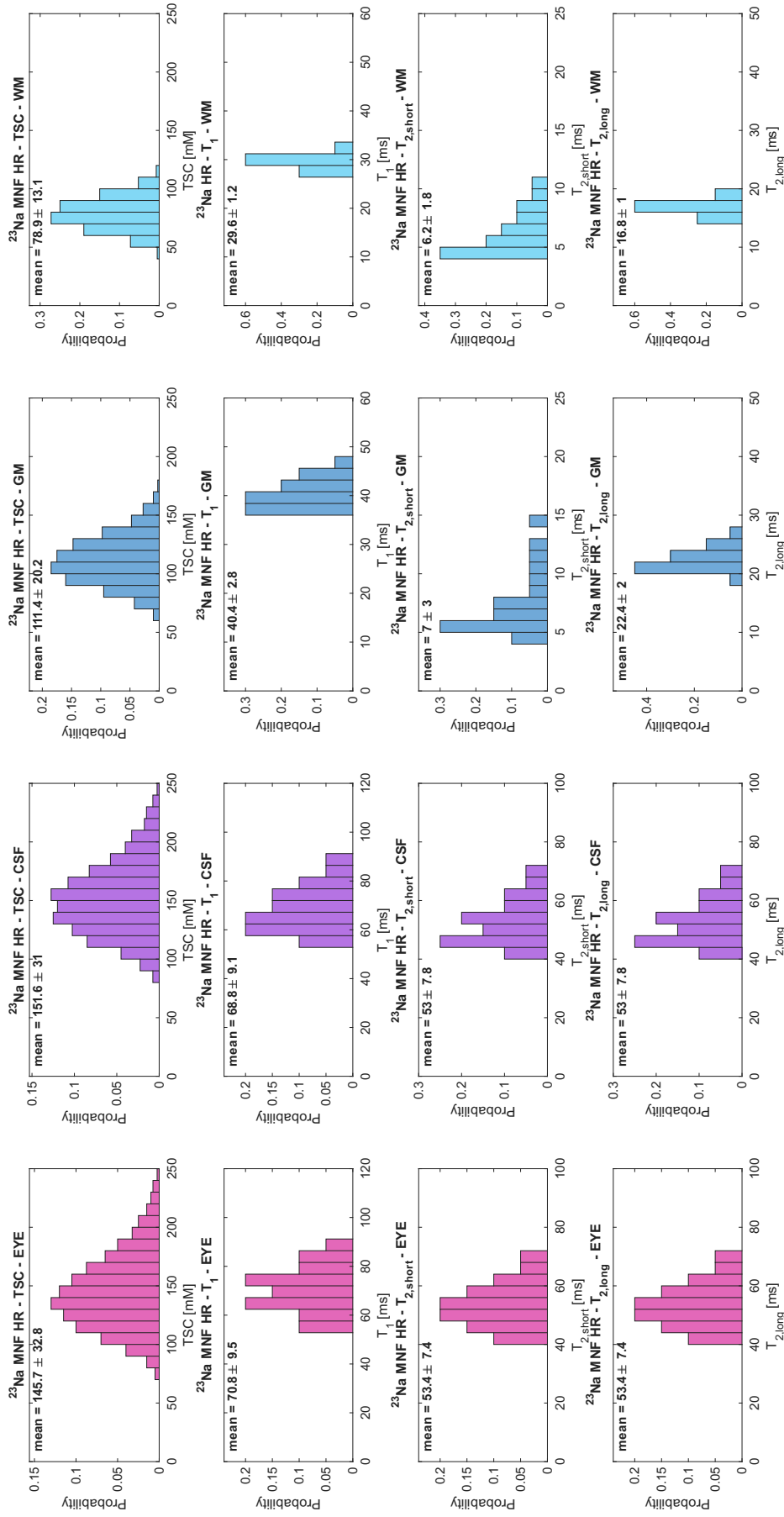


Figure S40. Histograms of the mean values from multiple measurements in subject 2, from the ^{23}Na MNF HR data (TSC, T_1 , $T_{2,short}$, $T_{2,long}$), in the EYE, CSF, GM and WM. The mean values of each metric were measured multiple times from different N_{ROI} and N_{REF} highest values in all the ROIs and in the reference ROI (eye), respectively, for TSC (for a total of 400 measurements), and from different N_{ROI} highest values in all the ROIs for the relaxation times (for a total of 20 measurements). Highest values used: $N_{ROI} = 5\%$ to 100% by steps of 5% (20 values), $N_{REF} = 5\%$ to 100% by steps of 5% (20 values).

Subject 3 - ^{23}Na MNF HR - All REF & ROI - MEAN

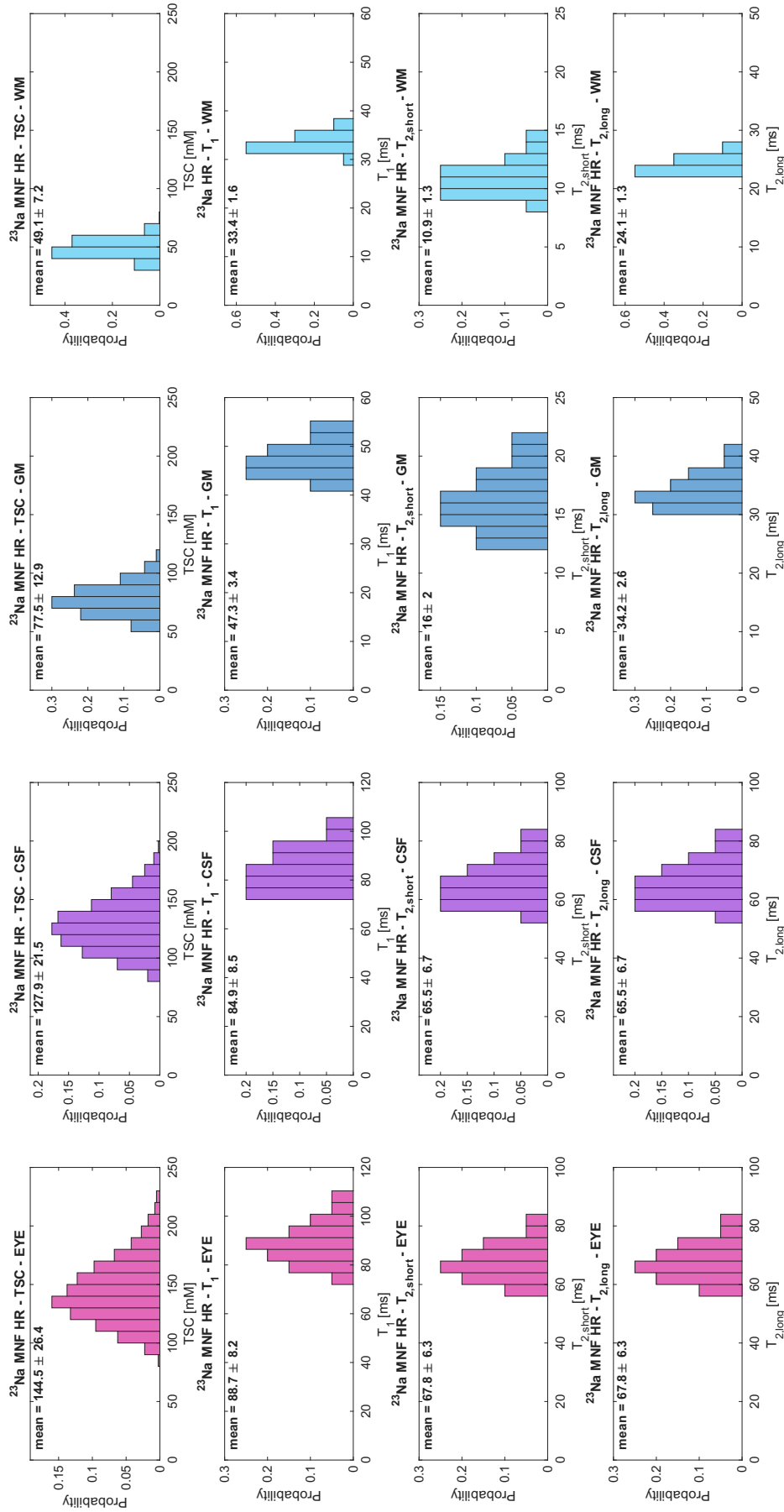


Figure S41. Histograms of the mean values from multiple measurements in subject 3, from the ^{23}Na MNF HR data (TSC, T_1 , $T_{2,short}$, $T_{2,long}$), in the EYE, CSF, GM and WM. The mean values of each metric were measured multiple times from different N_{ROI} and N_{REF} highest values in all the ROIs and in the reference ROI (eye), respectively, for TSC (for a total of 400 measurements), and from different N_{ROI} highest values in all the ROIs for the relaxation times (for a total of 20 measurements). Highest values used: $N_{ROI} = 5\%$ to 100% by steps of 5%, $N_{REF} = 5\%$ to 100% by steps of 5% (20 values).

Subject 4 - ^{23}Na MNF HR - All REF & ROI - MEAN

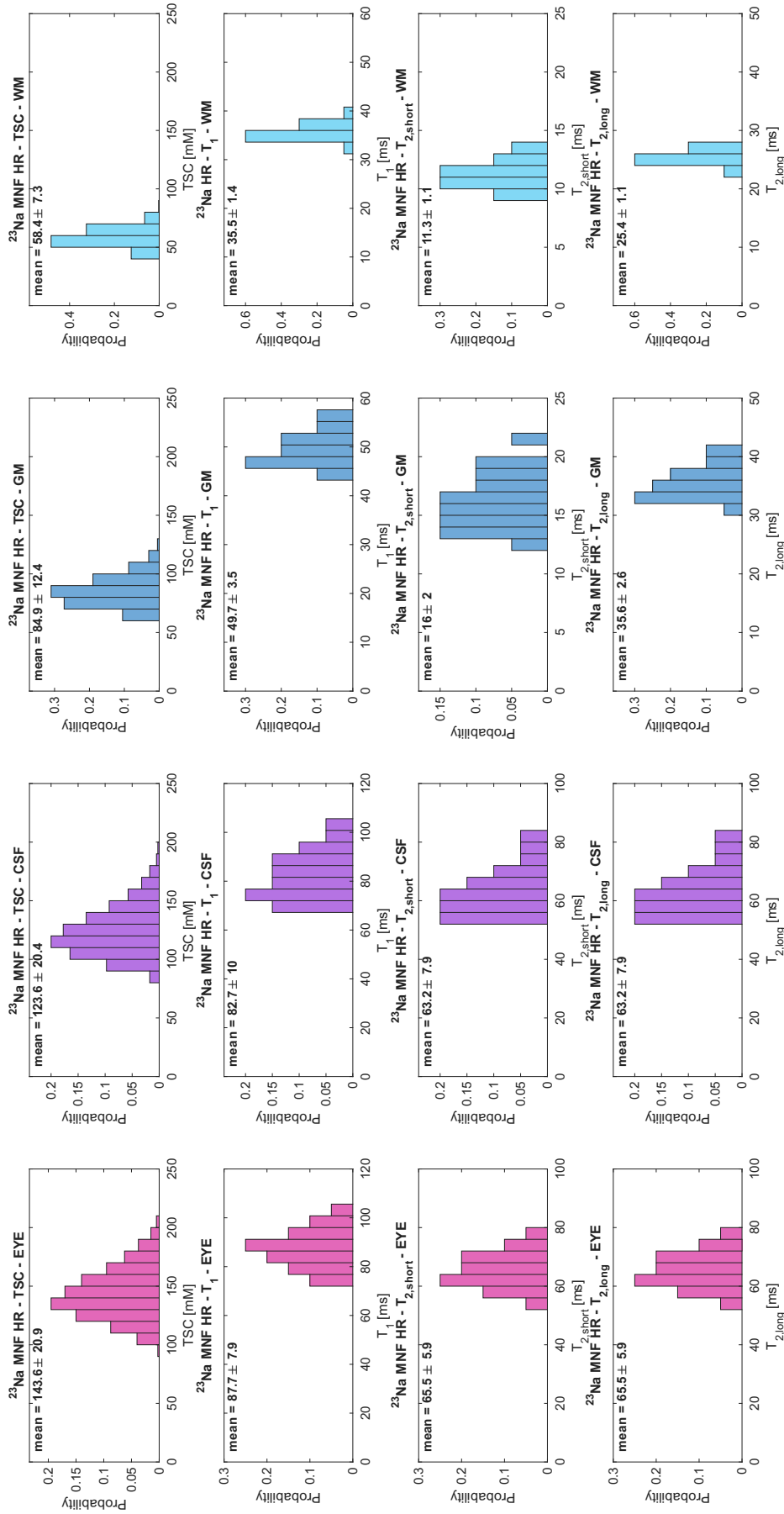


Figure S42. Histograms of the mean values from multiple measurements in subject 4, from the ^{23}Na MNF HR data (TSC, T_1 , $T_{2,short}$, $T_{2,long}$), in the EYE, CSF, GM and WM. The mean values of each metric were measured multiple times from different N_{ROI} and N_{REF} highest values in all the ROIs and in the reference ROI (eye), respectively, for TSC (for a total of 400 measurements), and from different N_{ROI} highest values in all the ROIs for the relaxation times (for a total of 20 measurements). Highest values used: $N_{ROI} = 5\%$ to 100% by steps of 5% (20 values), $N_{REF} = 5\%$ to 100% by steps of 5% (20 values).

Subject 5 - ^{23}Na MNF HR - All REF & ROI - MEAN

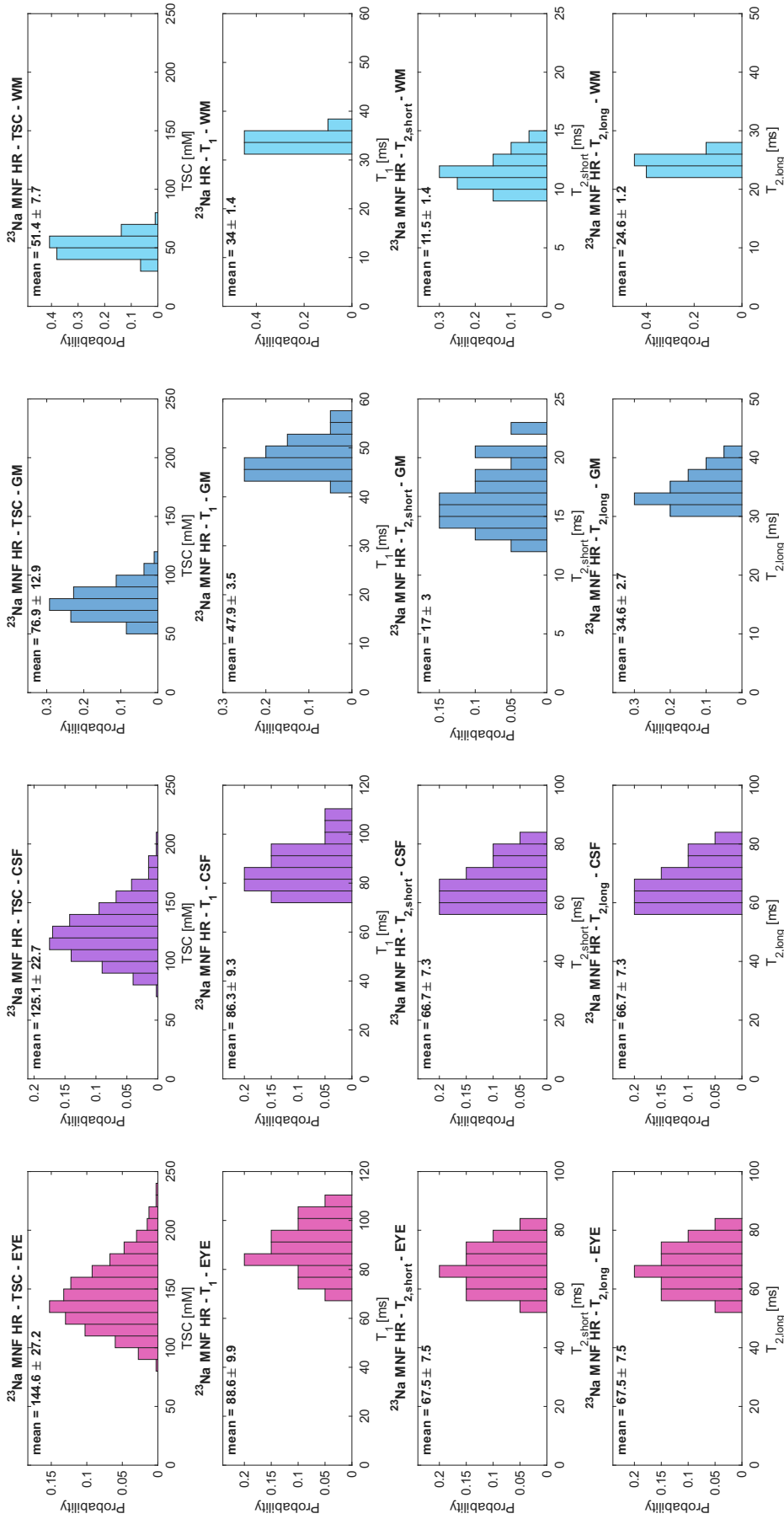


Figure S43. Histograms of the mean values from multiple measurements in subject 5, from the ^{23}Na MNF HR data (TSC, T_1 , $T_{2,short}$, $T_{2,long}$), in the EYE, CSF, GM and WM. The mean values of each metric were measured multiple times from different N_{ROI} and N_{REF} highest values in all the ROIs and in the reference ROI (eye), respectively, for TSC (for a total of 400 measurements), and from different N_{ROI} highest values in all the ROIs for the relaxation times (for a total of 20 measurements). Highest values used: $N_{ROI} = 5\%$ to 100% by steps of 5% (20 values), $N_{REF} = 5\%$ to 100% by steps of 5% (20 values).

Subject 6 - ^{23}Na MNF HR - All REF & ROI - MEAN

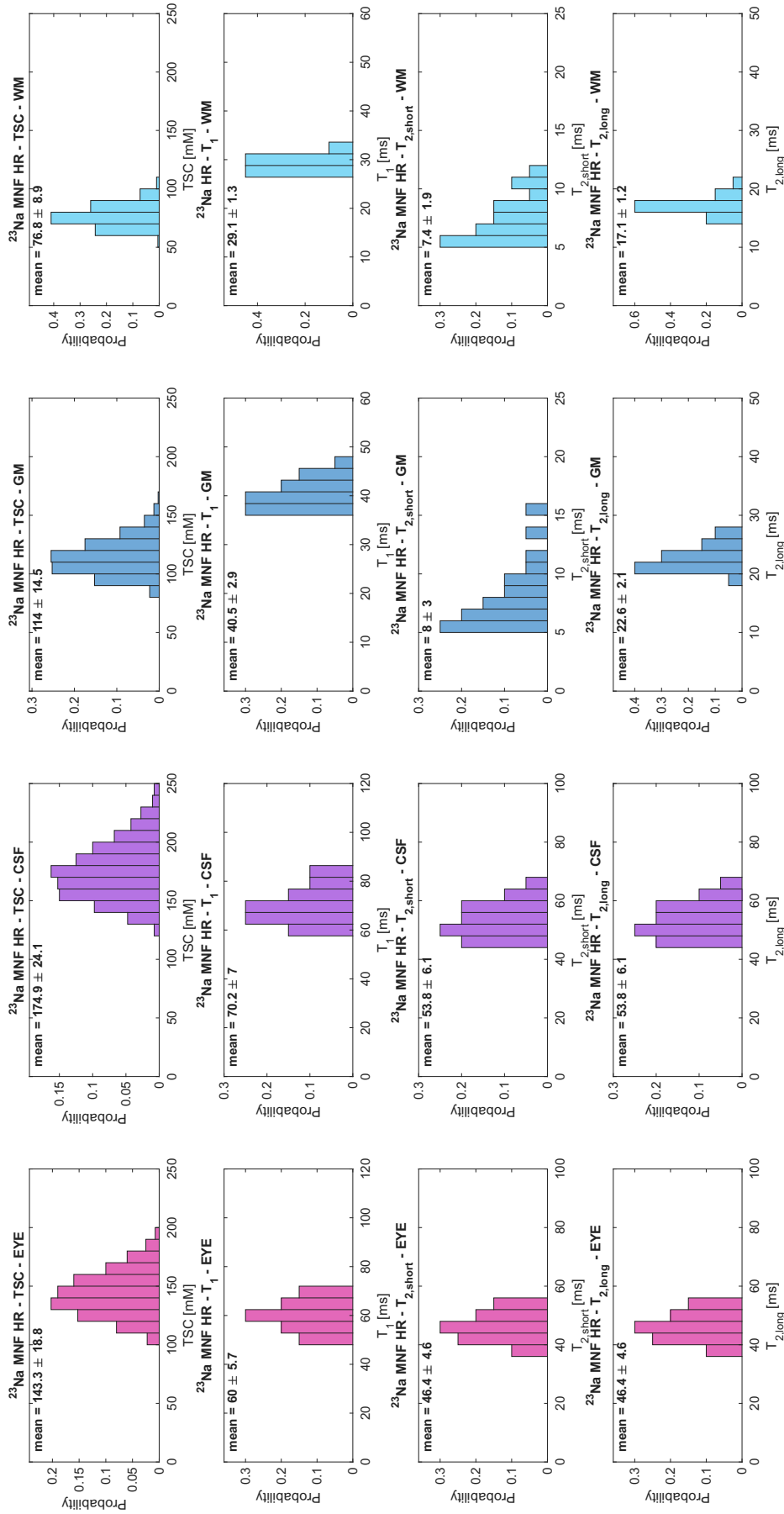


Figure S44. Histograms of the mean values from multiple measurements in subject 6, from the ^{23}Na MNF HR data (TSC, T_1 , $T_{2,short}$, $T_{2,long}$), in the EYE, CSF, GM and WM. The mean values of each metric were measured multiple times from different N_{ROI} and N_{REF} highest values in all the ROIs and in the reference ROI (eye), respectively, for TSC (for a total of 400 measurements), and from different N_{ROI} highest values in all the ROIs for the relaxation times (for a total of 20 measurements). Highest values used: $N_{ROI} = 5\%$ to 100% by steps of 5% (20 values), $N_{REF} = 5\%$ to 100% by steps of 5% (20 values).

Subject 7 - ^{23}Na MNF HR - All REF & ROI - MEAN

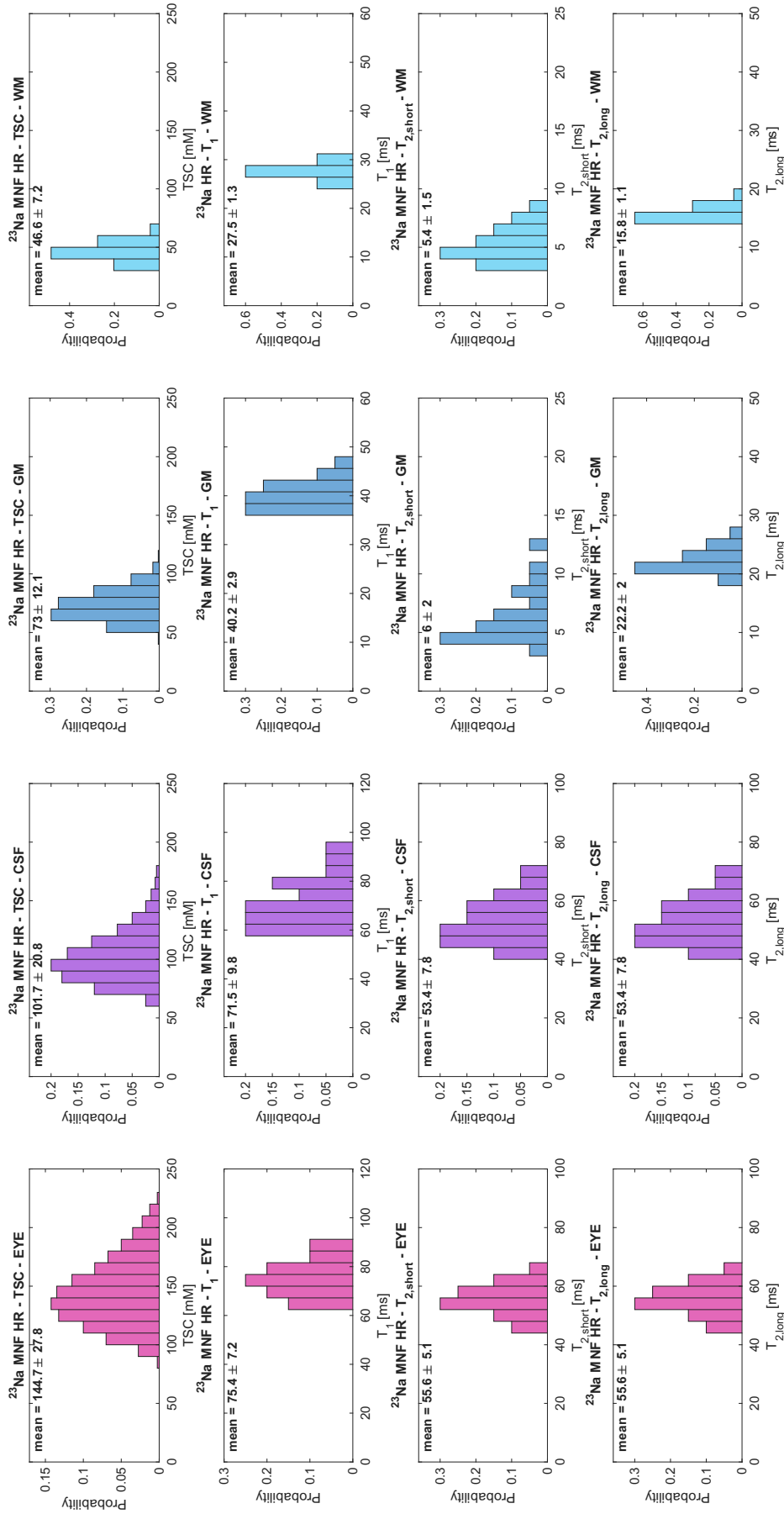


Figure S45. Histograms of the mean values from multiple measurements in subject 7, from the ^{23}Na MNF HR data (TSC, T_1 , $T_{2,short}$, $T_{2,long}$), in the EYE, CSF, GM and WM. The mean values of each metric were measured multiple times from different N_{ROI} and N_{REF} highest values in all the ROIs and in the reference ROI (eye), respectively, for TSC (for a total of 400 measurements), and from different N_{ROI} highest values in all the ROIs for the relaxation times (for a total of 20 measurements). Highest values used: $N_{ROI} = 5\%$ to 100% by steps of 5% (20 values), $N_{REF} = 5\%$ to 100% by steps of 5% (20 values).

Subject 1 - ^{23}Na MNF LR - All REF & ROI - MEAN

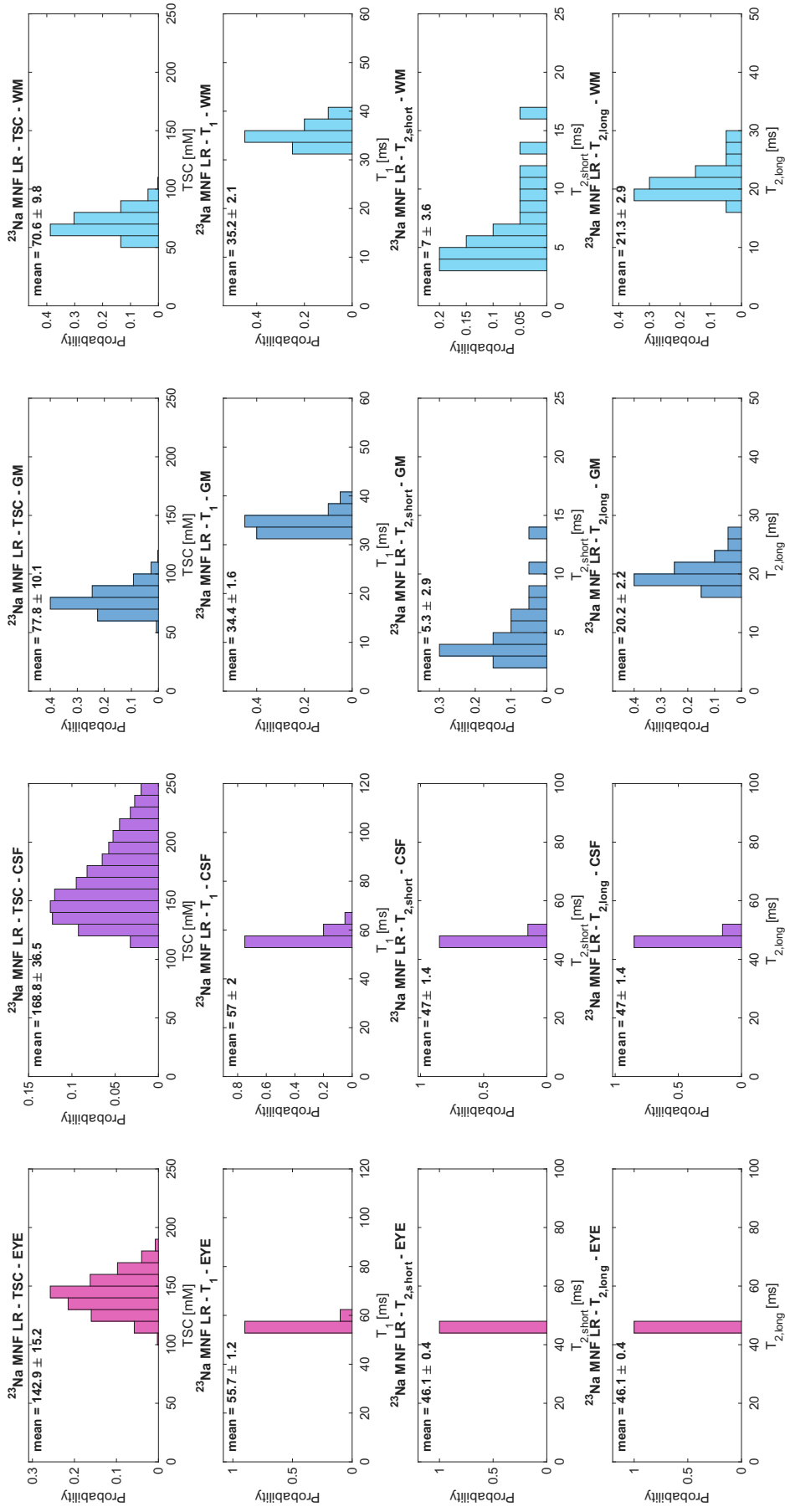


Figure S46. Histograms of the mean values from multiple measurements in subject 1, from the ^{23}Na MNF LR data (TSC, T_1 , $T_{2,short}$, $T_{2,long}$), in the EYE, CSF, GM and WM. The mean values of each metric were measured multiple times from different N_{ROI} and N_{REF} highest values in all the ROIs and in the reference ROI (eye), respectively, for TSC (for a total of 400 measurements), and from different N_{ROI} highest values in all the ROIs for the relaxation times (for a total of 20 measurements). Highest values used: $N_{ROI} = 5\%$ to 100% by steps of 5%, $N_{REF} = 5\%$ to 100% by steps of 5% (20 values).

Subject 2 - ^{23}Na MNF LR - All REF & ROI - MEAN

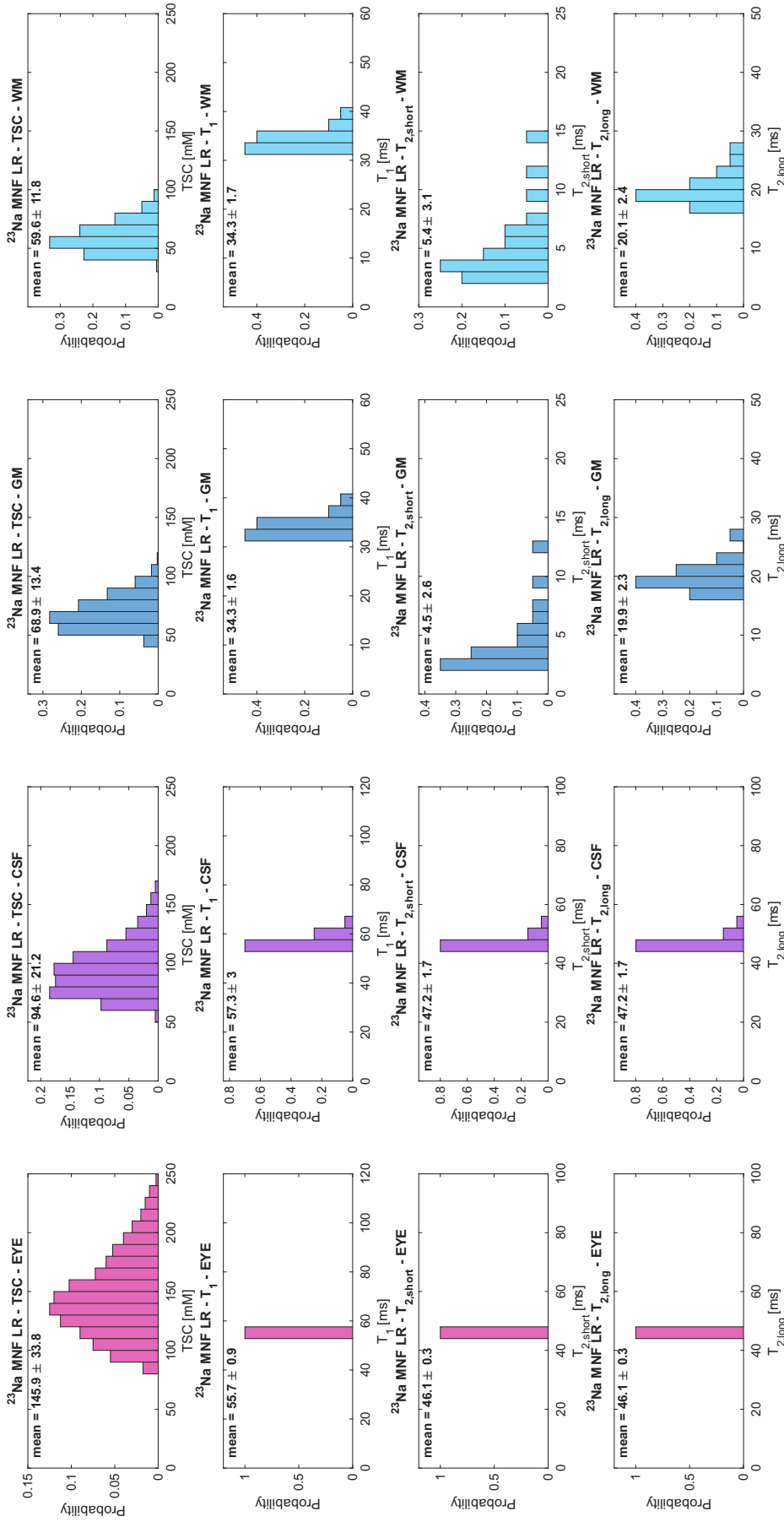


Figure S47. Histograms of the mean values from multiple measurements in subject 2, from the ^{23}Na MNF LR data (TSC, T_1 , $T_{2,short}$, $T_{2,long}$), in the EYE, CSF, GM and WM. The mean values of each metric were measured multiple times from different N_{ROI} and N_{REF} highest values in all the ROIs and in the reference ROI (eye), respectively, for TSC (for a total of 400 measurements), and from different N_{ROI} highest values in all the ROIs for the relaxation times (for a total of 20 measurements). Highest values used: $N_{\text{ROI}} = 5\%$ to 100% by steps of 5% (20 values), $N_{\text{REF}} = 5\%$ to 100% by steps of 5% (20 values).

Subject 3 - ^{23}Na MNF LR - All REF & ROI - MEAN

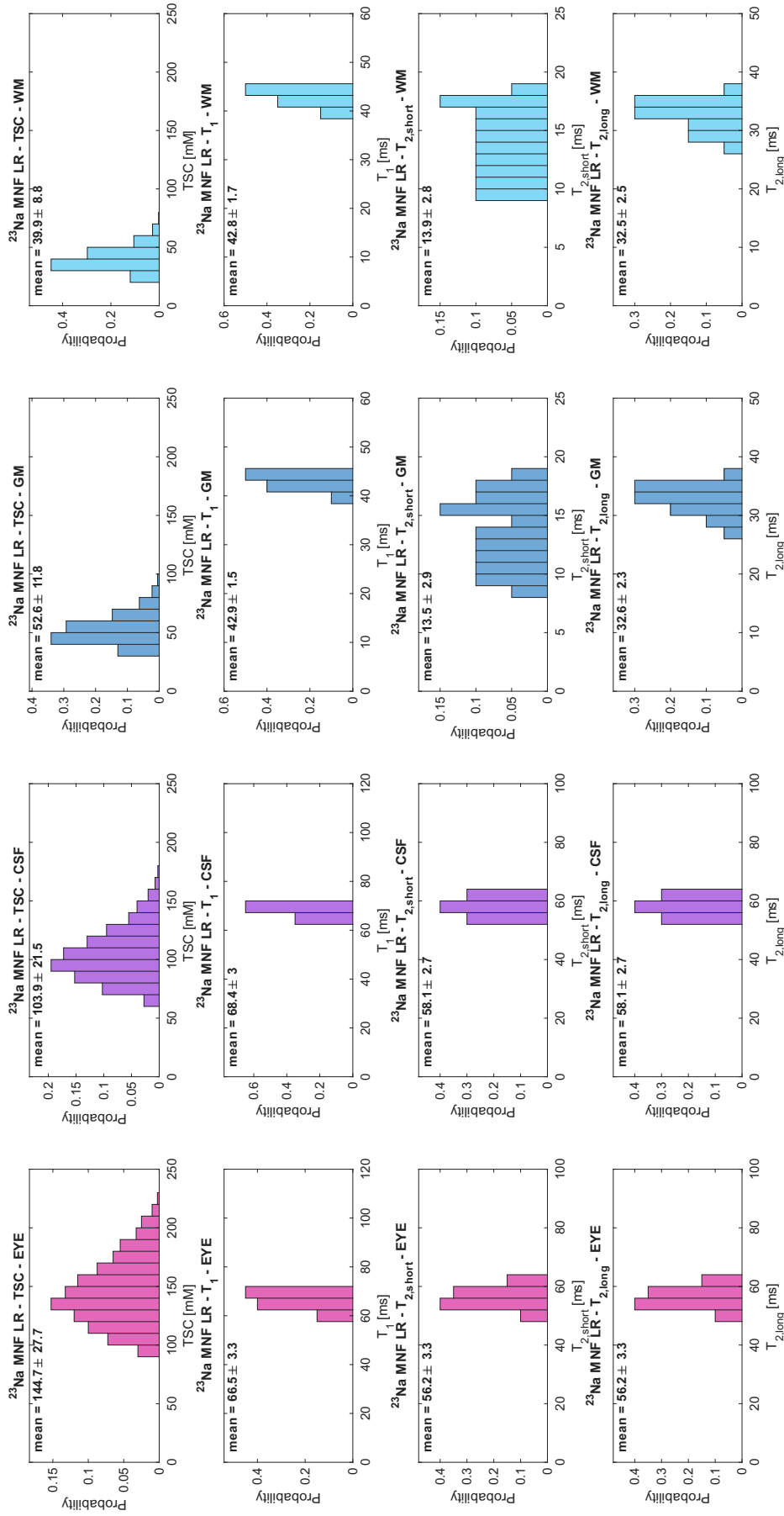


Figure S48. Histograms of the mean values from multiple measurements in subject 3, from the ^{23}Na MNF LR data (TSC, T_1 , $T_{2,short}$, $T_{2,long}$), in the EYE, CSF, GM and WM. The mean values of each metric were measured multiple times from different N_{ROI} and N_{REF} highest values in all the ROIs and in the reference ROI (eye), respectively, for TSC (for a total of 400 measurements), and from different N_{ROI} highest values in all the ROIs for the relaxation times (for a total of 20 measurements). Highest values used: $N_{ROI} = 5\%$ to 100% by steps of 5% (20 values), $N_{REF} = 5\%$ to 100% by steps of 5% (20 values).

Subject 4 - ^{23}Na MNF LR - All REF & ROI - MEAN

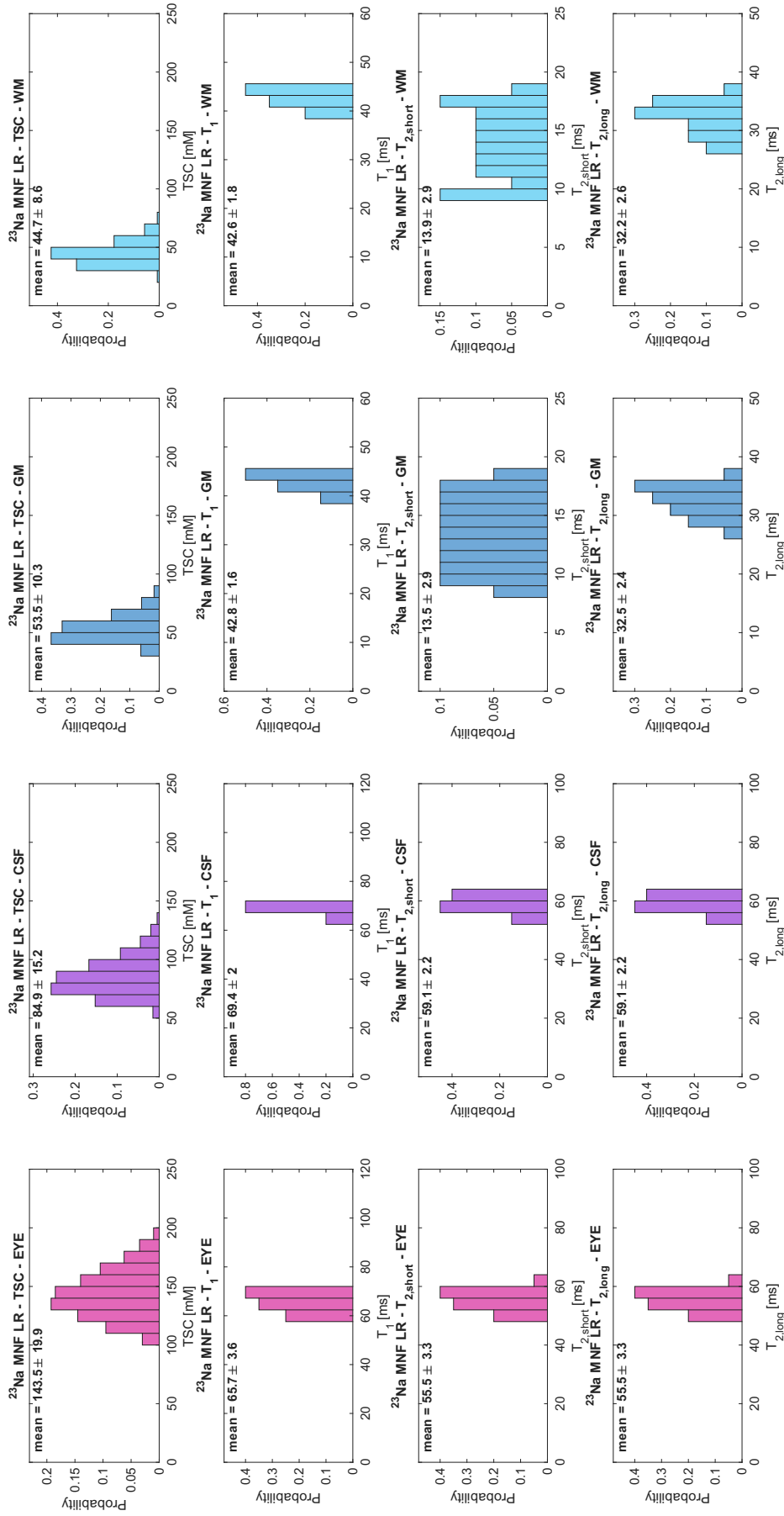


Figure S49. Histograms of the mean values from multiple measurements in subject 4, from the ^{23}Na MNF LR data (TSC, T_1 , $T_{2,short}$, $T_{2,long}$), in the EYE, CSF, GM and WM. The mean values of each metric were measured multiple times from different N_{ROI} and N_{REF} highest values in all the ROIs and in the reference ROI (eye), respectively, for TSC (for a total of 400 measurements), and from different N_{ROI} highest values in all the ROIs for the relaxation times (for a total of 20 measurements). Highest values used: $N_{\text{ROI}} = 5\%$ to 100% by steps of 5% (20 values), $N_{\text{REF}} = 5\%$ to 100% by steps of 5% (20 values).

Subject 5 - ^{23}Na MNF LR - All REF & ROI - MEAN

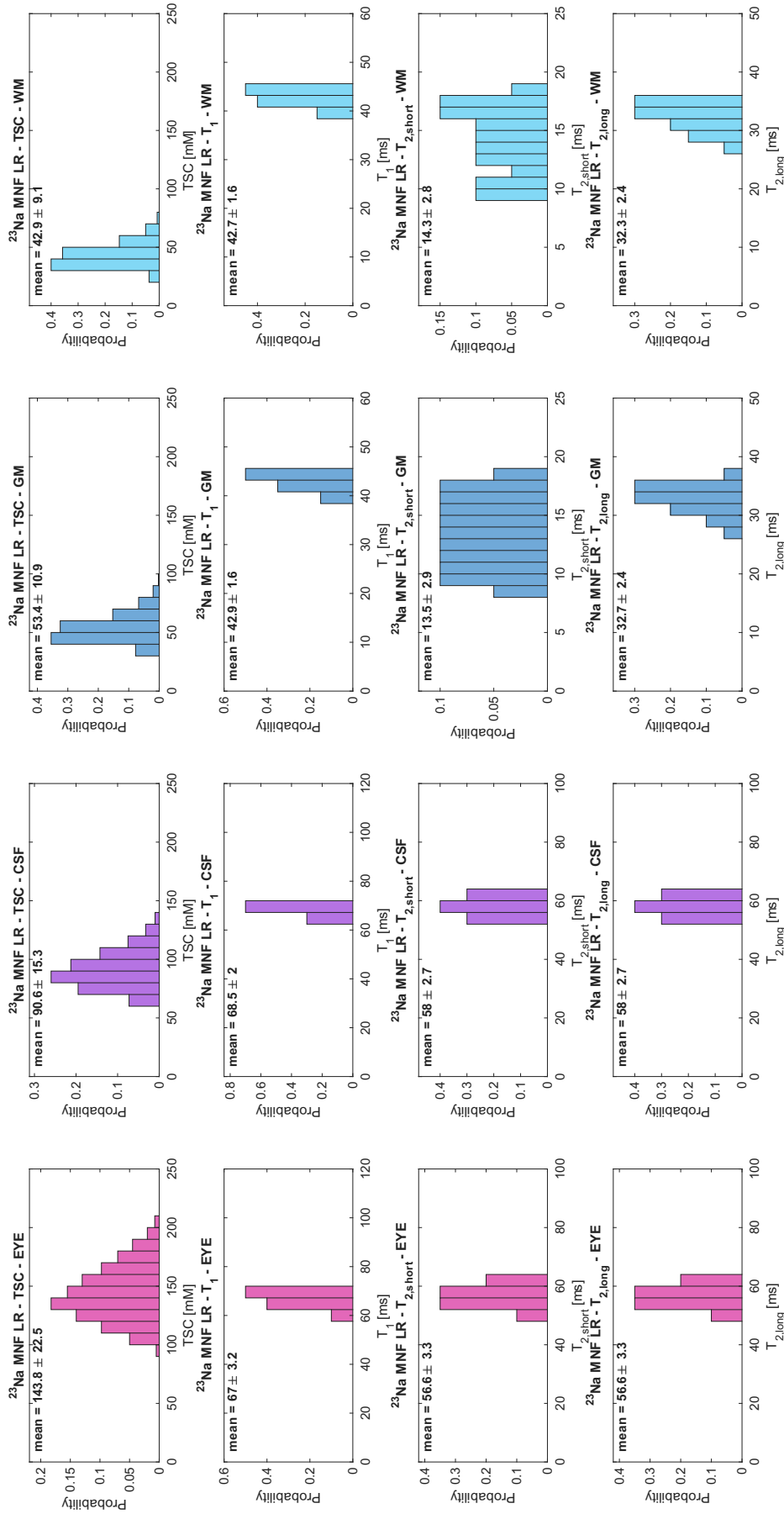


Figure S50. Histograms of the mean values from multiple measurements in subject 5, from the ^{23}Na MNF LR data (TSC, T_1 , $T_{2,short}$, $T_{2,long}$), in the EYE, CSF, GM and WM. The mean values of each metric were measured multiple times from different N_{ROI} and N_{REF} highest values in all the ROIs and in the reference ROI (eye), respectively, for TSC (for a total of 400 measurements), and from different N_{ROI} highest values in all the ROIs for the relaxation times (for a total of 20 measurements). Highest values used: $N_{\text{ROI}} = 5\%$ to 100% by steps of 5% (20 values), $N_{\text{REF}} = 5\%$ to 100% by steps of 5% (20 values).

Subject 6 - ^{23}Na MNF LR - All REF & ROI - MEAN

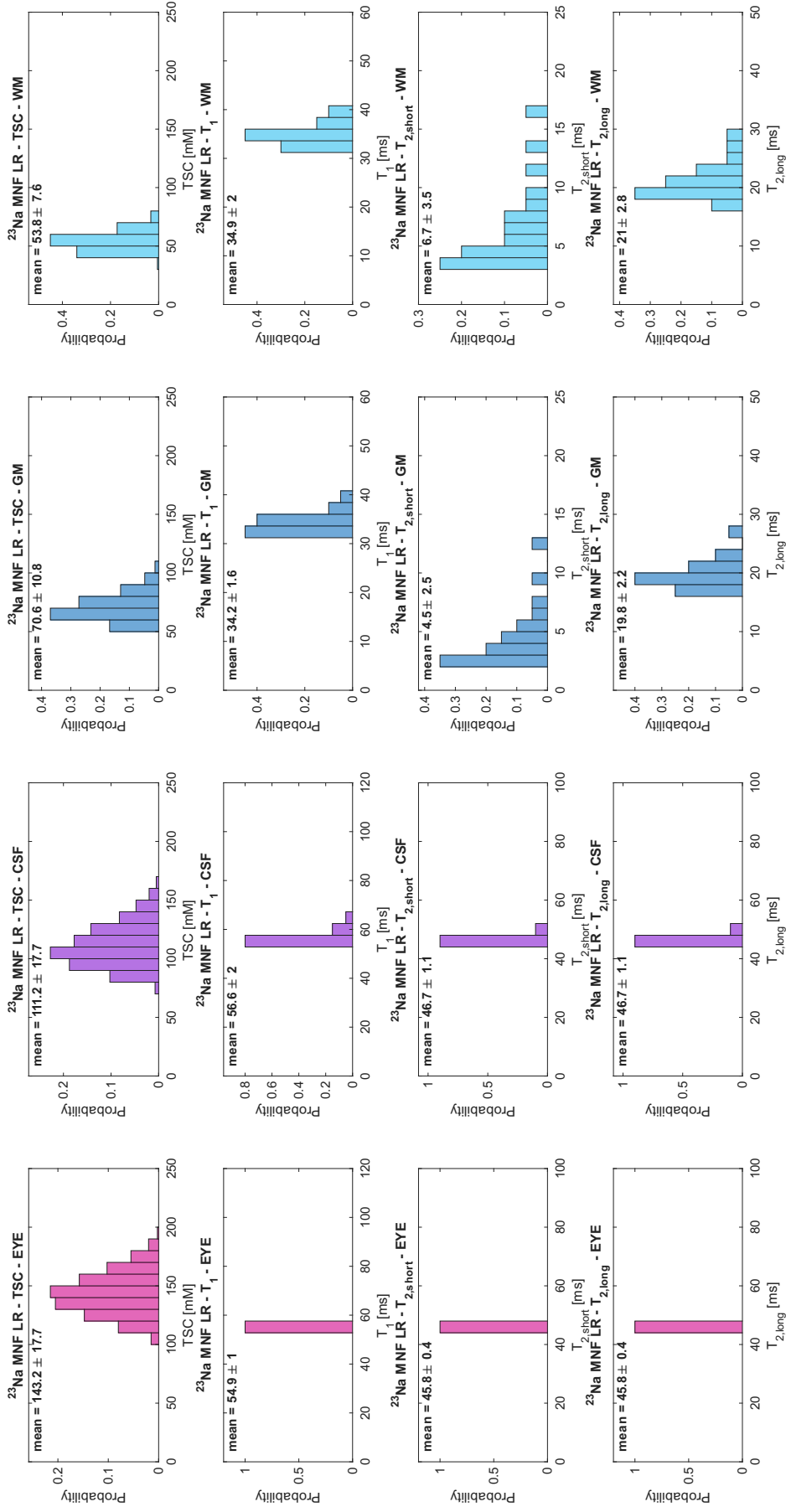


Figure S51. Histograms of the mean values from multiple measurements in subject 6, from the ^{23}Na MNF LR data (TSC, T_1 , $T_{2,\text{short}}$, $T_{2,\text{long}}$), in the EYE, CSF, GM and WM. The mean values of each metric were measured multiple times from different N_{ROI} and N_{REF} highest values in all the ROIs and in the reference ROI (eye), respectively, for TSC (for a total of 400 measurements), and from different N_{ROI} highest values in all the ROIs for the relaxation times (for a total of 20 measurements). Highest values used: $N_{\text{ROI}} = 5\%$ to 100% by steps of 5%, $N_{\text{REF}} = 5\%$ to 100% by steps of 5% (20 values).

Subject 7 - ^{23}Na MNF LR - All REF & ROI - MEAN

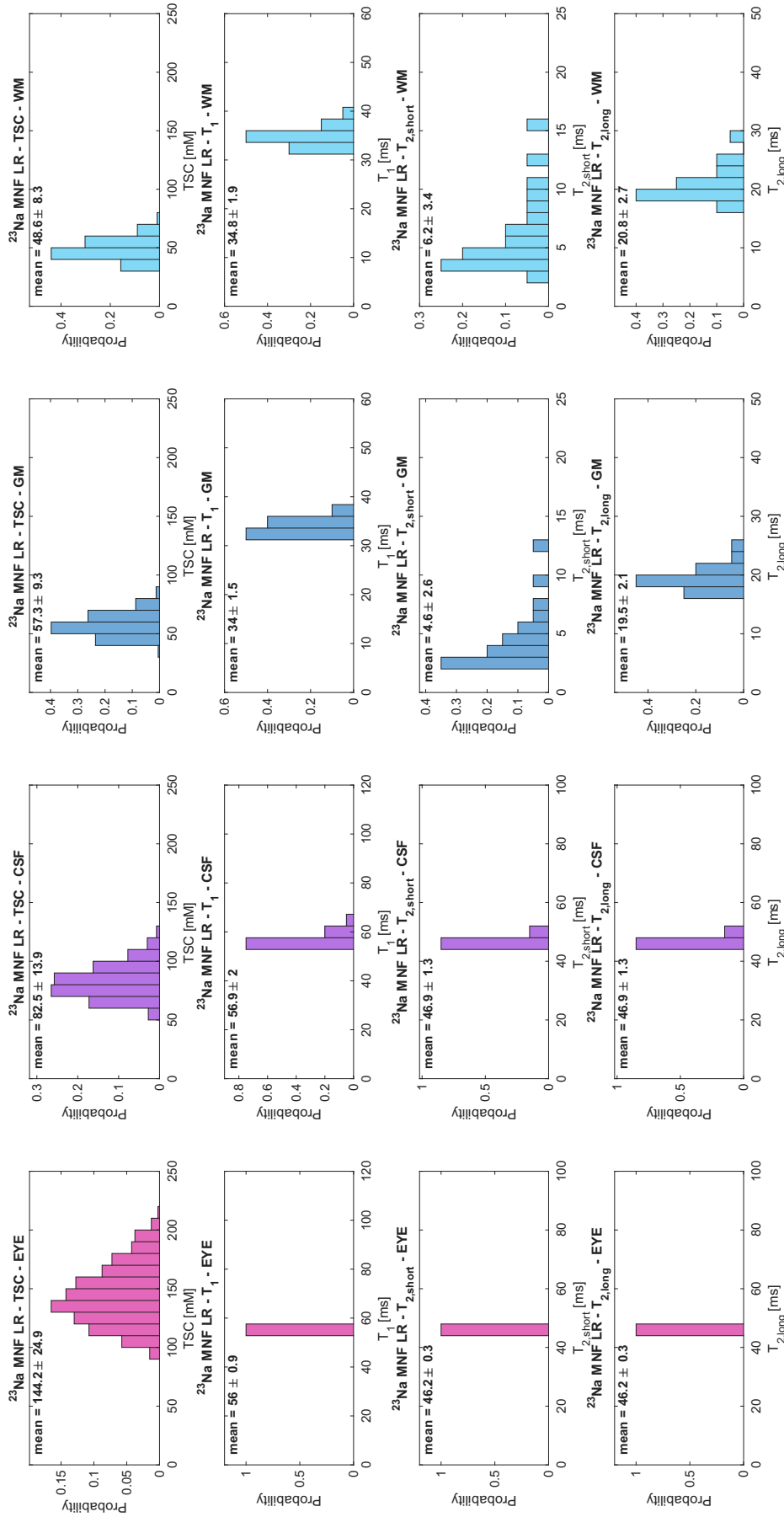


Figure S52. Histograms of the mean values from multiple measurements in subject 7, from the ^{23}Na MNF LR data (TSC, T_1 , $T_{2,short}$, $T_{2,long}$), in the EYE, CSF, GM and WM. The mean values of each metric were measured multiple times from different N_{ROI} and N_{REF} highest values in all the ROIs and in the reference ROI (eye), respectively, for TSC (for a total of 400 measurements), and from different N_{ROI} highest values in all the ROIs for the relaxation times (for a total of 20 measurements). Highest values used: $N_{\text{ROI}} = 5\%$ to 100% by steps of 5% (20 values), $N_{\text{REF}} = 5\%$ to 100% by steps of 5% (20 values).

Subject 5 - ^{23}Na FLORET - All REF & ROI - MEAN

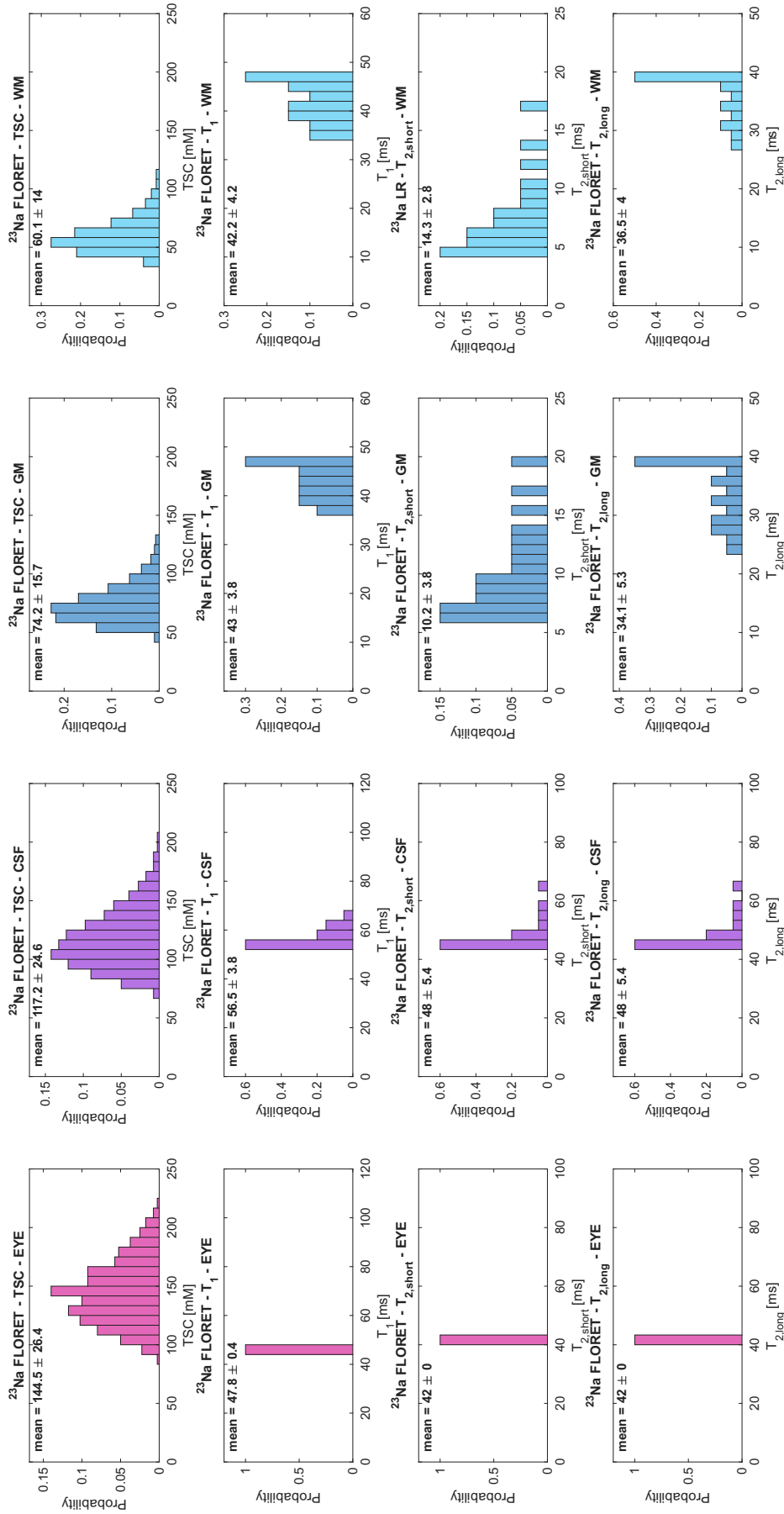


Figure S53. Histograms of the mean values from multiple measurements in subject 5, from the ^{23}Na FLORET data (TSC, T_1 , $T_{2,\text{short}}$, $T_{2,\text{long}}$), in the EYE, CSF, GM and WM. The mean values of each metric were measured multiple times from different N_{ROI} and N_{REF} highest values in all the ROIs and in the reference ROI (eye), respectively, for TSC (for a total of 400 measurements), and from different N_{ROI} highest values in all the ROIs for the relaxation times (for a total of 20 measurements). Highest values used: $N_{\text{ROI}} = 5\%$ to 100% by steps of 5% (20 values), $N_{\text{REF}} = 5\%$ to 100% by steps of 5% (20 values).

Subject 6 - ^{23}Na FLORET - All REF & ROI - MEAN

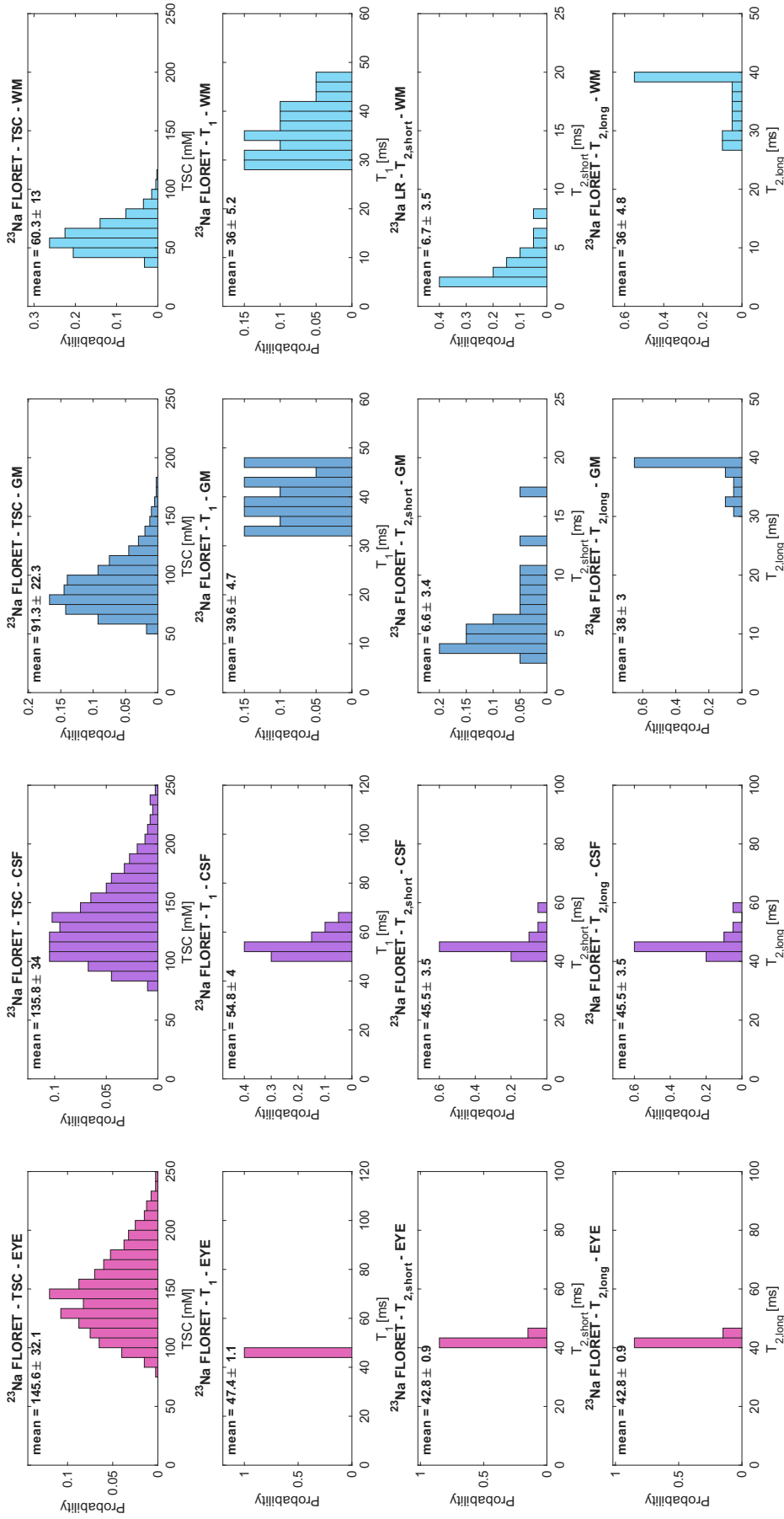


Figure S54. Histograms of the mean values from multiple measurements in subject 6, from the ^{23}Na FLORET data (TSC, T_1 , $T_{2,\text{short}}$, $T_{2,\text{long}}$), in the EYE, CSF, GM and WM. The mean values of each metric were measured multiple times from different N_{ROI} and N_{REF} highest values in all the ROIs and in the reference ROI (eye), respectively, for TSC (for a total of 400 measurements), and from different N_{ROI} highest values in all the ROIs for the relaxation times (for a total of 20 measurements). Highest values used: $N_{\text{ROI}} = 5\%$ to 100% by steps of 5% (20 values), $N_{\text{REF}} = 5\%$ to 100% by steps of 5% (20 values).

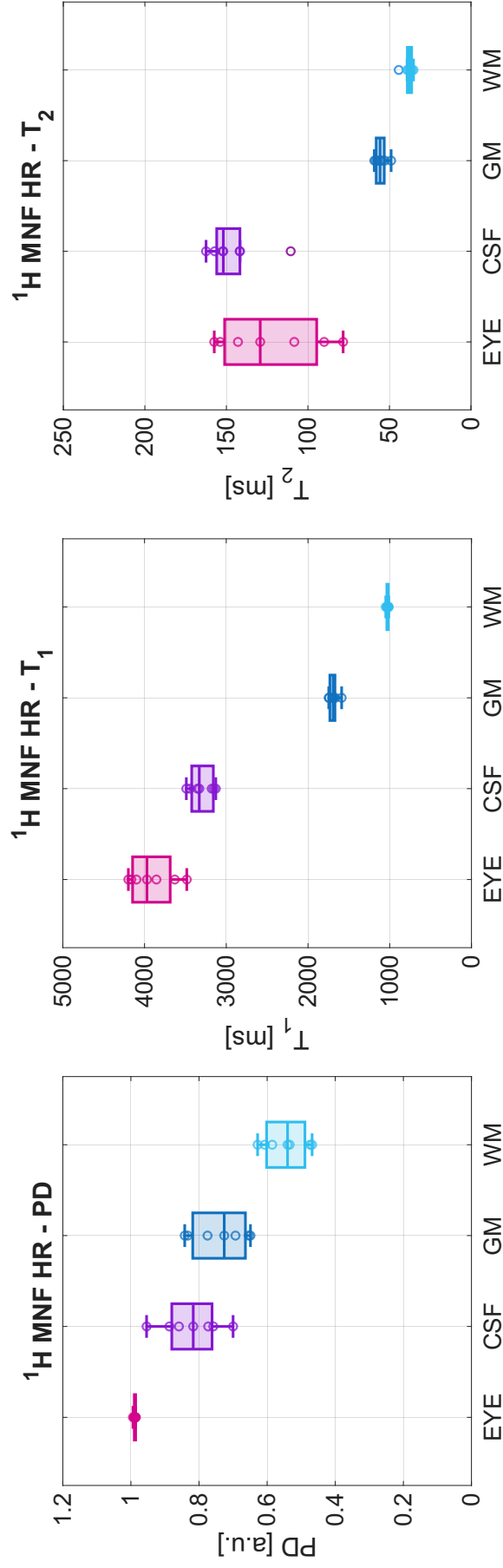


Figure S55. Boxplots of the mean values of the mean measurements using the N_{ROI} and N_{REF} values (histograms) from $N = 7$ subjects, from the $^1\text{H MNF HR}$ data (PD, T_1 , T_2), in the EYE, CSF, GM and WM. Highest values used: $N_{\text{ROI}} = 5\%$ to 100% by steps of 5% (20 values), $N_{\text{REF}} = 5\%$ to 100% by steps of 5% (20 values).

Note: This figure corresponds to Figure 3 in the article. It is just reproduced here for completeness of the Supplementary Information in order to show all data in the same file.

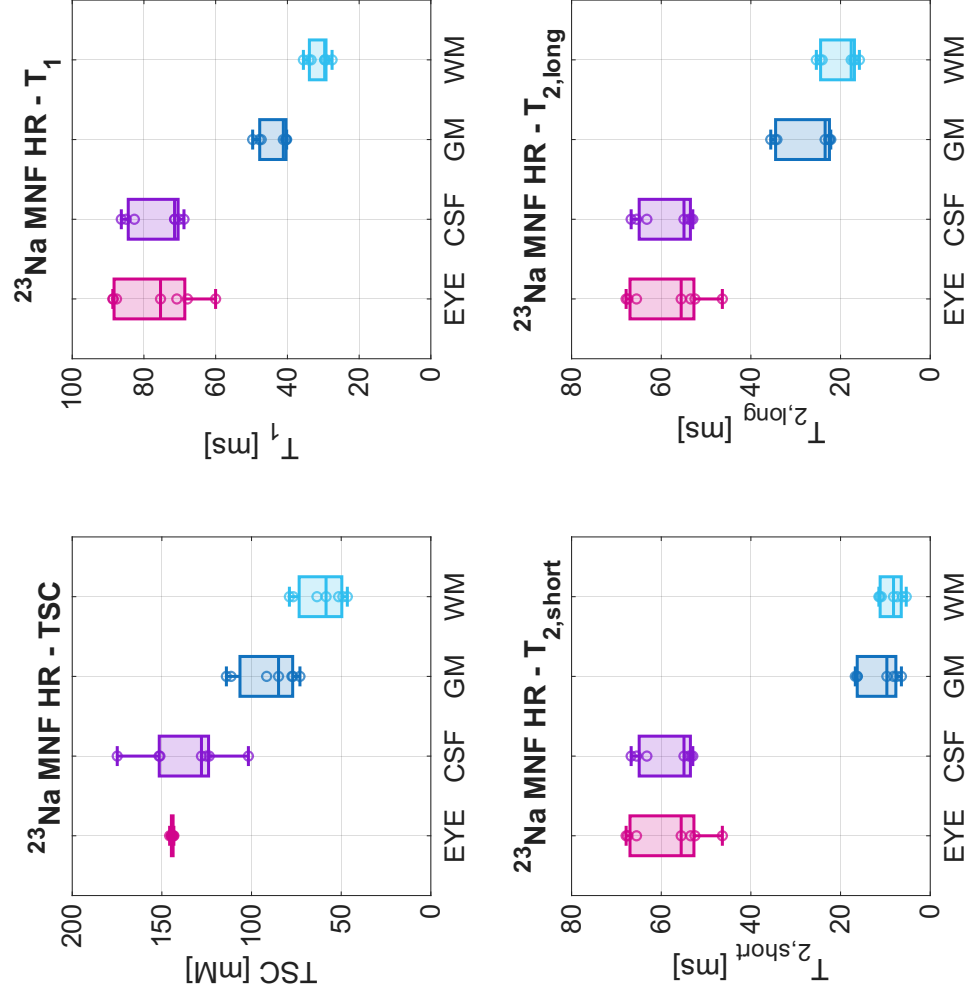


Figure S56. Boxplots of the mean values of the mean measurements using the N_{ROI} and N_{REF} values (histograms) from $N = 7$ subjects, from the ^{23}Na MNF HR data (TSC , T_1 , $T_{2,short}$, $T_{2,long}$), in the EYE, CSF, GM and WM. Highest values used: $N_{ROI} = 5\%$ to 100% by steps of 5% (20 values), $N_{REF} = 5\%$ to 100% by steps of 5% (20 values).

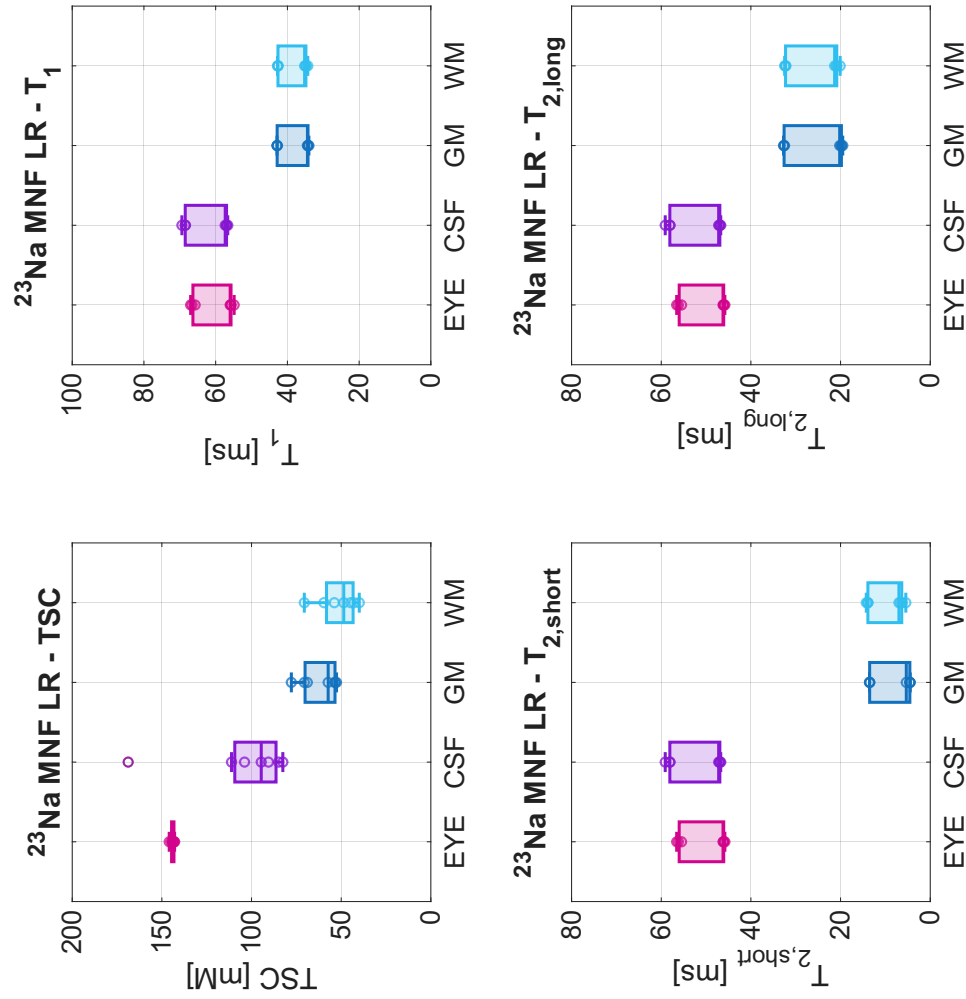


Figure S57. Boxplots of the mean values of the mean measurements using the N_{ROI} and N_{REF} values (histograms) from $N = 7$ subjects, from the ^{23}Na MNF LR data (TSC , T_1 , $T_{2,short}$, $T_{2,long}$), in the EYE, CSF, GM and WM. Highest values used: $N_{ROI} = 5\%$ to 100% by steps of 5% (20 values), $N_{REF} = 5\%$ to 100% by steps of 5% (20 values).

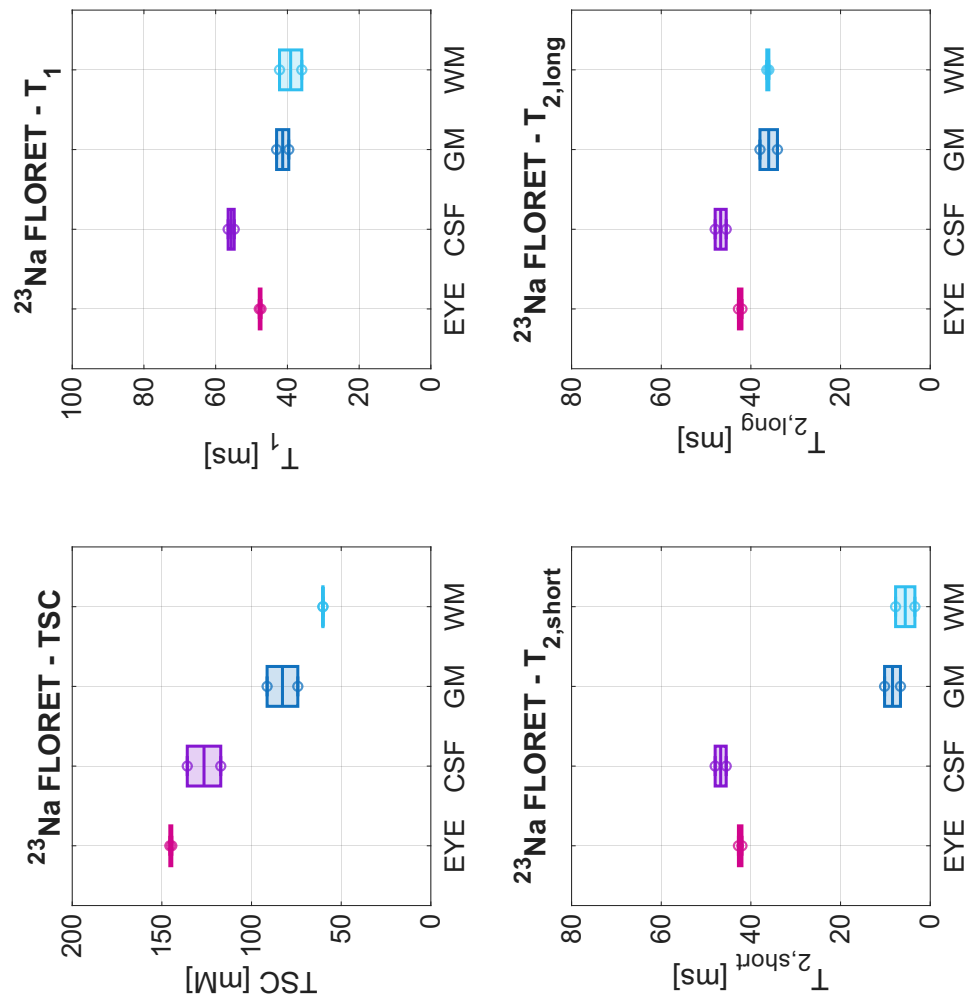


Figure S58. Boxplots of the mean values of the mean measurements using the N_{ROI} and N_{REF} values (histograms) from subjects 5 & 6, from the ^{23}Na FLORET data (T_{SC} , T_1 , $T_{2,\text{short}}$, $T_{2,\text{long}}$), in the EYE, CSF, GM and WM. Highest values used: $N_{\text{ROI}} = 5\%$ to 100% by steps of 5% (20 values), $N_{\text{REF}} = 5\%$ to 100% by steps of 5% (20 values).

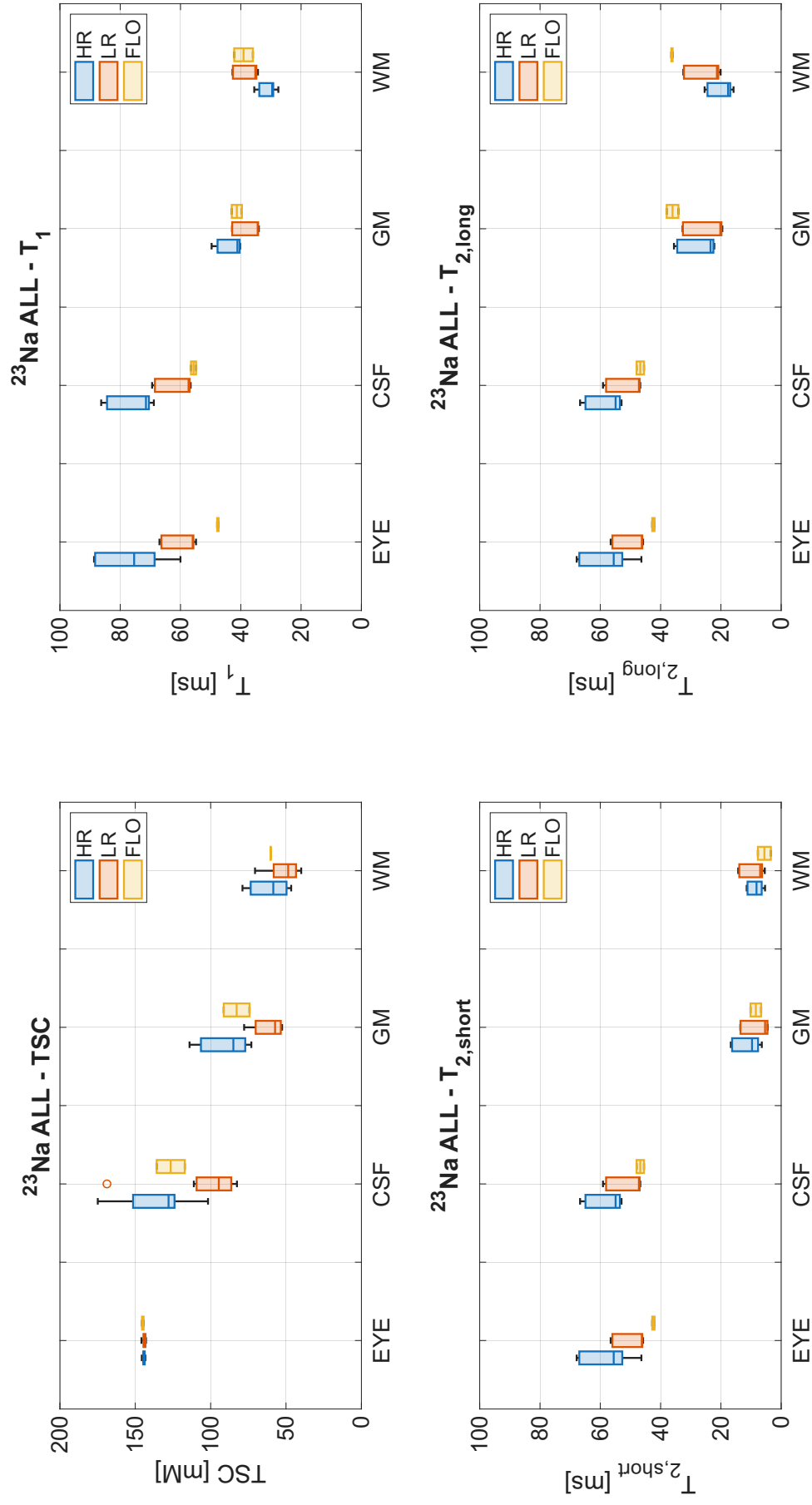


Figure S59. Boxplots for comparison of the mean values of the mean measurements using the N_{ROI} and N_{REF} values (histograms), from the ^{23}Na MNF HR (7 subjects), LR (7 subjects) and FLORET (FLO, 2 subjects: 5 and 6) data (T_{SC} , T_1 , $T_{2,\text{short}}$, $T_{2,\text{long}}$), in the EYE, CSF, GM and WM. Highest values used: $N_{\text{ROI}} = 5\%$ to 100% by steps of 5% (20 values), $N_{\text{REF}} = 5\%$ to 100% by steps of 5% (20 values).

Note: This figure corresponds to Figure 4 in the article. It is just reproduced here for completeness of the Supplementary Information in order to show all data in the same file.

4 TABLES: Multiple measurements in brain (20 N_{ROI} & 20 N_{REF} values)

4.1 Statistics

In this section, we present tables of the results shown in the figures in Section 2, where the measurements of all MNF and ^{23}Na FLORET metrics consist of the distribution of:

- The $N = 400$ *mean* PD and TSC values measured in all ROIs in each subject (from 20 $N_{ROI} \times 20 N_{REF}$ values).
- The $N = 20$ *mean* ^1H and ^{23}Na relaxation times values measured in all ROIs in each subject (from 20 N_{ROI} values).

4.1.1 Mean & standard deviation (std)

The overall mean and standard deviation (std) values of each distribution of *mean* values for each metric in each ROI was calculated using three statistical methods, and according to the two following steps:

1. Mean \pm std for each subject:

- Standard:** The standard mean \pm std was applied over all mean values in each dataset (or distribution) of size $N = 20$ or 400 (depending on the metric), resulting in a *final mean* and *std* for each subject.
- Jackknife:** Jackknife resampling (1, 2) consisted of the following two steps for each subject:
 - Calculate the mean value of each possible leave-one-out subsample of size $(N - 1)$ of the full dataset of size $N = 20$ or 400 mean values (depending on the metric), resulting in a new dataset of N mean values from N subsamples.
 - Calculate the *final mean* and *std* of this new dataset of N mean values from the N subsamples.

The Jackknife method can usually be used to reduce bias and variance in the estimation of statistical parameters (mean and std in our case).

- Bootstrap:** Bootstrap resampling (or bootstrapping) with replacement (1, 2) consisted of the following four steps for each subject:
 - Randomly and separately select N values from the full dataset of size $N = 20$ or 400 mean values (depending on the metric)—which means that some values can be selected multiple times, hence the term "replacement"—to generate a new dataset of N mean values (1 bootstrap).
 - Calculate the mean value of this new bootstrap dataset of N values.
 - Repeat steps i. and ii. $N_{btsp} = 1000$ times.
 - Calculate the *final mean* and *std* of the N_{btsp} mean values for each subject.

Similarly to Jackknife, bootstrapping can usually be used to reduce bias and variance in the estimation of statistical parameters (mean and std in our case).

- Mean \pm std over all subjects:** For each method, the mean \pm one std of both the *final mean* values and the *final std* values from each subject was calculated over all subjects.

4.1.2 Wilcoxon rank-sum test

The Wilcoxon rank-sum statistical test was applied between the *final mean* values from the *standard* method between all metrics from ^{23}Na MNF HR, LR and FLORET over all subjects in each ROI. Bonferroni correction (BC) was applied to the p values in order to take into account the number of tests ($N_{meas} = 3$) of each metric for each tissue: $p_{BC} = N_{meas} \cdot p$. Statistically significant differences between measurements, without and with BC, were therefore defined as p and $p_{BC} \leq 0.05$.

4.2 Summary of the measurements

Data Acquisition	Metrics	N _{REF} (PD & TSC)	N _{ROI} (all metrics)	ROIs	Statistical Methods	Subjects
¹ H MNF HR	PD, T ₁ , T ₂	5:5:100%	5:5:100%	EYE, CSE, GM, WM	Standard, Jackknife, Bootstrap	1-7
²³ Na MNF HR	TSC, T ₁ , T _{2,short} , T _{2,long}	5:5:100%	5:5:100%	EYE, CSE, GM, WM	Standard, Jackknife, Bootstrap	1-7
²³ Na MNF LR	TSC, T ₁ , T _{2,short} , T _{2,long}	5:5:100%	5:5:100%	EYE, CSE, GM, WM	Standard, Jackknife, Bootstrap	1-7
²³ Na FLORET	TSC, T ₁ , T _{2,short} , T _{2,long}	5:5:100%	5:5:100%	EYE, CSE, GM, WM	Standard, Jackknife, Bootstrap	5, 6

For N_{REF} and N_{ROI}, ranges of values are given as begin:step:end.

Table S1. Mean measurements from ^1H MNF HR in brain at 7 T: Results from 7 subjects for normalized proton density (PD), and relaxation times T_1 and T_2 . Results are presented as mean \pm one standard deviation (std) of both the mean and std values measured in each ROI and in each subject, from 3 statistical methods: (1) Standard mean \pm std; (2) Jackknife; (3) Bootstrap (n = 1000 bootstraps with replacement).

^1H MNF HR	PD			T_1 [ms]			T_2 [ms]		
	Statistical Method	Jackknife	Bootstrap	Standard	Jackknife	Bootstrap	Standard	Jackknife	Bootstrap
Eye (Vitreal Humor)									
Subject 1	0.986 \pm 0.106	0.986 \pm 0.000	0.986 \pm 0.005	3854.75 \pm 274.31	3854.75 \pm 0.69	3855.11 \pm 13.47	153.80 \pm 36.22	153.80 \pm 0.09	153.87 \pm 1.84
Subject 2	0.994 \pm 0.166	0.994 \pm 0.000	0.994 \pm 0.008	3970.30 \pm 277.91	3970.30 \pm 0.70	3970.67 \pm 13.52	142.89 \pm 40.90	142.89 \pm 0.10	142.97 \pm 2.02
Subject 3	0.990 \pm 0.145	0.990 \pm 0.000	0.990 \pm 0.007	4162.17 \pm 172.59	4162.17 \pm 0.43	4162.19 \pm 8.60	90.02 \pm 23.22	90.02 \pm 0.06	90.09 \pm 1.13
Subject 4	0.987 \pm 0.142	0.987 \pm 0.000	0.987 \pm 0.006	3629.98 \pm 243.11	3629.98 \pm 0.61	3629.98 \pm 11.80	129.23 \pm 24.94	129.23 \pm 0.06	129.23 \pm 1.28
Subject 5	0.987 \pm 0.114	0.987 \pm 0.000	0.986 \pm 0.006	4098.97 \pm 209.83	4098.97 \pm 0.53	4098.79 \pm 10.33	78.38 \pm 22.18	78.38 \pm 0.06	78.31 \pm 1.16
Subject 6	0.988 \pm 0.125	0.988 \pm 0.000	0.988 \pm 0.006	3483.27 \pm 262.88	3483.27 \pm 0.66	3483.02 \pm 13.06	157.43 \pm 32.05	157.43 \pm 0.08	157.47 \pm 1.65
Subject 7	0.986 \pm 0.113	0.986 \pm 0.000	0.986 \pm 0.006	4197.81 \pm 170.47	4197.81 \pm 0.43	4197.57 \pm 8.30	108.35 \pm 43.66	108.35 \pm 0.11	108.34 \pm 2.21
Mean \pm Std of Mean ¹	0.989 \pm 0.013	0.989 \pm 0.003	0.989 \pm 0.003	3913.89 \pm 273.63	3913.89 \pm 273.63	3913.89 \pm 273.65	122.87 \pm 31.25	122.87 \pm 31.25	122.90 \pm 31.29
Mean \pm Std of Std ²	0.130 \pm 0.022	0.000 \pm 0.000	0.006 \pm 0.001	230.16 \pm 46.11	0.58 \pm 0.12	11.30 \pm 2.24	31.88 \pm 8.72	0.08 \pm 0.02	1.61 \pm 0.43
Cerebrospinal Fluid (CSF)									
Subject 1	0.859 \pm 0.151	0.859 \pm 0.000	0.859 \pm 0.007	3488.56 \pm 486.05	3488.56 \pm 1.22	3488.42 \pm 23.70	157.14 \pm 50.18	157.14 \pm 0.13	157.14 \pm 2.61
Subject 2	0.773 \pm 0.130	0.773 \pm 0.000	0.773 \pm 0.007	3128.27 \pm 439.63	3128.27 \pm 1.10	3127.14 \pm 22.37	141.87 \pm 48.55	141.87 \pm 0.12	141.90 \pm 2.55
Subject 3	0.758 \pm 0.111	0.758 \pm 0.000	0.758 \pm 0.006	3446.52 \pm 329.35	3446.52 \pm 0.82	3446.78 \pm 16.61	152.28 \pm 45.19	152.28 \pm 0.11	152.08 \pm 2.30
Subject 4	0.700 \pm 0.099	0.700 \pm 0.000	0.699 \pm 0.005	3151.74 \pm 383.27	3151.74 \pm 0.96	3152.58 \pm 18.98	110.54 \pm 34.21	110.54 \pm 0.09	110.53 \pm 1.77
Subject 5	0.954 \pm 0.114	0.954 \pm 0.000	0.954 \pm 0.006	3351.52 \pm 345.46	3351.52 \pm 0.87	3351.52 \pm 17.24	162.45 \pm 45.85	162.45 \pm 0.11	162.41 \pm 2.25
Subject 6	0.887 \pm 0.116	0.887 \pm 0.000	0.887 \pm 0.006	3300.48 \pm 331.16	3300.48 \pm 0.83	3300.60 \pm 16.84	151.88 \pm 39.19	151.88 \pm 0.10	151.87 \pm 1.93
Subject 7	0.817 \pm 0.105	0.817 \pm 0.000	0.818 \pm 0.005	3177.57 \pm 419.45	3177.57 \pm 1.05	3177.27 \pm 21.92	141.63 \pm 48.45	141.63 \pm 0.12	141.53 \pm 2.44
Mean \pm Std of Mean	0.821 \pm 0.086	0.821 \pm 0.086	0.821 \pm 0.086	3296.39 \pm 445.47	3296.39 \pm 445.47	3296.37 \pm 445.58	145.40 \pm 17.12	145.40 \pm 17.12	145.35 \pm 17.11
Mean \pm Std of Std	0.118 \pm 0.017	0.000 \pm 0.000	0.006 \pm 0.001	390.62 \pm 60.17	0.98 \pm 0.15	19.67 \pm 2.95	44.52 \pm 5.78	0.11 \pm 0.01	2.26 \pm 0.31
Gray Matter (GM)									
Subject 1	0.833 \pm 0.086	0.833 \pm 0.000	0.833 \pm 0.004	1746.05 \pm 105.46	1746.05 \pm 0.26	1746.25 \pm 5.29	48.96 \pm 5.03	48.96 \pm 0.01	48.97 \pm 0.26
Subject 2	0.693 \pm 0.091	0.693 \pm 0.000	0.693 \pm 0.004	1588.40 \pm 97.55	1588.40 \pm 0.24	1588.27 \pm 4.85	52.81 \pm 10.08	52.81 \pm 0.02	52.81 \pm 0.50
Subject 3	0.654 \pm 0.079	0.654 \pm 0.000	0.654 \pm 0.004	1742.83 \pm 116.32	1742.83 \pm 0.29	1743.21 \pm 5.89	57.28 \pm 13.01	57.28 \pm 0.03	57.25 \pm 0.66
Subject 4	0.649 \pm 0.080	0.649 \pm 0.000	0.649 \pm 0.004	1701.45 \pm 109.11	1701.45 \pm 0.27	1701.29 \pm 5.76	54.30 \pm 10.77	54.30 \pm 0.03	54.32 \pm 0.54
Subject 5	0.842 \pm 0.087	0.842 \pm 0.000	0.842 \pm 0.004	1665.52 \pm 111.19	1665.52 \pm 0.28	1665.52 \pm 5.46	59.27 \pm 13.96	59.27 \pm 0.03	59.28 \pm 0.71
Subject 6	0.775 \pm 0.085	0.774 \pm 0.000	0.774 \pm 0.004	1692.51 \pm 109.56	1692.51 \pm 0.27	1692.58 \pm 5.57	58.40 \pm 12.34	58.40 \pm 0.03	58.37 \pm 0.63
Subject 7	0.726 \pm 0.074	0.726 \pm 0.000	0.725 \pm 0.004	1684.11 \pm 106.34	1684.11 \pm 0.27	1684.20 \pm 5.10	55.75 \pm 10.71	55.75 \pm 0.03	55.76 \pm 0.53
Mean \pm Std of Mean	0.799 \pm 0.080	0.799 \pm 0.080	0.799 \pm 0.080	1668.70 \pm 53.25	1668.70 \pm 53.25	1668.73 \pm 53.40	55.25 \pm 5.58	55.25 \pm 5.58	55.25 \pm 3.57
Mean \pm Std of Std	0.083 \pm 0.006	0.000 \pm 0.000	0.004 \pm 0.000	107.93 \pm 5.80	0.27 \pm 0.02	5.42 \pm 0.37	10.84 \pm 2.92	0.03 \pm 0.01	0.59 \pm 0.15
White Matter (WM)									
Subject 1	0.607 \pm 0.057	0.607 \pm 0.000	0.607 \pm 0.003	1048.45 \pm 43.83	1048.45 \pm 0.11	1048.36 \pm 2.25	44.28 \pm 9.36	44.28 \pm 0.02	44.28 \pm 0.48
Subject 2	0.534 \pm 0.065	0.534 \pm 0.000	0.534 \pm 0.003	1017.74 \pm 39.63	1017.74 \pm 0.10	1017.83 \pm 1.98	37.61 \pm 3.26	37.62 \pm 0.01	37.61 \pm 0.16
Subject 3	0.474 \pm 0.052	0.474 \pm 0.000	0.474 \pm 0.003	1028.61 \pm 53.80	1028.61 \pm 0.14	1028.50 \pm 2.71	35.23 \pm 2.68	35.23 \pm 0.01	35.23 \pm 0.14
Subject 4	0.468 \pm 0.051	0.468 \pm 0.000	0.469 \pm 0.003	1028.66 \pm 45.37	1028.66 \pm 0.11	1028.60 \pm 2.17	39.18 \pm 5.07	39.18 \pm 0.01	39.19 \pm 0.26
Subject 5	0.628 \pm 0.057	0.628 \pm 0.000	0.628 \pm 0.003	1020.43 \pm 46.22	1020.43 \pm 0.12	1020.52 \pm 2.27	36.91 \pm 3.60	36.91 \pm 0.01	36.91 \pm 0.18
Subject 6	0.585 \pm 0.058	0.585 \pm 0.000	0.585 \pm 0.003	1037.33 \pm 48.15	1037.33 \pm 0.12	1037.19 \pm 2.45	38.51 \pm 2.08	38.51 \pm 0.01	38.51 \pm 0.20
Subject 7	0.540 \pm 0.049	0.540 \pm 0.000	0.540 \pm 0.002	1011.49 \pm 49.62	1011.49 \pm 0.12	1011.50 \pm 2.44	36.20 \pm 2.96	36.20 \pm 0.01	36.19 \pm 0.15
Mean \pm Std of Mean	0.548 \pm 0.062	0.548 \pm 0.062	0.548 \pm 0.062	1027.53 \pm 12.52	1027.53 \pm 12.52	1027.53 \pm 12.45	38.28 \pm 2.97	38.28 \pm 2.97	38.27 \pm 2.97
Mean \pm Std of Std	0.056 \pm 0.005	0.000 \pm 0.000	0.003 \pm 0.000	46.66 \pm 4.50	0.12 \pm 0.01	2.32 \pm 0.23	4.43 \pm 2.31	0.01 \pm 0.01	0.22 \pm 0.12

Table S2. Mean measurements from ²³Na MNF HR in brain at 7 T: Results from 7 subjects for total sodium concentration (TSC) and relaxation times T₁, T_{2,short} and T_{2,long}. TSC is measured in mM (or mmol/L), with mean TSC in the eye (vitreous humor) used as internal reference (145 mM). Results are presented as mean ± one standard deviation (std) of both the mean and std values measured in each ROI and in each subject, from 3 statistical methods: (1) Standard mean ± std; (2) Jackknife; (3) Bootstrap (n = 1000 bootstraps with replacement). For the eyes (vitreous humor) and CSF; T_{2,long} = T_{2,short} ≡ T₂.

Statistical Method	TSC [mM]			T ₁ [ms]			T _{2,short} [ms]			T _{2,long} [ms]		
	Standard	Jackknife	Bootstrap	Standard	Jackknife	Bootstrap	Standard	Jackknife	Bootstrap	Standard	Jackknife	Bootstrap
Eye (Vitreous Humor)												
Subject 1	144.16 ± 24.62	144.16 ± 0.06	144.11 ± 1.25	67.86 ± 7.41	67.86 ± 0.02	67.85 ± 0.36	52.47 ± 5.89	52.47 ± 0.02	52.46 ± 0.29	52.47 ± 5.89	52.47 ± 0.02	52.47 ± 0.29
Subject 2	145.47 ± 32.82	145.67 ± 0.08	145.70 ± 1.69	70.83 ± 9.49	70.83 ± 0.02	70.83 ± 0.48	53.43 ± 7.41	53.43 ± 0.02	53.44 ± 0.37	53.43 ± 7.41	53.43 ± 0.02	53.44 ± 0.38
Subject 3	144.47 ± 26.45	144.47 ± 0.07	144.41 ± 1.31	88.68 ± 8.20	88.68 ± 0.02	88.68 ± 0.39	67.83 ± 6.32	67.83 ± 0.02	67.84 ± 0.31	67.83 ± 6.32	67.83 ± 0.02	67.82 ± 0.31
Subject 4	143.60 ± 20.91	143.60 ± 0.05	143.68 ± 1.06	87.66 ± 7.90	87.66 ± 0.02	87.66 ± 0.40	65.52 ± 5.94	65.52 ± 0.02	65.54 ± 0.29	65.52 ± 5.94	65.52 ± 0.02	65.53 ± 0.30
Subject 5	144.61 ± 27.22	144.61 ± 0.07	144.58 ± 1.33	88.56 ± 9.87	88.56 ± 0.03	88.58 ± 0.50	67.46 ± 7.49	67.46 ± 0.02	67.44 ± 0.38	67.46 ± 7.49	67.46 ± 0.02	67.47 ± 0.37
Subject 6	143.32 ± 18.79	143.32 ± 0.05	143.36 ± 0.88	60.02 ± 5.71	60.02 ± 0.01	60.02 ± 0.28	46.37 ± 4.58	46.37 ± 0.01	46.36 ± 0.24	46.37 ± 4.58	46.37 ± 0.01	46.37 ± 0.23
Subject 7	144.72 ± 27.79	144.72 ± 0.07	144.69 ± 1.43	75.40 ± 7.17	75.40 ± 0.02	75.36 ± 0.36	55.55 ± 5.13	55.55 ± 0.01	55.54 ± 0.30	55.55 ± 5.13	55.55 ± 0.01	55.54 ± 0.25
Mean ± Std of Mean	144.37 ± 0.78	144.37 ± 0.78	144.36 ± 0.76	77.00 ± 11.52	77.00 ± 11.52	77.00 ± 11.52	58.36 ± 8.51	58.36 ± 8.51	58.36 ± 8.51	58.36 ± 8.51	58.36 ± 8.51	58.36 ± 8.51
Mean ± Std of Std	25.51 ± 4.65	0.06 ± 0.01	1.28 ± 0.26	7.96 ± 1.42	0.02 ± 0.00	0.40 ± 0.08	6.11 ± 1.08	0.02 ± 0.00	0.30 ± 0.05	6.11 ± 1.08	0.02 ± 0.00	0.31 ± 0.06
Cerebrospinal Fluid (CSF)												
Subject 1	151.10 ± 29.00	151.10 ± 0.07	151.10 ± 1.40	71.40 ± 9.66	71.40 ± 0.02	71.41 ± 0.48	54.93 ± 8.06	54.93 ± 0.02	54.93 ± 0.40	54.93 ± 8.06	54.93 ± 0.02	54.93 ± 0.40
Subject 2	151.59 ± 31.04	151.59 ± 0.08	151.53 ± 1.50	68.94 ± 9.13	68.94 ± 0.02	68.85 ± 0.45	52.96 ± 7.76	52.96 ± 0.02	52.98 ± 0.38	52.96 ± 7.76	52.96 ± 0.02	52.96 ± 0.40
Subject 3	127.93 ± 21.52	127.93 ± 0.05	127.86 ± 1.05	84.94 ± 8.46	84.94 ± 0.02	84.94 ± 0.44	65.49 ± 6.65	65.49 ± 0.02	65.50 ± 0.33	65.49 ± 6.65	65.49 ± 0.02	65.52 ± 0.33
Subject 4	123.59 ± 20.39	123.59 ± 0.05	123.58 ± 1.03	82.67 ± 10.02	82.67 ± 0.03	82.69 ± 0.51	63.21 ± 7.87	63.21 ± 0.02	63.23 ± 0.40	63.21 ± 7.87	63.21 ± 0.02	63.21 ± 0.40
Subject 5	125.10 ± 22.72	125.10 ± 0.06	125.16 ± 1.14	86.31 ± 9.33	86.31 ± 0.02	86.33 ± 0.47	66.71 ± 7.27	66.71 ± 0.02	66.74 ± 0.36	66.71 ± 7.27	66.71 ± 0.02	66.72 ± 0.37
Subject 6	174.88 ± 24.11	174.88 ± 0.06	174.80 ± 1.17	70.17 ± 6.98	70.17 ± 0.02	70.16 ± 0.35	53.80 ± 6.13	53.80 ± 0.01	53.79 ± 0.30	53.80 ± 6.13	53.80 ± 0.02	53.80 ± 0.30
Subject 7	101.75 ± 20.84	101.75 ± 0.05	101.77 ± 1.03	71.46 ± 9.76	71.46 ± 0.02	71.44 ± 0.49	53.40 ± 7.80	53.40 ± 0.02	53.39 ± 0.39	53.40 ± 7.80	53.42 ± 0.02	53.40 ± 0.40
Mean ± Std of Mean	136.56 ± 24.12	136.56 ± 24.12	136.56 ± 24.12	76.54 ± 7.70	76.54 ± 7.70	76.55 ± 7.71	58.64 ± 6.19	58.64 ± 6.19	58.65 ± 6.20	58.64 ± 6.19	58.64 ± 6.19	58.65 ± 6.20
Mean ± Std of Std	24.23 ± 4.18	0.06 ± 0.01	1.19 ± 0.19	9.05 ± 1.04	0.02 ± 0.00	0.46 ± 0.05	7.36 ± 0.72	0.02 ± 0.00	0.37 ± 0.04	7.36 ± 0.72	0.02 ± 0.00	0.37 ± 0.04
Gray Matter (GM)												
Subject 1	91.58 ± 13.02	91.58 ± 0.03	91.58 ± 0.64	41.13 ± 2.71	41.13 ± 0.01	41.14 ± 0.14	9.67 ± 3.07	9.67 ± 0.01	9.67 ± 0.15	23.45 ± 1.93	23.45 ± 0.01	23.44 ± 0.10
Subject 2	111.41 ± 20.19	111.41 ± 0.05	111.41 ± 1.01	40.36 ± 2.81	40.36 ± 0.01	40.36 ± 0.14	7.50 ± 2.65	7.50 ± 0.01	7.50 ± 0.13	22.44 ± 2.01	22.44 ± 0.01	22.44 ± 0.10
Subject 3	77.49 ± 12.90	77.49 ± 0.03	77.51 ± 0.67	47.31 ± 3.36	47.31 ± 0.01	47.31 ± 0.16	16.27 ± 2.48	16.27 ± 0.01	16.27 ± 0.13	34.20 ± 0.01	34.20 ± 0.01	34.21 ± 0.13
Subject 4	84.94 ± 12.41	84.94 ± 0.03	84.96 ± 0.63	49.69 ± 3.49	49.69 ± 0.01	49.68 ± 0.18	16.29 ± 2.27	16.29 ± 0.01	16.29 ± 0.11	35.57 ± 2.62	35.57 ± 0.01	35.57 ± 0.13
Subject 5	76.91 ± 12.80	76.91 ± 0.03	76.92 ± 0.64	47.86 ± 3.51	47.86 ± 0.01	47.87 ± 0.18	16.71 ± 2.59	16.71 ± 0.01	16.71 ± 0.13	34.59 ± 2.68	34.59 ± 0.01	34.59 ± 0.13
Subject 6	114.02 ± 14.47	114.02 ± 0.04	114.02 ± 0.73	40.59 ± 2.93	40.59 ± 0.01	40.51 ± 0.15	18.18 ± 2.77	18.18 ± 0.01	18.18 ± 0.14	22.62 ± 2.06	22.62 ± 0.01	22.61 ± 0.10
Subject 7	73.01 ± 12.10	73.01 ± 0.03	73.02 ± 0.61	40.21 ± 2.89	40.21 ± 0.01	40.21 ± 0.15	6.43 ± 2.35	6.43 ± 0.01	6.43 ± 0.12	22.19 ± 2.02	22.19 ± 0.01	22.18 ± 0.10
Mean ± Std of Mean	89.91 ± 16.73	89.91 ± 16.73	89.92 ± 16.72	43.86 ± 4.21	43.86 ± 4.21	43.86 ± 4.20	11.56 ± 4.63	11.56 ± 4.63	11.56 ± 4.63	27.86 ± 6.50	27.86 ± 6.50	27.87 ± 6.50
Mean ± Std of Std	14.00 ± 2.83	0.04 ± 0.01	0.70 ± 0.14	3.10 ± 0.34	0.01 ± 0.00	0.16 ± 0.02	2.60 ± 0.27	0.01 ± 0.00	0.13 ± 0.01	2.28 ± 0.34	0.01 ± 0.00	0.11 ± 0.02
White Matter (WM)												
Subject 1	63.52 ± 8.36	63.52 ± 0.02	63.52 ± 0.43	29.60 ± 1.30	29.60 ± 0.00	29.60 ± 0.07	8.19 ± 2.03	8.19 ± 0.01	8.18 ± 0.10	17.63 ± 1.20	17.63 ± 0.00	17.63 ± 0.06
Subject 2	78.88 ± 13.13	78.88 ± 0.03	78.89 ± 0.67	29.57 ± 1.23	29.57 ± 0.00	29.57 ± 0.06	6.16 ± 1.78	6.16 ± 0.00	6.16 ± 0.09	16.84 ± 1.04	16.84 ± 0.00	16.84 ± 0.05
Subject 3	49.07 ± 7.21	49.07 ± 0.02	49.08 ± 0.36	33.40 ± 1.57	33.40 ± 0.00	33.40 ± 0.08	10.92 ± 1.94	10.92 ± 0.00	10.92 ± 0.07	24.10 ± 1.31	24.10 ± 0.00	24.10 ± 0.07
Subject 4	56.44 ± 7.27	56.44 ± 0.02	56.45 ± 0.36	35.54 ± 1.56	35.54 ± 0.00	35.54 ± 0.07	11.28 ± 1.15	11.28 ± 0.00	11.28 ± 0.06	25.40 ± 1.06	25.40 ± 0.00	25.40 ± 0.05
Subject 5	51.42 ± 7.72	51.42 ± 0.02	51.43 ± 0.39	34.03 ± 1.45	34.03 ± 0.00	34.03 ± 0.07	11.45 ± 1.41	11.45 ± 0.00	11.46 ± 0.07	24.57 ± 1.22	24.57 ± 0.00	24.57 ± 0.06
Subject 6	76.76 ± 8.91	76.76 ± 0.02	76.75 ± 0.44	29.13 ± 1.27	29.13 ± 0.00	29.13 ± 0.06	7.37 ± 1.90	7.37 ± 0.01	7.37 ± 0.09	17.12 ± 1.20	17.12 ± 0.00	17.12 ± 0.06
Subject 7	46.58 ± 7.20	46.58 ± 0.02	46.59 ± 0.36	27.55 ± 1.29	27.55 ± 0.00	27.55 ± 0.06	5.35 ± 1.51	5.36 ± 0.00	5.36 ± 0.07	15.80 ± 1.12	15.80 ± 0.00	15.80 ± 0.06
Mean ± Std of Mean	60.67 ± 13.05	60.67 ± 13.05	60.67 ± 13.05	31.26 ± 3.01	31.26 ± 3.01	31.26 ± 3.01	8.67 ± 2.54	8.67 ± 2.54	8.67 ± 2.54	20.21 ± 4.25	20.21 ± 4.25	20.21 ± 4.25
Mean ± Std of Std	8.54 ± 2.12	0.02 ± 0.01	0.43 ± 0.11	1.35 ± 0.11	0.00 ± 0.00	0.00 ± 0.01	1.59 ± 0.32	0.00 ± 0.00	0.08 ± 0.02	1.17 ± 0.09	0.00 ± 0.00	0.06 ± 0.00

Table S3. Mean values from the multiple measurements on the ²³Na MNF LR data in brain at 7 T: Results from 7 subjects for total sodium concentration (TSC) and relaxation times T₁, T_{2,short} and T_{2,long}. TSC is measured in mM (or mmol/L), with mean TSC in the eye (vitreous humor) used as internal reference (145 mM). Results are presented as mean ± one standard deviation (std) of both the mean and std values measured in each ROI and in each subject, from 3 statistical methods: (1) Standard mean ± std; (2) Jackknife; (3) Bootstrap (n = 1000 bootstraps with replacement). For the eyes (vitreous humor) and CSF; T_{2,long} = T_{2,short} ≡ T₂.

Statistical Method	TSC [mmM]			T ₁ [ms]			T _{2,short} [ms]			T _{2,long} [ms]		
	Standard	Bootstrap	Jackknife	Standard	Bootstrap	Jackknife	Standard	Bootstrap	Jackknife	Standard	Bootstrap	Jackknife
Eye (Vitreous Humor)												
Subject 1	142.90 ± 15.20	142.94 ± 0.75	55.74 ± 1.24	55.74 ± 0.00	55.74 ± 0.06	46.07 ± 0.41	46.07 ± 0.02	46.07 ± 0.41	46.07 ± 0.00	46.07 ± 0.02	46.07 ± 0.41	46.07 ± 0.00
Subject 2	145.91 ± 33.79	145.93 ± 1.69	55.71 ± 0.91	55.71 ± 0.00	55.71 ± 0.04	46.07 ± 0.41	46.07 ± 0.02	46.07 ± 0.41	46.07 ± 0.00	46.07 ± 0.02	46.07 ± 0.41	46.07 ± 0.00
Subject 3	144.71 ± 27.72	144.75 ± 1.34	66.55 ± 3.34	66.55 ± 0.01	66.55 ± 0.17	56.17 ± 3.30	56.17 ± 0.31	56.17 ± 3.30	56.17 ± 0.01	56.17 ± 0.31	56.17 ± 3.30	56.17 ± 0.01
Subject 4	143.47 ± 19.94	143.48 ± 1.03	65.74 ± 3.60	65.74 ± 0.01	65.73 ± 0.19	55.48 ± 3.31	55.48 ± 0.01	55.48 ± 3.31	55.48 ± 0.01	55.48 ± 0.01	55.48 ± 3.31	55.48 ± 0.01
Subject 5	143.83 ± 22.48	143.78 ± 1.10	66.98 ± 3.22	66.98 ± 0.01	66.98 ± 0.16	56.56 ± 3.27	56.56 ± 0.01	56.56 ± 3.27	56.56 ± 0.01	56.56 ± 0.01	56.56 ± 3.27	56.56 ± 0.01
Subject 6	143.19 ± 17.72	143.16 ± 0.85	54.85 ± 1.02	54.85 ± 0.00	54.85 ± 0.05	45.81 ± 0.38	45.81 ± 0.00	45.81 ± 0.38	45.81 ± 0.00	45.81 ± 0.00	45.81 ± 0.38	45.81 ± 0.00
Subject 7	144.22 ± 24.94	144.26 ± 1.26	55.96 ± 0.88	55.96 ± 0.00	55.96 ± 0.04	46.22 ± 0.33	46.22 ± 0.02	46.22 ± 0.33	46.22 ± 0.00	46.22 ± 0.02	46.22 ± 0.33	46.22 ± 0.00
Mean ± Std of Mean	144.03 ± 1.03	144.04 ± 1.04	60.22 ± 5.82	60.22 ± 5.82	60.22 ± 5.82	50.34 ± 5.37	50.34 ± 5.37	50.34 ± 5.37	50.34 ± 5.37	50.34 ± 5.37	50.34 ± 5.37	50.34 ± 5.37
Mean ± Std of Std	23.11 ± 6.33	1.15 ± 0.32	2.03 ± 1.28	0.01 ± 0.00	0.10 ± 0.06	1.62 ± 1.57	0.08 ± 0.08	1.62 ± 1.57	0.00 ± 0.00	0.08 ± 0.08	1.62 ± 1.57	0.00 ± 0.00
Cerebrospinal Fluid (CSF)												
Subject 1	168.80 ± 36.49	168.80 ± 1.82	57.02 ± 2.36	57.02 ± 0.01	57.02 ± 0.12	46.96 ± 1.36	46.96 ± 0.07	46.96 ± 1.36	46.96 ± 0.00	46.96 ± 0.07	46.96 ± 1.36	46.96 ± 0.00
Subject 2	94.59 ± 21.16	94.61 ± 1.07	57.34 ± 2.69	57.34 ± 0.01	57.34 ± 0.14	47.19 ± 1.65	47.19 ± 0.08	47.19 ± 1.65	47.19 ± 0.00	47.19 ± 0.08	47.19 ± 1.65	47.19 ± 0.00
Subject 3	103.90 ± 21.45	103.93 ± 1.06	68.43 ± 1.51	68.43 ± 0.01	68.43 ± 0.12	58.10 ± 2.69	58.10 ± 0.13	58.10 ± 2.69	58.10 ± 0.01	58.10 ± 0.13	58.10 ± 2.69	58.10 ± 0.01
Subject 4	84.93 ± 15.22	84.91 ± 0.74	69.42 ± 1.92	69.42 ± 0.01	69.41 ± 0.09	59.11 ± 2.24	59.11 ± 0.11	59.11 ± 2.24	59.11 ± 0.01	59.11 ± 0.11	59.11 ± 2.24	59.11 ± 0.01
Subject 5	90.57 ± 15.34	90.55 ± 0.76	68.51 ± 2.46	68.51 ± 0.01	68.51 ± 0.12	58.04 ± 2.68	58.04 ± 0.13	58.04 ± 2.68	58.04 ± 0.01	58.04 ± 0.13	58.04 ± 2.68	58.04 ± 0.01
Subject 6	111.16 ± 17.74	111.17 ± 0.89	56.63 ± 2.09	56.63 ± 0.01	56.64 ± 0.10	46.73 ± 1.14	46.73 ± 0.06	46.73 ± 1.14	46.73 ± 0.00	46.73 ± 0.06	46.73 ± 1.14	46.73 ± 0.00
Subject 7	82.54 ± 13.94	82.53 ± 0.70	56.95 ± 2.32	56.95 ± 0.01	56.95 ± 0.12	46.92 ± 1.29	46.92 ± 0.06	46.92 ± 1.29	46.92 ± 0.00	46.92 ± 0.06	46.92 ± 1.29	46.92 ± 0.00
Mean ± Std of Mean	105.21 ± 29.81	105.21 ± 29.82	62.04 ± 6.32	62.04 ± 6.32	62.04 ± 6.32	51.86 ± 6.14	51.86 ± 6.14	51.86 ± 6.14	51.86 ± 6.14	51.86 ± 6.14	51.86 ± 6.14	51.86 ± 6.14
Mean ± Std of Std	20.19 ± 7.76	1.01 ± 0.39	2.33 ± 0.26	0.01 ± 0.00	0.12 ± 0.02	1.86 ± 0.86	0.09 ± 0.03	1.86 ± 0.86	0.01 ± 0.00	0.09 ± 0.03	1.86 ± 0.86	0.01 ± 0.00
Gray Matter (GM)												
Subject 1	77.79 ± 10.14	77.81 ± 0.49	34.41 ± 1.56	34.41 ± 0.00	34.41 ± 0.08	5.34 ± 2.86	5.34 ± 0.01	5.34 ± 2.86	5.34 ± 0.01	5.34 ± 0.01	5.34 ± 2.86	5.34 ± 0.01
Subject 2	68.90 ± 13.40	68.90 ± 0.88	34.29 ± 1.64	34.29 ± 0.00	34.29 ± 0.08	4.45 ± 2.56	4.45 ± 0.01	4.45 ± 2.56	4.45 ± 0.01	4.45 ± 0.01	4.45 ± 2.56	4.45 ± 0.01
Subject 3	52.61 ± 11.79	52.61 ± 0.61	42.88 ± 1.51	42.88 ± 0.00	42.88 ± 0.07	13.55 ± 2.90	13.55 ± 0.01	13.55 ± 2.90	13.55 ± 0.01	13.55 ± 0.01	13.55 ± 2.90	13.55 ± 0.01
Subject 4	53.49 ± 10.34	53.49 ± 0.51	42.78 ± 1.92	42.78 ± 0.00	42.78 ± 0.08	13.52 ± 2.91	13.52 ± 0.01	13.52 ± 2.91	13.52 ± 0.01	13.52 ± 0.01	13.52 ± 2.91	13.52 ± 0.01
Subject 5	53.45 ± 10.89	53.47 ± 0.55	42.91 ± 1.60	42.91 ± 0.00	42.91 ± 0.08	13.49 ± 2.90	13.49 ± 0.01	13.49 ± 2.90	13.49 ± 0.01	13.49 ± 0.01	13.49 ± 2.90	13.49 ± 0.01
Subject 6	70.57 ± 10.83	70.58 ± 0.35	34.24 ± 1.59	34.24 ± 0.00	34.24 ± 0.08	4.54 ± 2.49	4.54 ± 0.01	4.54 ± 2.49	4.54 ± 0.01	4.54 ± 0.01	4.54 ± 2.49	4.54 ± 0.01
Subject 7	57.27 ± 9.27	57.25 ± 0.47	34.01 ± 1.48	34.01 ± 0.00	34.01 ± 0.07	4.56 ± 2.56	4.56 ± 0.01	4.56 ± 2.56	4.56 ± 0.01	4.56 ± 0.01	4.56 ± 2.56	4.56 ± 0.01
Mean ± Std of Mean	62.01 ± 10.22	62.02 ± 10.22	37.93 ± 4.61	37.93 ± 4.61	37.93 ± 4.61	8.49 ± 4.71	8.49 ± 4.71	8.49 ± 4.71	8.49 ± 4.71	8.49 ± 4.71	8.49 ± 4.71	8.49 ± 4.71
Mean ± Std of Std	10.95 ± 1.33	0.53 ± 0.07	1.57 ± 0.06	0.00 ± 0.00	0.08 ± 0.00	2.74 ± 0.19	0.01 ± 0.00	2.74 ± 0.19	0.01 ± 0.00	0.01 ± 0.00	2.74 ± 0.19	0.01 ± 0.00
White Matter (WM)												
Subject 1	70.57 ± 9.82	70.58 ± 0.48	35.20 ± 2.07	35.20 ± 0.01	35.20 ± 0.11	6.98 ± 3.64	6.98 ± 0.01	6.98 ± 3.64	6.98 ± 0.01	6.98 ± 0.01	6.98 ± 3.64	6.98 ± 0.01
Subject 2	59.63 ± 11.81	59.62 ± 0.60	34.31 ± 1.65	34.31 ± 0.00	34.32 ± 0.08	5.45 ± 3.07	5.45 ± 0.01	5.45 ± 3.07	5.45 ± 0.01	5.45 ± 0.01	5.45 ± 3.07	5.45 ± 0.01
Subject 3	39.93 ± 8.82	39.93 ± 0.45	42.76 ± 1.68	42.76 ± 0.00	42.76 ± 0.08	13.91 ± 2.83	13.91 ± 0.01	13.91 ± 2.83	13.91 ± 0.01	13.91 ± 0.01	13.91 ± 2.83	13.91 ± 0.01
Subject 4	44.72 ± 6.64	44.73 ± 0.44	42.56 ± 1.79	42.56 ± 0.00	42.56 ± 0.09	13.90 ± 2.90	13.90 ± 0.01	13.90 ± 2.90	13.90 ± 0.01	13.90 ± 0.01	13.90 ± 2.90	13.90 ± 0.01
Subject 5	42.91 ± 9.10	42.93 ± 0.44	42.86 ± 1.61	42.86 ± 0.00	42.86 ± 0.08	14.26 ± 2.79	14.26 ± 0.01	14.26 ± 2.79	14.26 ± 0.01	14.26 ± 0.01	14.26 ± 2.79	14.26 ± 0.01
Subject 6	53.84 ± 7.62	53.84 ± 0.38	34.91 ± 1.89	34.91 ± 0.01	34.91 ± 0.10	6.67 ± 3.55	6.67 ± 0.01	6.67 ± 3.55	6.67 ± 0.01	6.67 ± 0.01	6.67 ± 3.55	6.67 ± 0.01
Subject 7	48.56 ± 9.30	48.56 ± 0.42	34.81 ± 1.99	34.81 ± 0.01	34.82 ± 0.09	6.25 ± 3.38	6.25 ± 0.01	6.25 ± 3.38	6.25 ± 0.01	6.25 ± 0.01	6.25 ± 3.38	6.25 ± 0.01
Mean ± Std of Mean	51.45 ± 10.78	51.46 ± 10.78	38.17 ± 4.21	38.17 ± 4.21	38.17 ± 4.20	9.63 ± 4.14	9.63 ± 4.14	9.63 ± 4.14	9.63 ± 4.14	9.63 ± 4.14	9.63 ± 4.14	9.63 ± 4.14
Mean ± Std of Std	9.16 ± 1.35	0.46 ± 0.07	1.81 ± 0.18	0.00 ± 0.00	0.09 ± 0.01	3.17 ± 0.35	0.01 ± 0.00	3.17 ± 0.35	0.01 ± 0.00	0.01 ± 0.00	3.17 ± 0.35	0.01 ± 0.00

Table S4. Mean measurements from ^{23}Na FLORET in brain at 7 T: Results from 2 subjects (#5 and 6) for total sodium concentration (TSC) and relaxation times T_1 , $T_{2,\text{short}}$ and $T_{2,\text{long}}$. TSC is measured in mM (or mmol/L), with mean TSC in the eye (vitreous humor) used as internal reference (145 mM). Results are presented as mean \pm one standard deviation (std) of both the mean and std values measured in each ROI and in each subject, from 3 statistical methods: (1) Standard mean \pm std; (2) Jackknife; (3) Bootstrap (n = 1000 bootstraps with replacement). For the eyes (vitreous humor) and CSF, $T_{2,\text{long}} = T_{2,\text{short}} \equiv T_2$.

Statistical Method	TSC (mM)			T_1 (ms)			$T_{2,\text{short}}$ (ms)			$T_{2,\text{long}}$ (ms)		
	Standard	Jackknife	Bootstrap	Standard	Jackknife	Bootstrap	Standard	Jackknife	Bootstrap	Standard	Jackknife	Bootstrap
Eye (Vitreous Humor)												
Subject 5	144.47 \pm 26.40	144.47 \pm 0.07	144.45 \pm 1.28	47.84 \pm 0.44	47.84 \pm 0.00	47.84 \pm 0.02	42.00 \pm 0.00	42.00 \pm 0.00	42.00 \pm 0.00	42.00 \pm 0.00	42.00 \pm 0.00	42.00 \pm 0.00
Subject 6	145.56 \pm 32.13	145.56 \pm 0.08	145.65 \pm 1.62	47.37 \pm 1.06	47.37 \pm 0.00	47.37 \pm 0.05	42.78 \pm 0.94	42.78 \pm 0.94	42.78 \pm 0.94	42.78 \pm 0.94	42.78 \pm 0.94	42.78 \pm 0.05
Mean \pm Std of Mean	145.01 \pm 0.77	145.01 \pm 0.77	145.05 \pm 0.85	47.61 \pm 0.34	47.61 \pm 0.34	47.61 \pm 0.34	42.39 \pm 0.55	42.39 \pm 0.55	42.39 \pm 0.55	42.39 \pm 0.55	42.39 \pm 0.55	42.39 \pm 0.55
Mean \pm Std of Std	29.26 \pm 4.05	0.07 \pm 0.01	1.45 \pm 0.24	0.75 \pm 0.44	0.00 \pm 0.00	0.04 \pm 0.02	0.47 \pm 0.66	0.00 \pm 0.00	0.02 \pm 0.03	0.47 \pm 0.66	0.00 \pm 0.00	0.02 \pm 0.03
Cerebrospinal Fluid (CSF)												
Subject 5	117.17 \pm 24.63	117.17 \pm 0.06	117.18 \pm 1.21	56.52 \pm 3.81	56.52 \pm 0.01	56.54 \pm 0.20	47.98 \pm 5.35	47.98 \pm 0.01	47.97 \pm 0.27	47.98 \pm 5.35	47.98 \pm 0.01	47.96 \pm 0.26
Subject 6	135.84 \pm 34.03	135.84 \pm 0.09	135.82 \pm 1.69	54.83 \pm 4.04	54.83 \pm 0.01	54.85 \pm 0.20	45.51 \pm 3.51	45.51 \pm 0.01	45.52 \pm 0.18	45.51 \pm 3.51	45.51 \pm 0.01	45.52 \pm 0.17
Mean \pm Std of Mean	126.50 \pm 13.20	126.50 \pm 13.20	126.50 \pm 13.19	55.68 \pm 1.20	55.68 \pm 1.20	55.69 \pm 1.20	46.74 \pm 1.74	46.74 \pm 1.74	46.75 \pm 1.74	46.74 \pm 1.74	46.74 \pm 1.74	46.74 \pm 1.72
Mean \pm Std of Std	29.33 \pm 6.65	0.07 \pm 0.02	1.45 \pm 0.34	3.99 \pm 0.16	0.01 \pm 0.00	0.20 \pm 0.01	4.43 \pm 1.30	0.01 \pm 0.00	0.22 \pm 0.06	4.43 \pm 1.30	0.01 \pm 0.00	0.22 \pm 0.06
Gray Matter (WM)												
Subject 5	74.19 \pm 15.68	74.19 \pm 0.04	74.15 \pm 0.80	43.01 \pm 3.80	43.01 \pm 0.01	43.03 \pm 0.18	10.18 \pm 3.76	10.18 \pm 0.01	10.18 \pm 0.18	34.08 \pm 5.28	34.08 \pm 0.01	34.09 \pm 0.27
Subject 6	91.32 \pm 22.28	91.32 \pm 0.06	91.34 \pm 1.11	39.62 \pm 4.70	39.62 \pm 0.01	39.62 \pm 0.23	6.64 \pm 3.44	6.64 \pm 0.01	6.65 \pm 0.17	37.98 \pm 3.05	37.98 \pm 0.01	37.99 \pm 0.15
Mean \pm Std of Mean	82.75 \pm 12.11	82.75 \pm 12.11	82.75 \pm 12.16	41.31 \pm 2.40	41.31 \pm 2.40	41.32 \pm 2.41	8.41 \pm 2.51	8.41 \pm 2.51	8.41 \pm 2.50	36.03 \pm 2.76	36.03 \pm 2.76	36.04 \pm 2.76
Mean \pm Std of Std	18.98 \pm 4.67	0.05 \pm 0.01	0.95 \pm 0.22	4.25 \pm 0.64	0.01 \pm 0.00	0.21 \pm 0.03	3.60 \pm 0.23	0.01 \pm 0.00	0.18 \pm 0.01	4.17 \pm 1.58	0.01 \pm 0.00	0.21 \pm 0.09
White Matter (GM)												
Subject 5	60.14 \pm 13.99	60.14 \pm 0.04	60.14 \pm 0.67	42.20 \pm 4.21	42.20 \pm 0.01	42.20 \pm 0.21	7.73 \pm 3.25	7.73 \pm 0.01	7.73 \pm 0.16	36.46 \pm 4.00	36.46 \pm 0.01	36.45 \pm 0.19
Subject 6	60.25 \pm 13.00	60.25 \pm 0.03	60.26 \pm 0.65	35.99 \pm 5.22	35.99 \pm 0.01	35.99 \pm 0.26	3.42 \pm 1.59	3.42 \pm 0.02	3.42 \pm 0.08	36.00 \pm 4.84	36.00 \pm 0.02	35.99 \pm 0.24
Mean \pm Std of Mean	60.19 \pm 0.08	60.19 \pm 0.08	60.20 \pm 0.08	39.09 \pm 4.39	39.09 \pm 4.39	39.09 \pm 4.40	5.57 \pm 3.04	5.57 \pm 3.04	5.58 \pm 3.05	36.23 \pm 0.32	36.23 \pm 0.32	36.22 \pm 0.33
Mean \pm Std of Std	13.50 \pm 0.70	0.03 \pm 0.00	0.66 \pm 0.02	4.72 \pm 0.72	0.01 \pm 0.00	0.23 \pm 0.04	2.42 \pm 1.17	0.01 \pm 0.01	0.12 \pm 0.06	4.42 \pm 0.59	0.01 \pm 0.00	0.22 \pm 0.04

Table S5. Wilcoxon rank-sum statistical tests between mean measurements (standard method) from ^{23}Na MNF HR, LR and FLORET (FLO), over all subjects, for each ROI: Bonferroni correction (BC) was applied to the p values in order to take into account the number of tests ($N_{\text{meas}} = 3$) of each metric for each tissue: $p_{\text{BC}} = N_{\text{meas}} \cdot p$. The h and h_{BC} values correspond to statistically significant differences between measurements, using standard p and p_{BC} of 0.05 as threshold: $h = 1$ if $p \leq 0.05$ (statistically significant), and $h = 0$ otherwise; $h_{\text{BC}} = 1$ if $p_{\text{BC}} \leq 0.05$ (statistically significant), and $h_{\text{BC}} = 0$ otherwise.

ROI	Metric	Test	p	h	p_{BC}	h_{BC}
EYE	TSC	HR/LR	0.45571	0	1.36710	0
EYE	TSC	HR/FLO	0.50000	0	1.50000	0
EYE	TSC	LR/FLO	0.33333	0	1.10000	0
EYE	T1	HR/LR	0.00408	1	0.01224	1
EYE	T1	HR/FLO	0.05556	0	0.16667	0
EYE	T1	LR/FLO	0.05556	0	0.16667	0
EYE	T2s	HR/LR	0.09732	0	0.29196	0
EYE	T2s	HR/FLO	0.05556	0	0.16667	0
EYE	T2s	LR/FLO	0.05556	0	0.16667	0
EYE	T2l	HR/LR	0.09732	0	0.29196	0
EYE	T2l	HR/FLO	0.05556	0	0.16667	0
EYE	T2l	LR/FLO	0.05556	0	0.16667	0
CSF	TSC	HR/LR	0.03788	1	0.11364	0
CSF	TSC	HR/FLO	0.66667	0	2.00000	0
CSF	TSC	LR/FLO	0.22222	0	0.66667	0
CSF	T1	HR/LR	0.00117	1	0.00350	1
CSF	T1	HR/FLO	0.05556	0	0.16667	0
CSF	T1	LR/FLO	0.05556	0	0.16667	0
CSF	T2s	HR/LR	0.12821	0	0.38462	0
CSF	T2s	HR/FLO	0.05556	0	0.16667	0
CSF	T2s	LR/FLO	0.50000	0	1.50000	0
CSF	T2l	HR/LR	0.12821	0	0.38462	0
CSF	T2l	HR/FLO	0.05556	0	0.16667	0
CSF	T2l	LR/FLO	0.50000	0	1.50000	0
GM	TSC	HR/LR	0.00408	1	0.01224	1
GM	TSC	HR/FLO	0.66667	0	2.00000	0
GM	TSC	LR/FLO	0.11111	0	0.33333	0
GM	T1	HR/LR	0.12821	0	0.38462	0
GM	T1	HR/FLO	0.50000	0	1.50000	0
GM	T1	LR/FLO	0.33333	0	1.00000	0
GM	T2s	HR/LR	0.12821	0	0.38462	0
GM	T2s	HR/FLO	0.66667	0	2.00000	0
GM	T2s	LR/FLO	0.88889	0	2.66670	0
GM	T2l	HR/LR	0.12821	0	0.38462	0
GM	T2l	HR/FLO	0.33333	0	1.00000	0
GM	T2l	LR/FLO	0.05556	0	0.16667	0
WM	TSC	HR/LR	0.16492	0	0.49476	0
WM	TSC	HR/FLO	0.88889	0	2.66670	0
WM	TSC	LR/FLO	0.22222	0	0.66667	0
WM	T1	HR/LR	0.00699	1	0.02098	1
WM	T1	HR/FLO	0.05556	0	0.16667	0
WM	T1	LR/FLO	0.88889	0	2.66670	0
WM	T2s	HR/LR	0.71037	0	2.13110	0
WM	T2s	HR/FLO	0.33333	0	1.00000	0
WM	T2s	LR/FLO	0.50000	0	1.50000	0
WM	T2l	HR/LR	0.12821	0	0.38462	0
WM	T2l	HR/FLO	0.05556	0	0.16667	0
WM	T2l	LR/FLO	0.05556	0	0.16667	0

5 REFERENCES

1. Shao, J. & Tu, D. *The jackknife and bootstrap* (Springer Science & Business Media, 2012).
2. Efron, B. *The jackknife, the bootstrap and other resampling plans* (SIAM, 1982).